AD-A023 527

ENERGY MANAGEMENT TECHNIQUES FOR FUEL CONSERVATION IN MILITARY TRANSPORT AIRCRAFT

Analytic Sciences Corporation

Prepared for:

Air Force Flight Dynamics Laboratory

February 1976

DISTRIBUTED BY:

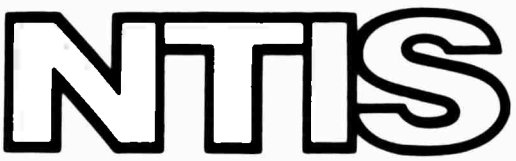

National Technical Information Service
U. S. DEPARTMENT OF COMMERCE

DISCLAIMER NOTICE

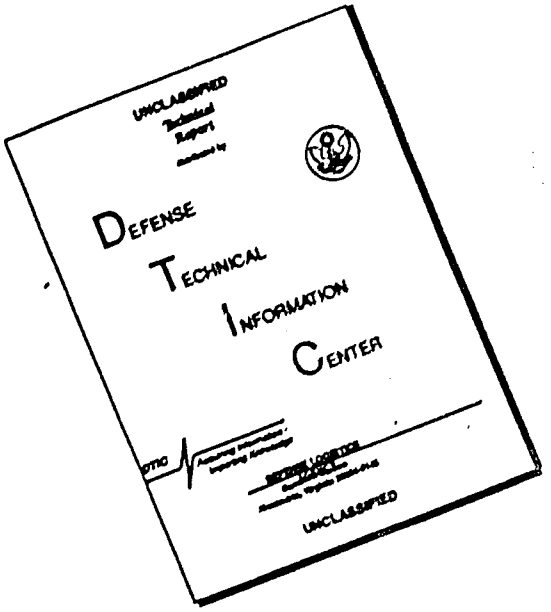

THIS DOCUMENT IS BEST QUALITY AVAILABLE. THE COPY FURNISHED TO DTIC CONTAINED A SIGNIFICANT NUMBER OF PAGES WHICH DO NOT REPRODUCE LEGIBLY.

120147

AFFDL-TR-75-156

AD A023527

ENERGY MANAGEMENT TECHNIQUES FOR FUEL CONSERVATION IN MILITARY TRANSPORT AIRCRAFT

THE ANALYTIC SCIENCES CORPORATION
SIX JACOB WAY
READING, MASSACHUSETTS 01867

13 FEBRUARY 1976

TECHNICAL REPORT AFFDL-TR-75-156
FINAL REPORT FOR PERIOD 6 JANUARY 1975 – 6 FEBRUARY 1976

Approved for public release; distribution unlimited

REPRODUCED BY
NATIONAL TECHNICAL
INFORMATION SERVICE
U. S. DEPARTMENT OF COMMERCE
SPRINGFIELD, VA. 22161

DDC
RECEIVED
APR 27 1976
B

AIR FORCE FLIGHT DYNAMICS LABORATORY
AIR FORCE WRIGHT AERONAUTICAL LABORATORIES
Air Force Systems Command
Wright-Patterson Air Force Base, Ohio 45433

NOTICE

When Government drawings, specifications, or other data are used for any purpose other than in connection with a definitely related Government procurement operation, the United States Government thereby incurs no responsibility nor any obligation whatsoever; and the fact that the government may have formulated, furnished, or in any way supplied the said drawings, specifications, or other data, is not to be regarded by implication or otherwise as in any manner licensing the holder or any other person or corporation, or conveying any rights or permission to manufacture, use, or sell any patented invention that may in any way be related thereto.

Copies of this report should not be returned unless return is required by security considerations, contractual obligations, or notice on a specific document.

This report has been reviewed by the Information Office (OI) and is releasable to the National Technical Information Service (NTIS). At NTIS, it will be available to the general public, including foreign nations.

This technical report has been reviewed and is approved for publication.

Ralph E. Guth

RALPH E. GUTH
Project Engineer

FOR THE COMMANDER

Paul E Blatt

PAUL E. BLATT
Chief
Control Systems Development Branch
Flight Control Division
AF Flight Dynamics Laboratory

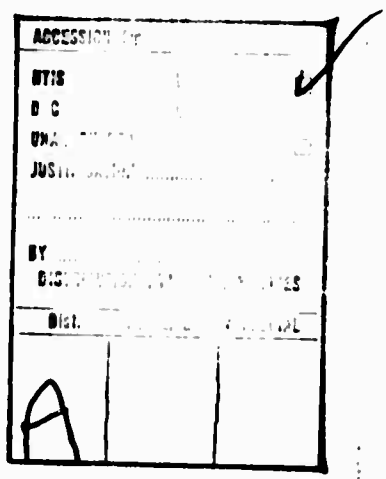

Copies of this report should not be returned unless return is required by security considerations, contractual obligations, or notice on a specific document.

AIR FORCE - 19 APRIL 1976 - 100

UNCLASSIFIED

SECURITY CLASSIFICATION OF THIS PAGE (When Data Entered)

REPORT DOCUMENTATION PAGE	READ INSTRUCTIONS BEFORE COMPLETING FORM
1. REPORT NUMBER: AFFDL-TR-75-156	2. GOVT ACCESSION NO. / 3. RECIPIENT'S CATALOG NUMBER
4. TITLE (and Subtitle): ENERGY MANAGEMENT TECHNIQUES FOR FUEL CONSERVATION IN MILITARY TRANSPORT AIRCRAFT	5. TYPE OF REPORT & PERIOD COVERED: FINAL 6 Jan. 75 - 6 Feb. 76
	6. PERFORMING ORG. REPORT NUMBER: TR-545-1
7. AUTHOR(s): Robert F. Stengel, Fred J. Marcus	8. CONTRACT OR GRANT NUMBER(s): F33615-75-C-3039
9. PERFORMING ORGANIZATION NAME AND ADDRESS: The Analytic Sciences Corporation, Six Jacob Way, Reading, Massachusetts 01867	10. PROGRAM ELEMENT, PROJECT, TASK AREA & WORK UNIT NUMBERS: Prog. Element: 62201F, Project: 1987, Task: 02, W.U.: 71
11. CONTROLLING OFFICE NAME AND ADDRESS: Air Force Flight Dynamics Laboratory, Air Force Wright Aeronautical Labs., Wright-Patterson AFB, Ohio 45433	12. REPORT DATE: February 1976
	13. NUMBER OF PAGES: 219
14. MONITORING AGENCY NAME & ADDRESS (if different from Controlling Office)	15. SECURITY CLASS. (of this report): UNCLASSIFIED
	15a. DECLASSIFICATION DOWNGRADING SCHEDULE

16. DISTRIBUTION STATEMENT (of this Report)

APPROVED FOR PUBLIC RELEASE: DISTRIBUTION UNLIMITED

17. DISTRIBUTION STATEMENT (of the abstract entered in Block 20, if different from Report)

18. SUPPLEMENTARY NOTES

19. KEY WORDS (Continue on reverse side if necessary and identify by block number)

Energy Management
Fuel Conservation
Flight Profiles
Control Algorithms

20. ABSTRACT (Continue on reverse side if necessary and identify by block number)

This report presents the results of an investigation of energy management techniques for fuel conservation in a large transport aircraft, the USAF C-141A. Using the methods of optimal control theory and numerical simulation, fuel-optimal flight paths are computed and compared with conventional vertical profiles for typical mission scenarios. Algorithms for on-board guidance to minimize fuel use are synthesized and evaluated, and functional requirements for system implementation are developed. (Cont.)

DD FORM 1 JAN 73 1473 EDITION OF 1 NOV 65 IS OBSOLETE

UNCLASSIFIED

SECURITY CLASSIFICATION OF THIS PAGE (When Data Entered)

20. (Continued)

Concepts for flight testing this throttle/energy management technique are presented. It is concluded that substantial fuel economies can be realized with current aircraft by careful shaping of the flight profile and that the methods applied to the C-141A aircraft can be applied successfully to other aircraft types.

FOREWORD

The investigation described in this report was performed by The Analytic Sciences Corporation (TASC), Six Jacob Way, Reading, Massachusetts under Contract No. F33615-75-C-3039, Project 1987, Task 02, for the Air Force Flight Dynamics Laboratory, Wright-Patterson Air Force Base, Ohio. The work was sponsored by the Control Systems Development Branch of the Flight Control Division. Mr. Ralph E. Guth (AFFDL/FGL) served as Technical Monitor for this contract.

The period of performance was January 1975 to February 1976.

The study was directed by Dr. Robert F. Stengel of TASC. Engineering investigation was conducted by Mr. Fred J. Marcus, who received engineering support from Mr. Paul W. Berry and Mr. John R. Broussard. Mr. Larry Murano assisted in computer program development.

This report was submitted by the authors in February 1976.

TABLE OF CONTENTS

TABLE OF CONTENTS (Continued)

LIST OF ILLUSTRATIONS

LIST OF ILLUSTRATIONS (Continued)

LIST OF TABLES

LIST OF SYMBOLS

VARIABLES	DESCRIPTION
A	State deviation penalty matrix
a	Speed of sound
a_{ii}	Diagonal elements of penalty matrix a
B	Control vector deviation penalty matrix
b_{ii}	Diagonal elements of penalty matrix B
C	Variational optimization control perturbation weighting matrix
c	Elements of weighting matrix C
C_D	Aircraft drag coefficient
C_L	Aircraft lift coefficient
CDCCL	Table of drag coefficient values
CLALP	Table of lift curve slopes
CLBAS	Basic lift coefficient
CMCL	Table of pitching moments due to lift
CMIT	Pitching moment-coefficient due to stabilator deflection angle
CMO	Pitching moment table
CMTH	Pitching moment due to thrust
CR	Crossrange
CRALO	Zero lift flexibility parameter table
CRCLA	Lift flexibility parameter table
CRCMC	CMCL flexibility parameter table
CRCMO	CMO flexibility parameter table

LIST OF SYMBOLS (Continued)

VARIABLES	DESCRIPTION
c.g.	Aircraft center of gravity
D	Aircraft drag
d	Flight conditions for gain scheduling
E	Specific total energy
F	Total engine thrust
^{o}F	Degrees farenheit
$\underline{f}$	Vector of aircraft state derivatives
$\underline{f}_{\underline{x}}$	$\partial \underline{f}/\partial \underline{x}$
$\underline{f}_{\underline{u}}$	$\partial \underline{f}/\partial \underline{u}$
g	Gravitational acceleration
H	Hamiltonian for the variational optimization cost function
$H_{\underline{u}}$	$\partial H/\partial \underline{u}$
h	Altitude
HN	Normalized altitude
IAS	Indicated airspeed
J	Total scalar cost
K	Matrix of linear-optimal perturbation guidance gains
$K_{\theta 1}, K_{\theta 2}, K_{\theta 3}$	Gains employed in ad hoc guidance law
k	Elements of gain matrix, K
L	Aircraft lift
ℓ	In-flight scalar cost function
$\ell_{\underline{x}}$	$\partial \ell/\partial \underline{x}$
$\ell_{\underline{u}}$	$\partial \ell/\Delta \underline{u}$
M	Mach number
m	Aircraft mass
MAC	Mean aerodynamic chord
MN	Normalized Mach number
N	Integer index-variable limit

LIST OF SYMBOLS (Continued)

VARIABLES	DESCRIPTION
NRT	Normal-rated thrust
P	Solution of matrix Riccati equation
p	Parameters to be optimized
q	Dynamic pressure
R	Range
S	Aircraft reference area
SR	Specific range (nautical miles/lb fuel)
STAB	Stabilator deflection angle
T	Throttle setting (0 to 1)
t	Time
TAS	True airspeed
TEMP	Atmospheric temperature
UN	Normalized atmospheric temperature deviation
$\underline{u}$	Vector of control variables
V	Ground relative velocity
V_W	Wind velocity
W	Aircraft weight
$\underline{x}$	Vector of state variables

VARIABLES (Greek)	
α	Angle of attack
α_O	Zero-lift angle of attack
α_T	Engine angle of incidence
γ	Flight path angle
δ	Atmospheric pressure ratio (pressure at altitude divided by sea level pressure)
ϵ	Suppression factor used for integrating equations of motion

LIST OF SYMBOLS (Continued)

VARIABLES (Greek)	DESCRIPTION
ρ	Atmospheric density correlation
	Coefficient between gain values and flight conditions (Chapter 6)
ω	Fuel flow rate
ξ	Aircraft heading angle
θ	Pitch angle
Φ	Scalar terminal state cost function
ϕ	Roll angle
σ	Standard deviation
$\underline{\lambda}$	Costate variable vector
μ	Weight ratio

VARIABLES (Subscripts)	
D	Desired value
i	Index variable
opt	Optimum value
SL	Sea level

VARIABLES (Superscripts)	
*	Optimal solution

VARIABLES (Punctuation)	
$(\dot{})$	Derivative of quantity with respect to time
$(\,)'$	Derivative of quantity with respect to path length
$\partial()/\partial()$	Partial derivative of one variable with respect to another
$()^T$	Transpose of vector or matrix
$(\bar{})$	Mean value
$(\underline{\ })$	Vector quantity
$\Delta(\,)$	Perturbation variable

I. INTRODUCTION

1.1 BACKGROUND

The "energy crisis" has caused virtually every segment of American society to reconsider energy-use policies. The immediate concern for running out of fuel has lessened, but we are left with greatly increased fuel costs, the continuing threat of localized shortfalls, and the reminder that natural sources of hydrocarbon fuels eventually will run dry.

Throughout recent developments, the military has been guaranteed a war reserve of fuel, and the nation's defense posture has not been compromised significantly. Nevertheless, fuel-use efficiency is a central issue of military preparedness for several reasons. First, there are obvious tactical and strategic reasons: if the average specific fuel consumption of a military aircraft can be improved, it can fly farther and/or carry a bigger payload. If the net fuel use per mission is reduced, more missions can be flown with a fixed amount of fuel. From a budgetary viewpoint, the cost of fuel per mission is another important factor, with per-gallon costs averaging 3 to 4 times what they were a year ago. Impacts of fuel shortages on training schedules, crew proficiency, reserve-unit support, trans-shipment and utility flying, and aircraft deployment also are major issues. Furthermore, in times of national emergency, the availability of the war reserve of fuel itself could be jeopardized.

The seriousness of this situation suggests not only that future aircraft be designed for increased fuel efficiency, but that fuel-optimality of the operations of current aircraft be examined in detail. Although numerous studies of improved aircraft operations have been made, few comprehensive evaluations of fuel-optimal climb-to-descent flight profiles have been conducted for existing aircraft. The technology for conducting such studies exists and has been demonstrated for individual flight profiles, but it has rarely been applied in such a way that sensitivities to mission variations and parameter uncertainties are fully understood.

In the past, aircraft fuel efficiency often has been considered to be synonymous with cruise efficiency, as essential efforts in designing aircraft have centered on maximizing range (Refs. 1 to 5). During maximum-range flight, a transport- or bomber-type aircraft spends a major portion of its time at the cruise condition, and there is strong justification for the point of view that minimizing fuel used during cruise minimizes overall fuel use. When day-to-day operations of such aircraft are examined, however, it is found that average stage lengths ("hops") are substantially below maximum range. Any practical approach to saving fuel must consider the reduced range of flight involved in normal transport and training operations, as well as the maximum range of the aircraft.

In recent years, research emphasis has shifted from range-maximizing equilibrium flight ("Breguet Cruise") to fuel-minimizing dynamic flight ("Energy-State" climb and descent), and, in fact, the fuel-optimality of cruise itself has been questioned (Ref. 6) and defended (Ref. 7). Building on the "energy-maneuverability" and "excess power" concepts introduced in the 1950's, approximate techniques for analyzing

minimum-time-to-climb and minimum-fuel-to-climb problems were developed (Refs. 8 to 17). These provide valuable insights concerning the importance of managing kinetic and potential energy, taking account of factors such as specific fuel consumption, altitude-Mach number effects of thrust, and Mach-dependent drag rise in shaping climb profiles. For fuel-minimizing climb, these profiles consist of two types of arcs: those which maximize total energy gained per unit of fuel expended and "zoom" climb or dive segments which provide kinetic-potential energy interchange. Recent developments have been directed at computing and matching arcs using asymptotic expansions and singular perturbation theory (Refs. 18 to 21), and practical approaches to specifying optimal flight path segments are treated in Refs. 22 and 23.

These approaches have identified the character of fuel-optimal flight paths, although, in most instances, the comparison between approximate and exact results (obtained by numerical optimization) has not been pursued extensively. The present study seeks to fill this gap by investigation of fuel-optimal flight paths which contain climb, cruise, and descent segments, which are computed with a detailed mathematical model of an existing aircraft, and which could be repeated in actual aircraft operations.

1.2 SCOPE AND TECHNICAL APPROACH

This report presents an analysis of the application of integrated throttle/flight path energy management techniques to a military transport aircraft. The purpose is to establish quantitative data on fuel economies and range extension achievable for typical mission scenarios. Specific algorithms designed to optimize throttle setting and flight trajectory within operational mission constraints are synthesized and

evaluated. An on-board system to implement the energy management functions in real time is defined, and a test concept for system validation and flight test is presented, considering alternative manual and automatic control modes.

Unified guidance algorithms are developed using a common conceptual and methodological approach, namely that associated with modern control theory. The design technique can be summarized as follows:

- Compute nonlinear, fuel-optimal trajectories for a specific aircraft type and typical mission scenarios.
- Compute linear-optimal perturbation guidance gains along these fuel-optimal trajectories.
- Integrate the reference trajectories and perturbation guidance gains to form an on-board throttle/energy management algorithm.

Further details of this technical approach can be found in the remainder of the report. Factors which may constrain fuel saving measures (e.g., air traffic control and mission scenarios) are identified, and the specific "ground rules" for system design are established, using the C-141A transport aircraft as a basis for detailed analysis.

1.3 SUMMARY OF RESULTS

The major tasks of this project were defined at the outset as:

- Aircraft Selection
- Constraint Definition
- Algorithm Development
- Concept Validation
- System Synthesis
- Test Concept

These tasks are summarized briefly. Aircraft Selection required the choice of a specific aircraft for detailed study, together with the reasons for making the selection. Constraint Definition identified the operational limitations and control objectives to be applied in the investigation. Algorithm Development provided throttle/energy management equations which were considered most suitable for achieving the stated objectives. Concept Validation was achieved by a quantitative comparison of fuel-optimal and conventional flight policies. System Synthesis was directed at design for real-time implementation of the energy management algorithms. Test Concept developed a methodology for planning and executing flight tests to demonstrate flight policies for fuel conservation.

The C-141A jet transport was chosen as a baseline for study. This aircraft type constitutes the single greatest user of jet fuel in the Air Force, and its flight operations are flexible enough that substantial variations in vertical profile could be flown without altering mission constraints and objectives.

Fuel savings from a few percent to more than 20 percent can be realized by reshaping the aircraft's vertical flight profile. The actual saving depends on stage length and the flight profile taken as a reference (the latter ambiguity is eliminated by choosing the optimal profile as a base and evaluating the excess fuel use of various conventional flight paths); however, the comparison with handbook profiles and cruise points used for pre-flight planning suggests that substantial savings can be realized in day-to-day operations.

Fuel-optimal flight conditions for the subject aircraft are not sharply peaked, and major fuel savings can be accomplished by operating in the vicinity of the optimum condition. Aerodynamic substantiating data and documented standard procedures provide valuable reference points for fuel optimization, although certain results require consideration of the specific stage length and vehicle weight, particularly for short-range flights. For example, the optimum climb schedule for short-range flights uses a constant Mach number and reduced throttle setting, whereas the medium- to long-range flight calls for constant indicated airspeed and maximum throttle setting during the climb.

The time penalty associated with fuel-optimal flight paths is not great, and the decreased fuel costs can lead to decreased direct operating costs. Except for long-range cruise at an altitude substantially below the unconstrained optimum cruise point (in which case, the fuel-optimal cruise speed is sharply reduced), the total flight times of optimal and conventional profiles are comparable. While it is difficult to account for total operating costs of the military transport (since several Air Force Commands share the costs), a comparison with airline operating costs suggests that the C-141A's fuel costs now exceed time-based costs on most flights; hence, reduced fuel use would result in reduced operating costs.

The development of fuel-minimizing guidance laws can be separated into two parts: generating the optimal flight path and issuing commands which force the aircraft to follow the path in the presence of disturbances. Simplified reference profiles can be established from the precise optimal flight paths, and the path-following guidance laws are readily formulated using linear-optimal control theory. The latter design process leads to a combined throttle/energy management

structure of very simple form. Such a system can be synthesized for flight test using a small digital computer, and it could be incorporated within navigation and control systems now under development.

Alternatives for flight testing center around two concepts. The first uses a dedicated, well-instrumented aircraft flying under carefully controlled conditions. The second approach is to conduct "piggy-back" experiments during operational missions. Both types of flight test should be carried out to maximize results with minimum cost.

1.4 ORGANIZATION OF THE REPORT

This report treats several aspects of the aircraft fuel conservation problem. Chapter 2 reviews aircraft selection, mission constraints, and prior developments related to fuel conservation. Chapter 3 describes the mathematical basis for the investigation. Optimal performance results for the C-141A are given in Chapter 4, and these results are compared with conventional flight paths in Chapter 5. Fuel-optimal guidance algorithms are developed in Chapter 6, and test planning is discussed in Chapter 7. The report is concluded by Chapter 8. Mathematical tools are described in Appendices A and B.

II. AIRCRAFT USE FACTORS AND PROSPECTS FOR FUEL CONSERVATION

2.1 OVERVIEW

With an annual fuel usage in the vicinity of more than 4 billion gallons and an associated bill of about $2 billion (Ref. 24), the U.S. Air Force has strong motivation to consider alternatives for conserving fuel. Projected cost increases will make fuel conservation even more important in years to come. In the long-term, improved aircraft configurations and propulsion systems can be expected to reduce fuel use, but for the short- and mid-term, it is necessary to consider improvements in the maintenance, operations, and subsystems of existing aircraft.

Although this investigation is directed at improving the technology base for fuel-efficient aircraft operations, particular attention is devoted to obtaining results which can assist the Air Force in reducing aircraft fuel use in the near-term. To achieve this objective, aircraft use factors must be considered in the context of mission requirements, airspace limitations, crew workload, and the probability that fuel-saving procedures can be incorporated in day-to-day operations. This chapter discusses these factors.

There are three topics covered here. Section 2.2 treats the selection of a subject aircraft, including the basic characteristics of four aircraft types and the criteria for selection. Section 2.3 presents mission profiles and

constraints for the chosen aircraft, the C-141A transport. Section 2.4 reviews energy management concepts for fuel-efficient flight, and the chapter is summarized in Section 2.5.

2.2 AIRCRAFT SELECTION

To assure that the energy management development provides usable results at an early stage, a single aircraft type must be defined for detailed study. Breakdowns of aircraft fuel use by aircraft class and type assist the selection of this study aircraft. Nearly 90 percent of aircraft fuel used by the Air Force is used by four aircraft classes:

- Cargo 32.7%
- Fighter/Reconnaissance 25.4%
- Bomber/Reconnaissance 18.1%
- Tanker 11.9%

Six aircraft types use almost 70 percent of the fuel (c. 1973):

- C-141 14.9%
- B-52 14.2%
- F-4 14.1%
- KC-135 11.2%
- C-5 7.2%
- C-130 6.9%

These lists indicate that over half the fuel is used by large aircraft (cargo, bomber, and tanker), and four aircraft types consume the bulk of this (C-141, B-52, KC-135, and C-5). These aircraft were candidates for study in this investigation (Ref. 25).

A useful analysis could be made for any one of these aircraft, and the four types are sufficiently similar that

the results obtained for one type are generally applicable to the other three. In addition to the total fuel consumed by each fleet, other factors affect the selection, e.g., availability of aerodynamic and engine data, mission scenarios, operational constraints, and Air Force Command flying policies. These aspects are summarized below for each aircraft type.

2.2.1 The Candidate Aircraft Types

C-141A - Over 275 of these aircraft have been delivered to the Air Force for use in long-range strategic transport. Maximum range with 31,000-lb payload is about 5,600 nm, and normal cruise Mach number is 0.72 to 0.767. Maximum loaded weight is approximately 300,000 lb. This aircraft has been the subject of past throttle/energy management studies (Refs. 1 and 2); hence, there is a body of performance data available for ready comparison. As a major element of the Military Aircraft Command (MAC), potential fuel savings with this aircraft would be significant if the throttle/energy management techniques developed in this program were implemented at the squadron level. The aircraft was first test flown in 1963, and its low-bypass-ratio turbofan engine shares its core (TF33) with the earlier vintage B-52. The C-141A is in the same weight class as the KC-135, both of which are lighter than the C-5A or B-52; hence, fuel costs for testing throttle/energy management techniques would be relatively low.

C-5A - This aircraft is more than twice as heavy as the C-141A, and it carries three times the payload. The number of C-5A's in MAC inventory is one-third the number of C-141A's, and the potential C-5A fleet fuel saving is approximately one half that of the C-141A (subject to actual

use factors). Cruise characteristics of the aircraft are similar to the C-141A, although policies directed at increasing aircraft fatigue life by reducing average flight loads provide additional constraints on this aircraft. The C-5A possesses the most modern standard avionics suite in this list of aircraft, and a fuel management computer is included as part of the standard equipment. The actual costs of testing are likely to be higher than those of any other aircraft in the group. The moderate-bypass-ratio turbofan engine (TF39) is more representative of current and future technology than the engines in the other three aircraft types.

KC-135 - Since 1956, the Air Force has ordered over 400 of this aircraft type. It was initially equipped with the J57 turbojet engine, although a few aircraft are equipped with the TF33 turbofan engine. The original version has a "normal" cruising speed of 510 kt, somewhat faster than the C-141A and C-5A, and it is the lightest aircraft in the group (270,000-lb maximum loaded weight). The potential Air Force-wide fuel savings with this Strategic Air Command (SAC) aircraft (some also are assigned to MAC) must be evaluated in light of refueling mission constraints, which could preclude flying for best fuel consumption for extended periods of time.

B-52 - The Stratofortress was designed over 20 years ago, first flying in 1952. Production of the Air Force's 711 aircraft of this type was completed by 1962. Early versions have a maximum loaded weight of 400,000 lb and are equipped with eight J57 turbojet engines; later models are 100,000-lb heavier and use TF33 turbofan engines. Normal cruise speed of the aircraft is 490 kt. The initial analysis and development for fuel-minimizing cruise which preceded Refs. 1 and 2 was directed at the turbojet-powered B-52 (Ref. 26); hence, data for comparison are available. This aircraft is

SAC's major user of fuel, and it is likely to retain this status for the next several years; thus, squadron-level implementation of fuel-saving flight policies could have substantial effect. Mission constraints could be more restrictive for this aircraft than for the other three, although fuel optimality is a consideration in achieving strategic flexibility.

2.2.2 The Selected Aircraft

There are several reasons for choosing the C-141A. This aircraft type constitutes the single greatest user of jet fuel in the Air Force, and virtually all of the C-141A aircraft delivered to the Air Force have identical aerodynamic, thrust, and inertial characteristics (allowing for nominal aircraft-to-aircraft variation); hence, the results of the study are applicable to all aircraft in the C-141A fleet. (By comparison, the B-52 and KC-135 fleets contain both turbojet- and turbofan-powered aircraft, and results of the study depend on engine type; therefore direct results would be less widespread than for the C-141A). The C-141A has been the subject of previous fuel-use studies, and all data required to formulate the mathematical model are available. Most of the aircraft in the C-141A fleet are approaching the mid-point of their service life (now projected at 40,000 flight hours); therefore, the specific energy management techniques developed here could be applied over an extended period of time. The proposal to modify the entire C-141A fleet to the "stretched" C-141B configuration would have little effect on this result, as the range of parameter variations studied includes the C-141B performance characteristics.

The use of a transport aircraft rather than a bomber or tanker type provides fewer constraints in determining

fuel-optimal flight policies, as point-to-point navigation rather than strategic (or tactical) navigation is involved. This further increases the possibility that throttle/energy management techniques developed in this contract ultimately could find their way into early operational use. In addition, fuel-efficient transport flight sets the stage for later studies incorporating strategic or tactical constraints.

2.3 MISSION DEFINITIONS AND CONSTRAINTS

For fuel-use studies and flight profile planning, C-141A missions can be separated into three classes with associated utilization percentages (Ref. 25):

- Training 16%
- Exercise 38%
- Airlift 46%

Excluding aborted or diverted missions, touch-and-go training, air drop exercises, and other low-altitude missions, over 80 percent of the flight hours can be expected to be logged on missions which reach normal cruising altitudes (greater than 15,000 ft). These missions are considered candidates for detailed study. The average duration of missions in this category is 5 hours, with minimum and maximum values of 1 and 10 hours, respectively. Corresponding ranges are 2,000, 300, and 4,200 nm. Payloads range from negligible to 24 tons, with an average value of 10.4 tons.

2.3.1 Air Traffic Control

While air traffic control (ATC) presents one of the most restrictive constraints on aircraft energy management, it should be recognized as a factor which can be altered

and influenced to achieve desirable objectives. The need for an ATC system arises from possibly conflicting demands for the use of airspace, as shown in Fig. 1; hence, if these demands can be coordinated, or if air traffic is light, ATC becomes less of a constraint. Conversely, if airspace surveillance is inadequate, if ATC policies are particularly rigid and unyielding, or if air traffic is heavy, then the constraint is increased. Designs for throttle/energy management in a variable ATC environment must be sufficiently flexible as to take best advantage of the prevailing constraints (or lack thereof) to save fuel.

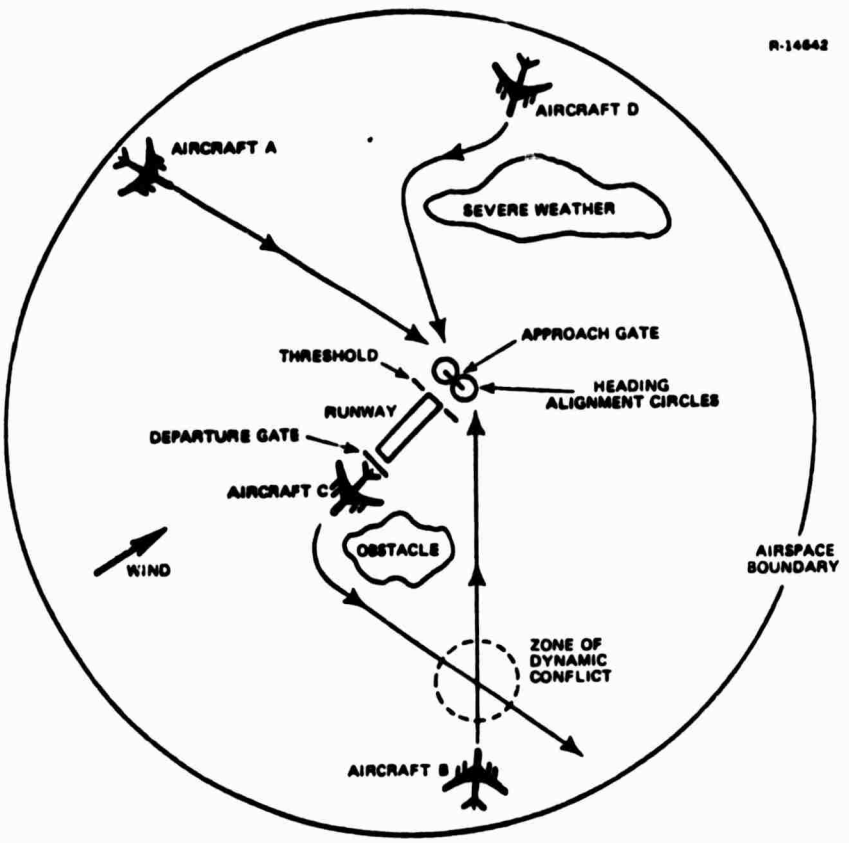

Figure 1 Overview for Constraint Definition

The ATC system imposes "hard" constraints on position and velocity in a time-based framework. The ATC system effectively establishes a network of corridors and time-slots within which an aircraft can travel. Explicitly or implicitly, the aircraft is assumed to be constrained to a "4-D" volume in time and space, surrounded by a region which the aircraft must not enter. Current civil ATC rules make this assumption implicitly, restricting aircraft to predetermined altitudes and airlanes; future systems predicated on all aircraft having area navigation ("R-Nav") capabilities could assign allowable "4-D" volumes explicitly in a very flexible way.

For the time being, a military transport operating without special priorities in the civil ATC system must fly according to fairly restrictive rules. For example, over the continental United States, cruise altitude must be held constant, altitude is assigned with 2,000-ft spacing below 29,000 ft and with 4,000-ft spacing above. Assigned altitude (a function of other traffic) may not be optimal (Refs. 27 to 29). Indicated airspeed must be held below 250 kt at altitudes under 10,000 ft. The throttle/energy management technique developed here handles such constraints in an efficient and direct way.

2.3.2 Atmospheric Conditions

Winds, atmospheric profiles of pressure and temperature, and severe weather (Fig. 1) all must be considered in establishing optimal flight paths, although only the latter falls into the category of a "hard" constraint. These factors regularly play a part in military and commercial route and altitude preflight planning (Refs. 30 and 31), which attempts to minimize fuel or direct operating costs.

Avoiding severe weather is similar to collision or obstacle avoidance, and a similar approach can be applied in both cases. The more difficult problem is identifying the potential conflict, which is beyond the scope of the study. Wind and atmospheric profile variations can be accounted for in the basic guidance algorithms, while guidance to avoid severe weather can be treated as an altitude/route determination problem, thus fitting into the same framework as ATC constraints.

2.3.3 Vehicle Constraints

The following chapters illustrate that fuel-optimal flight of a jet transport does not call for abrupt maneuvers and takes place at moderate dynamic pressure (and, therefore, indicated airspeed) and Mach number. Consequently, the vehicle's structural limitations do not have any bearing on shaping the vertical flight profile to minimize fuel use, and the flight condition does not exceed low dynamic pressure buffet limits. Although the performance ceiling of a lightly loaded C-141A is in the vicinity of 50,000 ft (Ref. 32), cabin pressurization cannot be maintained at adequate levels for passengers above 41,000 ft. As for most jet-powered aircraft, the ability to make idle-thrust descents also is limited by cabin pressurization requirements. (In order to maintain adequate cabin pressure levels, one or more powerplants must have sufficient speed to drive the appropriate subsystems.)* Cabin deck angle (pitch Euler angle) during fuel-optimal climb may be greater than conventional climb angle, but the vehicle contains no

*Pressurization constraints have not been applied in the following analyses, as they could be revised by subsystem modification, or, for cargo flights, by the air crew using breathing equipment. During descent, the C-141A maintains adequate pressurization at idle thrust.

inherent limitation which would prevent the higher angle. Flight paths investigated here pertain to the "clean" aircraft configuration (flaps, spoilers, and landing gear are retracted and the rear cargo door is closed), so restrictions on the deployment of these devices are not pertinent.

2.4 ENERGY MANAGEMENT FOR FUEL CONSERVATION

Fuel-conservative flight has always been a major goal in aeronautical development, so the recent concern for saving fuel is an intensification of prior interests rather than a new subject for study. Numerous aspects of aircraft operations can be examined for possible fuel savings, but the area which is addressed here is energy management, i.e., the regulation of an individual aircraft's kinetic and potential energy so that a minimum amount of powerplant fuel (chemical energy) is expended to achieve mission objectives.* As mentioned in the Introduction (Section 1.1), much prior analytical work in this area has been directed at the equilibrium cruise condition, during which specific total energy is approximately constant, and at climbs and descents, which result in transition to higher or lower energy.

Figure 2 illustrates the relationships between specific energy and basic flight variables, expressed in conventional units. The plot presents contours of specific total energy, E, and indicated airspeed (in knots), KIAS,

*It will be recalled that the aircraft's kinetic energy is $mV^2/2$, where m is aircraft mass and V is velocity. Potential energy is mgh, where g is gravitational acceleration and h is height. The aircraft's total energy is the sum of the two, and its specific total energy (or energy per unit weight), E, is $V^2/2g + h$.

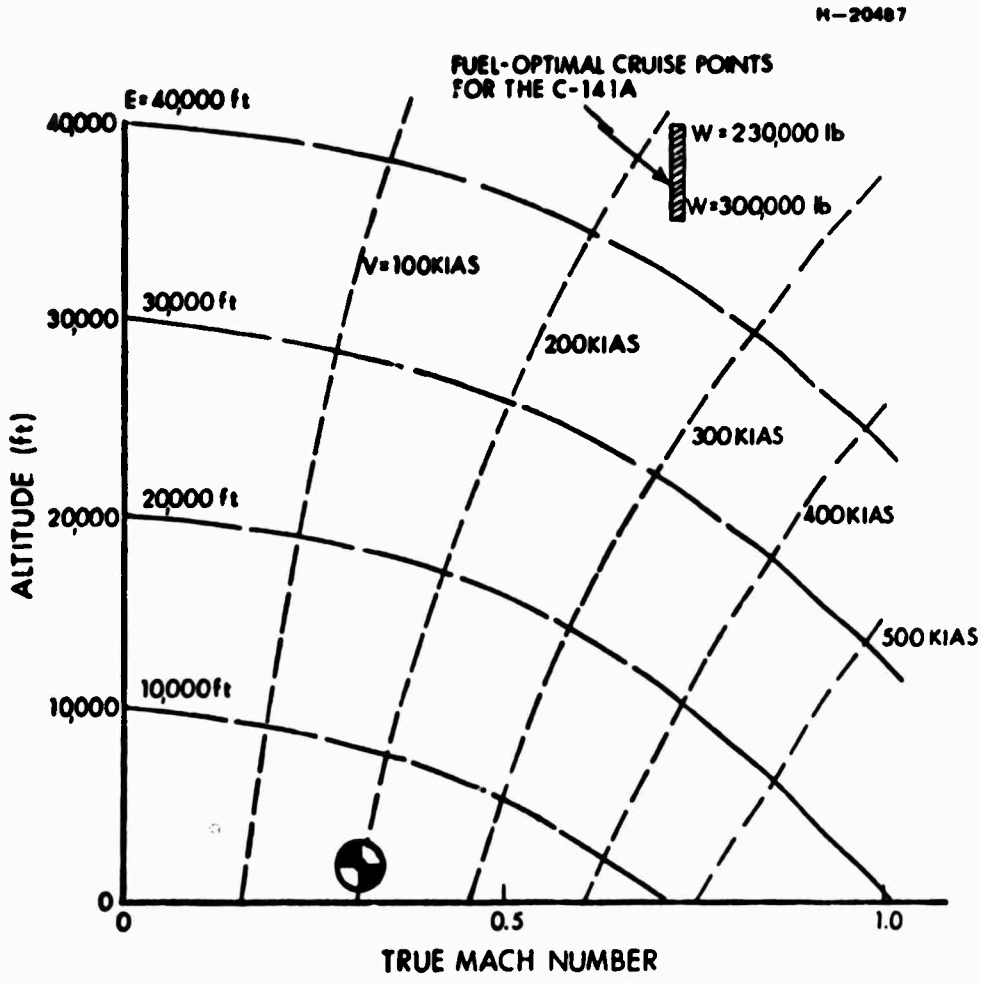

Figure 2 Contours of Constant Specific Total Energy (E) and Indicated Airspeed, in Knots (KIAS). Initial and Final Point for Climb-Cruise-Descent-Studies Indicated by "●"

as functions of altitude and true Mach number, M. (M and KIAS are computed using the 1962 Standard Atmosphere, Ref. 33).* Note that E has the dimensions of altitude, and, in fact, altitude is equivalent to specific potential energy. On a typical flight, the aircraft climbs from the

*Indicated airspeed (IAS) and calibrated airspeed (CAS) are assumed to be identical. IAS is computed as $1.689(2q/\rho_{SL})^{\frac{1}{2}}$, where q is the dynamic pressure (lb/ft^2) and ρ_{SL} is the sea level air density ($slugs/ft^3$).

lower left to the upper right of this figure and back, with commensurate variations in specific energy. Although M is held constant during fuel-optimal cruise of the C-141A, the figure shows that specific energy increases (due to altitude increase) as fuel is burned and the aircraft loses weight. This leads to a subtle effect on specific range (nautical miles travelled per pound of fuel expended), which is described in Chapter 4.

Figure 3 illustrates the general pattern for climb to and descent from the cruise point. Contours of constant specific energy change per unit of fuel burned ($\partial E/\partial m$) can be defined; if these contours are considered to portray a three-dimensional convex figure, the "ridge line" of this contour defines a fuel-minimizing climb path. Similarly, contours of constant drag force define a minimum-drag (or maximum-range) glide path for descent from the cruise condition.

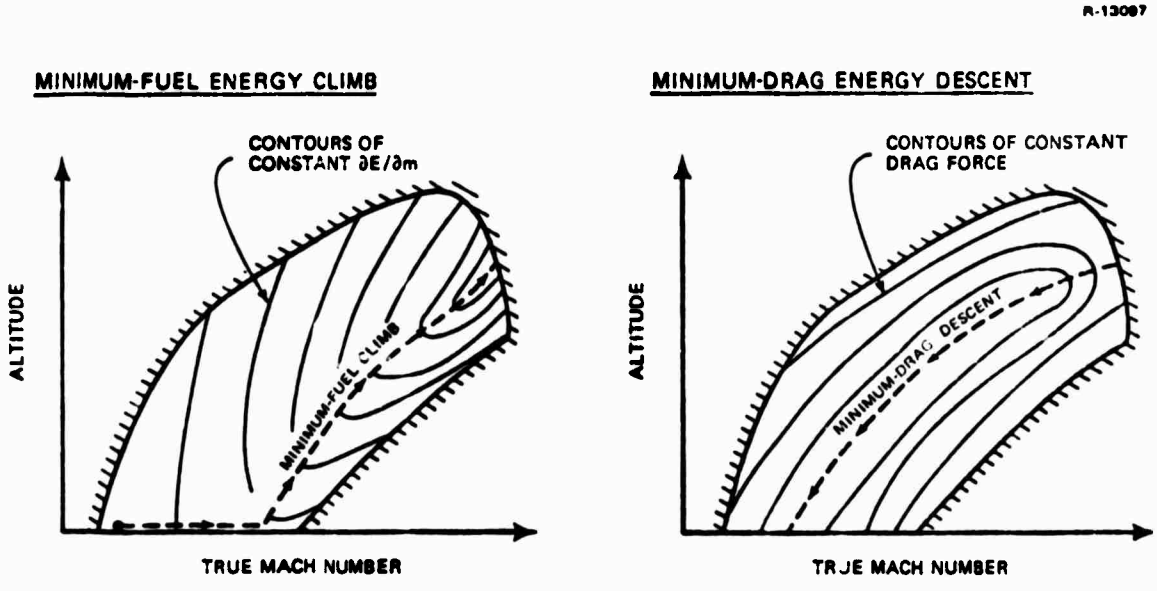

Figure 3 Fuel-Optimal Energy Transitions

As a result, fuel-optimal flight profiles tend to look like Fig. 4, which shows climb, descent, and two fuel-minimizing cruise alternatives -- a Breguet cruise-climb and a decelerating, constant-altitude cruise. The latter cruise is less efficient than the cruise-climb, but it is more efficient than a constant-Mach, constant-altitude cruise. In later chapters it will be seen that all fuel-optimal flight paths have the general shape shown in Fig. 4, including short-range trajectories without well-defined cruise segments. Specifically, climb speeds are faster than descent speeds, and the flight profile approaches operational boundaries (defined by buffet onset or by maximum operating velocity, V_{MO}, or Mach number, M_{MO}) only in the vicinity of cruise.

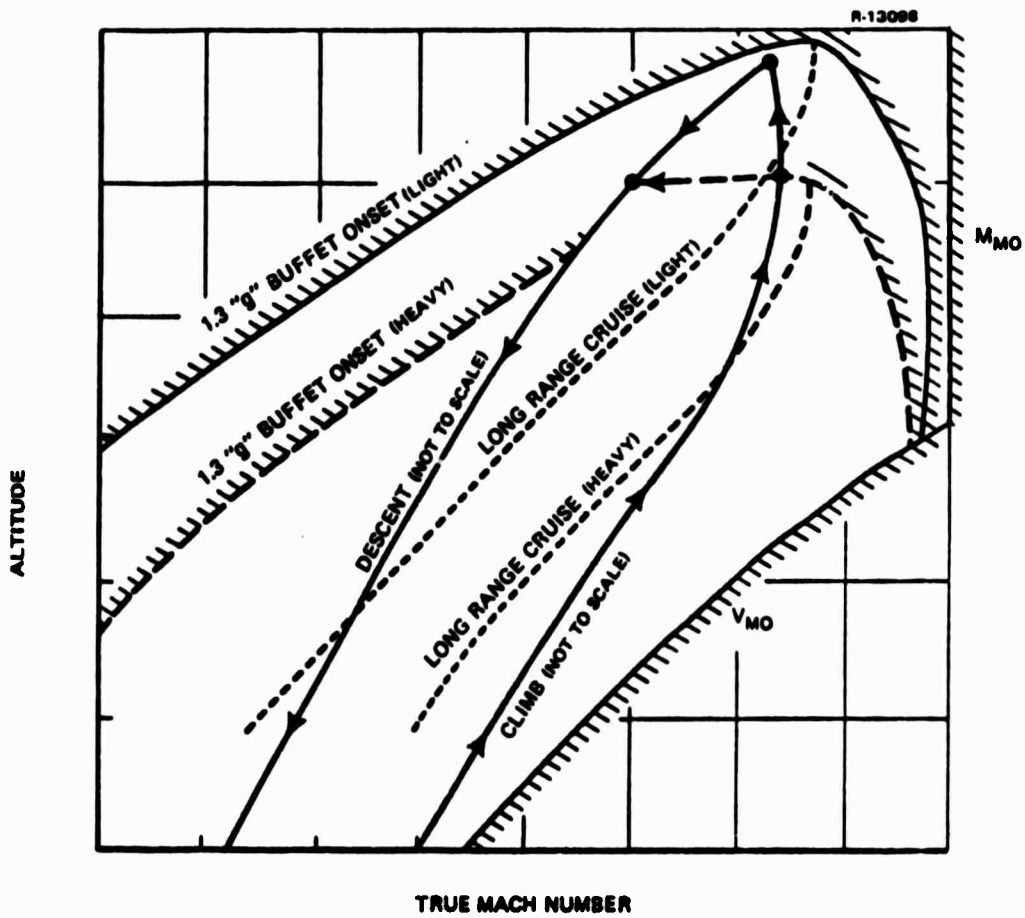

Figure 4 Fuel-Optimal Climb-Cruise-Descent Profile

Although these trends in the vertical flight path are known, actual flight operations may depart from this type of profile. Standard operating procedures frequently call for the descent-speed profile to be the reverse of the climb-speed profile, and many operators erroneously use higher-speed "barber-pole descents" (flying along the M_{MO}-V_{MO} boundary) to save fuel. Because the duration of the barber-pole descent is short, the apparent use of fuel during descent is low, and the aircraft can stay at cruising altitude (where specific range is high) longer. Nevertheless, the total fuel used during the cruise segment and descent is greater than that used on a fuel-optimal trajectory, especially if spoilers are used to increase descent rate by increasing drag.

Cruise segments often are flown one or two percent faster than the speed for best specific range for two reasons. The first reason is to reduce time-based direct operating costs, although, at present fuel rates, the net cost saving may be negligible. The second reason is to provide speed/thrust stability, i.e., to assure that speed excursions due to atmospheric disturbances are nulled inherently without throttle adjustment (Refs. 34 and 35). The additional fuel used in manual throttle adjustment can more than offset the penalty associated with the higher speed, and conventional autothrottles may have a similar effect in strong turbulence. This suggests that improved automatic systems could help by augmenting speed stability without throttle "hunting" and by automatically following a fuel-optimal altitude/speed schedule.

A number of general suggestions related to energy management for fuel conservation can be found in Ref. 36. In addition to recommendations regarding routing, fuel

reserves, ATC clearances, and center-of-gravity location, there are the following:

- Consider the use of area navigation equipment
- Adjust en route speed control to optimum values
- Cruise at optimum altitude
- Use optimum climb schedules
- Use idle-thrust descent
- Use lowest practical flap settings during landing
- Consider advanced onboard avionics for real-time selection of optimum flight profiles.

These suggestions indicate directions for fuel saving which are considered practical by industry representatives, and they make note of the special importance attached to augmenting navigation, guidance, and control systems to assist the pilot in saving fuel.

Practical implementation of fuel-saving flight policies for an individual aircraft requires detailed information regarding the actual state of the aircraft's engines, aerodynamic efficiency, and loading. There are a number of reasons why handbook data on a particular aircraft type may be inadequate for realizing fuel savings on an individual aircraft of that type. Aircraft of a particular design series often have modifications which occur during production. Rigging of aircraft control surfaces and of engine actuator settings changes with each overhaul, while aircraft use patterns and aging processes affect aerodynamic efficiency and the calibration of engine instruments and fuel gauges. Consequently, fuel-use efficiency for a particular aircraft is dependent on a real-time method for sensing these changes and estimating their effects.

This study addresses crucial elements of a throttle/energy management system which can optimize the flight paths of individual aircraft, namely the determination of fuel-optimal flight paths for the C-141A and the synthesis of guidance algorithms for following these paths. This development assumes that the aircraft's characteristics are known, and it demonstrates sensitivities to variations in the important parameters. The complete system should include fuel-use estimation logic to provide a continuing calibration of the relationship between throttle setting and the thrust/fuel-consumption characteristics of each engine, and it would be aided by improved thrust measuring devices, as reported, for example, in Ref. 37.

2.5 CHAPTER SUMMARY

This chapter has presented the process by which the C-141A was chosen as the study aircraft, the mission characteristics and limitations for this aircraft, and basic principles of energy management for aircraft fuel conservation. It was decided that the potential fuel-savings payoff of the study would be greatest by examining the C-141A. This single jet transport type consumes 15 percent of the Air Force's aircraft fuel, and over 80 percent of its missions could be flown with fuel-minimizing procedures. Prospects for flying fuel-optimal profiles on a day-to-day basis are enhanced by an automatic throttle/energy management system which follows optimal altitude/speed schedules, which augments cruising speed stability without undue throttle "hunting", and which adapts to variations in aircraft characteristics.

III. MATHEMATICAL FORMULATIONS FOR OPTIMIZATION AND ANALYSIS

3.1 OVERVIEW

Trajectory optimization consists of determining a "best" trajectory to accomplish a desired mission. The mission is defined by the aircraft's initial conditions, the terminal conditions, and the in-flight constraints imposed upon the trajectory. To be "best", or optimal, implies that a trajectory satisfies the mission requirements and also minimizes some cost function used to evaluate trajectory performance. For the present purpose of minimizing fuel use, the obvious cost function is the amount of fuel consumed in flying a given mission.

An aircraft trajectory is characterized by the time histories of the vehicle states (altitude, velocity, flight path angle, etc.) and the associated control histories (e.g., angle-of-attack and throttle setting). The dynamic relationships between the control and state histories are defined by the aircraft's equations of motion. As these equations must be satisfied by any physically realizable trajectory, they are included in the constraints which the optimal trajectory must satisfy. The aircraft equations of motion which are used for the current fuel minimization analysis are presented in Section 3.2.

All types of aircraft obey the same set of motion equations. What differs from one aircraft type to another is not the functional form of the equations, but rather the

magnitudes of the effects of the control histories upon the trajectory state response. For example, a particular throttle setting results in different values of thrust and fuel flow rate from one aircraft to another. Similarly, a given value of angle of attack yields values of lift and drag which are aircraft-dependent. The mathematical model which is used to describe the C-141A aircraft is reviewed in Section 3.3 of this report and presented in detail in Appendix B. Combining these models with the aircraft equations of motion fully specifies the interrelationships of the vehicle's control and state histories.

In order to examine trajectory performance and to exercise optimization techniques, a means of trajectory generation must be available. Given the aircraft's equations of motion and mathematical model, all that is needed to generate a trajectory by integration techniques is some means of specifying the control history. Reference trajectories are computed using control histories which represent standard aircraft operations, as described in Section 3.4. The present study embodies three alternatives for guidance command generation. These three techniques (Open-loop, ad hoc, and linear-optimal perturbation guidance) are discussed in Section 3.4. Trajectory generation by any of these means does insure a physically realizable trajectory. As long as the guidance commands are maintained within an allowable range, the vehicle model and motion equations accurately reflect the vehicle's state history.

Numerous methods exist for performing trajectory optimization (Refs. 38 to 40). Parametric optimization, variational optimization (using first- or higher-order algorithms), dynamic programming, and quasi-linearization

algorithms are but a few of the commonly used approaches for optimization. Each technique has its inherent advantages and disadvantages. For this reason, two optimization tools have been applied to the fuel-minimization problem under consideration.

Parametric optimization is a straightforward method for finding the maximum or minimum of a function which is determined by a finite set of parameters. Partial derivatives are not required, and the integration of sensitivity equations is unnecessary, thus making parametric optimization the simplest of the optimization methods. A number of problems concerned with fuel-minimization can be formulated as parameter optimization problems, and this analysis tool has proved to be useful in this study.

Variational optimization, while more complex than the parametric method, provides the capability to perform optimization in a more general framework. A first-order gradient algorithm is used here, as it has demonstrated its effectiveness in numerous aerospace trajectory optimization applications (Refs. 41 to 45). Higher-order algorithms have somewhat better convergence characteristics in some test cases (Ref. 39), but their performance is not uniformly superior, and the complexities involved in implementing these higher-order techniques are not justified for the current problem.

Descriptions of the parametric and steepest-descent optimization algorithms are presented in Sections 3.5 and 3.6, respectively. These descriptions provide only the details of the optimization techniques without the burden of theoretical derivation, which can be found in Ref. 39. The chapter is summarized in Section 3.7.

3.2 AIRCRAFT EQUATIONS OF MOTION

In this section, the "point-mass" equations of motion applicable to the aircraft fuel minimization are derived.* First, the three-degree-of-freedom (3-DOF) equations are presented. The two-degree-of-freedom (2-DOF) equations describing motion in a vertical plane then are derived as a subset of the 3-DOF model. These 2-DOF equations provide the basis for all fuel minimization analysis performed in this report. A change of independent variable from time to range is shown to further simplify trajectory optimization analysis. Finally, the usefulness of a new technique for reducing the computer time necessary for trajectory integration is demonstrated.

The 3-DOF aircraft equations of motion, assuming zero sideslip angle and neglecting round, rotating earth effects, can be written as

$$\dot{V} = T\left(\frac{NRT}{m}\right) \cos(\alpha+\alpha_T) - \frac{\rho}{2}(V+V_w)^2 C_D \frac{S}{m} - g \sin\gamma \qquad (3.2\text{-}1)$$

$$\dot{\gamma} = \left[T\left(\frac{NRT}{mV}\right) \sin(\alpha+\alpha_T) + \frac{\rho}{2V}(V+V_w)^2 C_L \frac{S}{m}\right] \cos\phi - \frac{g}{V}\cos\gamma \qquad (3.2\text{-}2)$$

$$\dot{h} = V \sin\gamma \qquad (3.2\text{-}3)$$

$$\dot{R} = V \cos\gamma \cos\xi \qquad (3.2\text{-}4)$$

$$\dot{CR} = V \cos\gamma \sin\xi \qquad (3.2\text{-}5)$$

$$\dot{\xi} = -\left[T\left(\frac{NRT}{mV}\right) \sin(\alpha+\alpha_T) + \frac{\rho}{2V}(V+V_w)^2 C_L \frac{S}{M}\right] \sin\phi/\cos\gamma \qquad (3.2\text{-}6)$$

$$\dot{m} = \omega(T, NRT, M, h) \qquad (3.2\text{-}7)$$

where the dependent variables are

*"Point-mass" equations of motion describe the dynamics of the aircraft's center of gravity, and they assume that angular maneuvers can be accomplished in negligible time.

V = Earth-relative velocity, fps

γ = Flight path angle, deg

h = Altitude, ft

R = Range, ft

CR = Crossrange, ft

ξ = Horizontal heading angle, deg

m = Aircraft mass, slugs

ω = Fuel mass flow rate, slugs/sec

The model parameters include engine normal-rated thrust (NRT), throttle setting (T), vehicle lift and drag coefficients (C_L and C_D), angle of attack (α), thrust-vector incidence angle (α_T), vehicle reference area (S), atmospheric density (ρ), gravitational acceleration (g), and vehicle Mach number (M). The term V_w represents the atmospheric wind velocity and is assumed to be aligned with the vehicle's velocity vector. This assumption is appropriate for the determination of horizontal-wind effects during cruising flight ($\gamma \simeq 0$), which is discussed in Section 4.2.4. In the preceding equations, total engine thrust is modeled as the product of normal-rated thrust (summed for each operating engine), and throttle setting.

The 2-DOF equations are obtained from the above set by constraining roll angle, crossrange, and heading to be zero. The resulting set of equations can be expressed as

$$\dot{V} = T\left(\frac{NRT}{m}\right) \cos(\alpha+\alpha_T) - \frac{\rho}{2}(V+V_w)^2 C_D \frac{S}{m} - g \sin\gamma \qquad (3.2\text{-}8)$$

$$\dot{\gamma} = T\left(\frac{NRT}{mV}\right) \sin(\alpha+\alpha_T) - \frac{\rho}{2V}(V+V_w)^2 C_L \frac{S}{m} - \frac{g}{V}\cos\gamma \qquad (3.2\text{-}9)$$

$$\dot{h} = V \sin \gamma \qquad (3.2\text{-}10)$$

$$\dot{R} = V \cos \gamma \qquad (3.2\text{-}11)$$

$$\dot{m} = \omega(T, NRT, M, h) \qquad (3.2\text{-}12)$$

Since the above dynamic equations have no explicit dependence on time, their number can be reduced by redefining the independent variable to be one or a combination of the dependent variables. The new independent variable must be monotonic along the trajectory to avoid singular points and multivalued control histories. For certain applications, specific total energy, E, is an appropriate choice of independent variable (Refs. 42 and 45). During aircraft cruising flight, however, E, is only slightly changing and may not be monotonic.

For the present analysis, the trajectory path length, R, proves to be a good choice of independent variable. Not only is path length a monotonic trajectory variable, but the initial and final points of an aircraft mission actually define total path length for planar trajectories. Use of path length as the independent variable also enables the optimization problem to be formulated in the "fixed-" (rather than "free-") endpoint framework. Typically, fixed-endpoint optimization analysis is simpler to perform because the sensitivities of the terminal state conditions with respect to terminal point variations need not be considered (Refs. 38 and 39).

Conversion of the dynamic equations to utilize path length rather than time as the independent variable is accomplished by invoking the chain rule for derivatives. For example, the rate of change of velocity with respect to path length is

$$\frac{dV}{dR} = \left(\frac{dV}{dt}\right)\left(\frac{dt}{dR}\right) = \frac{dV}{dt}\Big/\frac{dR}{dt} \qquad (3.2\text{-}13)$$

Equation (3.2-11) can be rearranged to yield the relationship between time and path length as

$$\frac{dt}{dR} = 1/(V \cos \gamma) \qquad (3.2\text{-}14)$$

The use of the chain rule and the time/path-length relationship of Eq. (3.2-14) results in the following set of 2-DOF motion equations:

$$V' = \left[T\left(\frac{NRT}{m}\right) \cos (\alpha+\alpha_T) - \frac{\rho}{2} (V+V_w)^2 C_D \frac{S}{m} - g \sin \gamma\right]/(V \cos \gamma) \qquad (3.2\text{-}15)$$

$$\gamma' = \left[T\left(\frac{NRT}{m}\right) \sin (\alpha+\alpha_T) + \frac{\rho}{2} (V+V_w)^2 C_L \frac{S}{m} - g \cos \gamma\right]/(V^2 \cos \gamma) \qquad (3.2\text{-}16)$$

$$h' = \tan \gamma \qquad (3.2\text{-}17)$$

$$m' = \omega(T,NRT,M,h)/(V \cos \gamma) \qquad (3.2\text{-}18)$$

where ()' is used to represent derivatives with respect to path length rather than time.

Although angle of attack, α, appears as an independent control parameter in the equations of motion, the use of pitch angle, θ, as a control variable is desirable. Reference 46 demonstrates that the use of θ in place of α for control tends to damp the undesirable phugoid oscillations which arise with constant angle-of-attack commands. In the case of the planar trajectory equations, the relationship between pitch angle and angle of attack is given simply as

$$\theta = \alpha + \gamma \qquad (3.2\text{-}19)$$

The equations of motion derived in this section are driven by many vehicle-dependent effects on lift, drag, and thrust. A description of these vehicle parameters is presented in the following section.

3.3 C-141A PARAMETERS

The aircraft equations of motion presented in Section 3.2 are valid for all types of aircraft. The study of a particular aircraft necessitates the specification of those parameters driving the equations of motion which are vehicle-dependent. The parameters which must be defined are the aircraft's lift and drag coefficients, C_L and C_D, reference area, S, normal-rated thrust from the engines, NRT, and fuel consumption rate, ω.

A complete description of the mathematical model of the C-141A is presented in Appendix B. This model includes all the numerical values of the vehicle-dependent parameters. Only the functional relationships of these parameters are given here, in order to review those quantities which affect trajectory performance.

The complex functional interrelationships of the C-141A vehicle and atmospheric parameters are summarized by the following equations:

$$C_L = f(\alpha, h, M, q, NRT, T) \qquad (3.3\text{-}1)$$

$$C_D = f(C_L, M) \qquad (3.3\text{-}2)$$

$$NRT = f(h, M, TEMP) \qquad (3.3\text{-}3)$$

$$\omega = f(NRT, T, \delta, TEMP) \quad (3.3\text{-}4)$$

$$M = f(V, TEMP) \quad (3.3\text{-}5)$$

$$q = f(V, \rho) \quad (3.3\text{-}6)$$

$$TEMP = f(h) \quad (3.3\text{-}7)$$

$$\rho = f(h) \quad (3.3\text{-}8)$$

$$\delta = f(h) \quad (3.3\text{-}9)$$

The atmospheric model parameters include total temperature (TEMP), density (ρ), and pressure ratio (δ). The vehicle's dynamic pressure (q) and Mach number (M) are computed from both the dependent variables of the equations of motion and the environmentally determined (atmospheric) quantities.

All of the above expressions are highly nonlinear functions of the model parameters. The environmental models employed in the current study are those of the 1962 Standard Atmosphere (Ref. 33). A number of sources (Refs. 1, 2, 32, 47, and 48) are used to define the C-141A model. These sources are chosen to provide a complete and valid mathematical vehicle representation. The fuel-minimization study accounts for all the major factors which influence vehicle performance.

3.4 REFERENCE TRAJECTORY COMPUTATION

Generation of aircraft trajectories is an important part of fuel-minimization analysis. The vehicle equations of motion and the mathematical model of the C-141A are two of the

three components necessary for trajectory computation. Addition of a guidance algorithm enables the generation of complete trajectory histories by means of numerical integration. The resulting profiles are also physically realizable as long as the guidance commands are maintained within allowable bounds. (In the current context, the terms "guidance" and "control" are used interchangeably; in a complete on-board system, the "control system" would produce the forces and moments required to follow the "guidance commands.").

Both open-loop and closed-loop guidance techniques may be used to compute aircraft controls. Open-loop guidance systems specify control histories as functions of an independent dynamic variable, while closed-loop commands are based upon values of the dependent variables of the equations of motion. In the present study, control commands (pitch angle and throttle setting) which are specified as functions of path length (the independent variable in the motion equations) provide open-loop guidance. Controls computed from dependent trajectory variables, such as altitude and velocity, form a closed-loop guidance law.

Open-loop guidance algorithms have only limited usefulness for actual vehicle implementation. The effects of winds and other uncertain conditions preclude specifying guidance commands in a totally open-loop fashion. Mathematical trajectory optimization techniques do, however, employ this form of control specification. The variational optimization analysis described in Section 3.6 demonstrates the use of open-loop guidance systems for analytical trajectory shaping.

Closed-loop guidance algorithms can be employed for both mathematical vehicle studies and direct aircraft control. A perturbation guidance system, which generates control

commands based upon the difference between desired and actual flight conditions, is a form of closed-loop guidance. The use of this guidance technique for aircraft implementation (linear-optimal perturbation guidance) is examined in Section 6.2. Simple ad hoc perturbation techniques serve the purposes of the parametric optimization efforts undertaken in this study.

The ad hoc guidance command generation used for parametric optimization in the current analysis is described by the following equations:

$$\dot{\theta} = K_{\theta_1} (V_D - V) + K_{\theta_2} (\dot{V}_D - \dot{V}) \qquad (3.4\text{-}1)$$

$$\dot{T} = K_T (E_D - E) \qquad (3.4\text{-}2)$$

where $\dot{\theta}$ and $\dot{T}$ are the time derivatives of the commanded pitch angle and throttle setting, V and E are the aircraft's velocity and specific total energy, respectively, and the subscript D denotes desired values of these quantities. The derivative of desired velocity, $\dot{V}_D$, is computed by dividing the change in V_D over each computation interval by the interval's time increment.

The specific energy term in Eq. (3.4-2) is a function of the vehicle's velocity and altitude,

$$E = h + \frac{V^2}{2g} \qquad (3.4\text{-}3)$$

where g is the earth's gravitational acceleration. The use of energy, rather than altitude, in the throttle command equation reduces the effects of phugoid oscillation (the interchange of kinetic and potential energy) on the trajectory response.

The desired values in Eqs. (3.4-1) and (3.4-2) may themselves be derived quantities. For example, it may be desired to fly a constant-altitude (h_D)/constant-Mach number (M_D) trajectory. In this case, desired values of velocity and energy would be computed as

$$V_D = M_D\, a \tag{3.4-4}$$

$$E_D = h_D + \frac{V_D^2}{2g} \tag{3.4-5}$$

where a is the speed of sound.

The vehicle equations of motion derived in Section 3.2 belong to a class of differential equations commonly called "stiff" (Refs. 49 and 50). This class of differential equations is characterized by the fact that large differences exist between the response times of the individual equations. In the current study, the flight path angle equation is much faster than the velocity, altitude, and mass equations. Typically, this necessitates using extremely small step sizes in the numerical integration procedure to accurately determine the trajectory characteristics.

In the current efforts, a simple time-scaling procedure has been employed to enable increased integration intervals. The time constant of the flight path angle differential equation is modified to be more compatible with that of the velocity equation. This is accomplished by using a suppression factor, ε, to lower the value of γ' obtained from Eq. (3.2-16). Note that in the limit, $\varepsilon = 1$, and the flight path angle equation is exact; as ε approaches 0, the dynamic effect of flight path angle change becomes negligible, and the equation becomes an algebraic constraint. This constraint frequently is employed in approximate trajectory

optimization methods, e.g., the energy-state method mentioned in Section 1.1. To insure that this suppression factor does not substantially alter the resultant trajectories, flight paths generated both with and without the suppression factor are compared. Altitude profiles for suppressed (ε = 0.05) and unsuppressed (ε = 1.0) sets of motion equations are presented in Fig. 5. The profiles are generated employing the ad hoc guidance algorithm demonstrating a climb in altitude from 34,000 to 35,000 ft. The small differences in overall profiles ensure that the suppressed equation set provides an excellent representation of the vehicle dynamics while allowing the computer time needed for trajectory integration to be reduced by a factor of nearly five. The unsuppressed trajectory settles at the desired altitude more quickly and

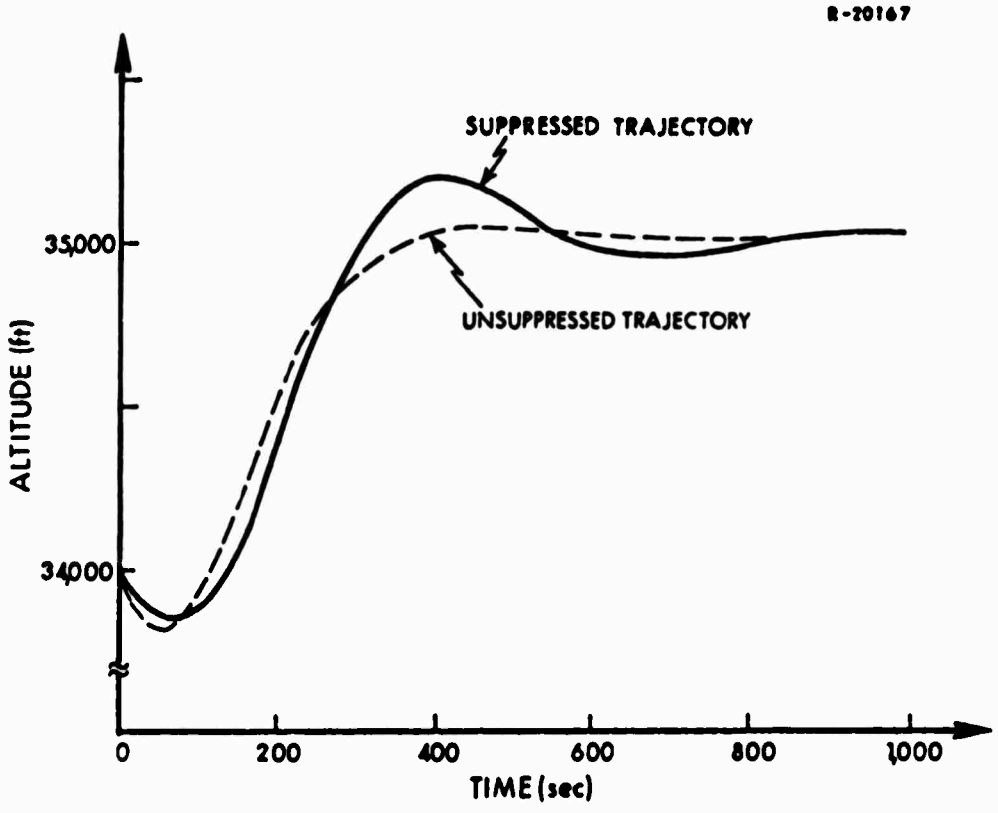

Figure 5 Altitude Profiles for Nominal and Suppressed Equations of Motion

with less overshoot than the suppressed version does because the unsuppressed motion equations have a faster flight path angle response.

3.5 PARAMETRIC OPTIMIZATION OF FLIGHT PATHS

The basic concepts of parametric optimization and its applications in determining fuel-optimal aircraft trajectories are reviewed in this section. Parametric optimization's major advantage over other optimization methods lies in the fact that it requires only function evaluations, not partial derivative or gradient evaluations. It tends to be a computationally efficient technique (Ref. 51). Of course, the use of this optimization tool is limited to that class of problems in which the cost function can be minimized by a finite set of parameters. Furthermore, if the initial choice of parameters is inappropriate or inadequate, further improvements over the parametric optimum are possible.

Relative comparisons of trajectory performance are made possible by assigning a scalar cost value to each trajectory. Trajectory A is considered to be superior to trajectory B if the cost associated with A is lower than that of B. An optimal profile is one which provides the lowest possible cost.

For the fuel minimization study at hand, the scalar cost function, J, used to characterize trajectory cost has the form

$$J = \phi(\underline{x}(R_f)) + \int_{R_0}^{R_f} L(\underline{x}, \underline{u}, R)\, dR \qquad (3.5\text{-}1)$$

where

J = total scalar cost function

$\underline{x}(R_f)$ = final values of dependent trajectory state variables: velocity, (V), altitude (h), flight path angle (γ), mass (m) and time (t)

$\underline{u}$ = vector of control variables: pitch angle (θ) and throttle setting (T)

R_0, R_f = initial and final values of the independent variable: range

L = scalar in-flight cost function

Φ = scalar cost function of final state variables

The terminal cost function, Φ, is used to penalize the trajectory for not meeting desired terminal conditions, such as final altitude and velocity, and to provide a direct penalty for the amount of fuel consumed. The in-flight cost function, L, penalizes the trajectory for violating desired flight path quantities, such as exceeding a maximum altitude or Mach number. A complete list of penalty functions available for use in the C-141A fuel minimization analysis is presented in Appendix A.2.

As previously noted, parametric optimization determines the lowest cost, J*, of a function which can be described by a finite set of parameters, i.e.,

$$J^* = \min J(p_1, p_2 \ldots p_N) \qquad (3.5\text{-}2)$$

where the p_i are the parameters which can be varied. The results of the optimization procedure are J*, the optimal cost, and the p_i^*(i=1 to N), which are the parameter values that yield the lowest cost.

The ad hoc closed-loop guidance algorithm described in Section 3.4 provides the means by which the fuel-minimization analysis can be cast in parametric form. The parameters which can be varied are those quantities which define the

desired trajectory characteristics (velocity, V_D, and energy E_D) and are inputs of the ad hoc guidance equations. The parametric optimization provides the optimum values of these parameters for particular trajectory segments.

Two examples of parametric optimization are illustrated in Fig. 6. In the first case (Fig. 6a), a two-segment profile which minimizes fuel used during a climb is generated, with the profile terminating at an optimal cruise condition (specified by weight over atmospheric pressure ratio, W/δ, and Mach number, M). The two parameters which are optimized are 1) the value of indicated airspeed, IAS, during the initial climb phase, and 2) the Mach number during the second portion of the climb. The results of the optimization are the best values of IAS and M to fly if this type of profile is to be implemented during the climb.

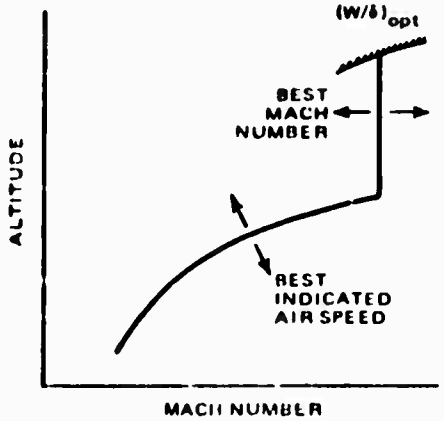

- 2 SEGMENT CLIMB PROFILE AT MAXIMUM THROTTLE SETTING
- MINIMUM FUEL USE USING CONVENTIONAL PROCEDURES

a) CLIMB OPTIMIZATION

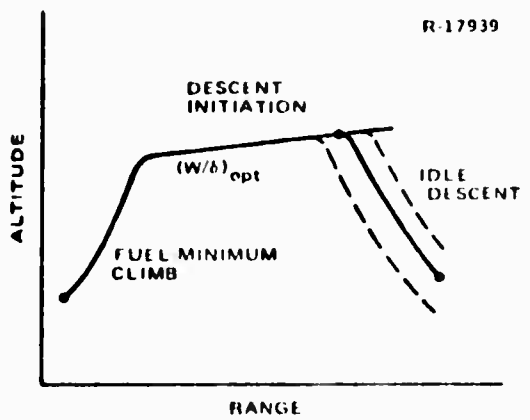

- CONVENTIONAL PROCEDURES THROUGHOUT ENTIRE PROFILE
- CONSTRAINTS (e.g., constant cruise altitude), WINDS, AND VEHICLE VARIATIONS INCORPORATED

b) DESCENT POINT OPTIMIZATION

Figure 6 Examples of Parametric Optimization

The second example (Fig. 6b) demonstrates the use of single-parameter optimization. In this case, the point for initiating descent is chosen to match the desired values of terminal altitude and velocity. Thus, complete near-optimal trajectory profiles can be generated by appropriate use of parametric optimization methods.

The parametric optimization procedure determines the best parameter values by successive function evaluations. A single parameter case, Fig. 7a, serves as a simple example of the optimization concepts. As shown in the figure, the cost function of parameter p, J(p), is evaluated three times: for values of p equal to x, (x - x), and (x + x). A parabola is then fitted to the three values of cost associated with these parameter values, and a final function evaluation is performed at the predicted minimum of the parabola. If the cost function were truly parabolic in the parameter, p, only one such iteration would serve to locate the true minimum. For most situations, however, the cost function is not exactly parabolic, and the sequence of function evaluations must be repeated several times to approach the optimum point as closely as desired.

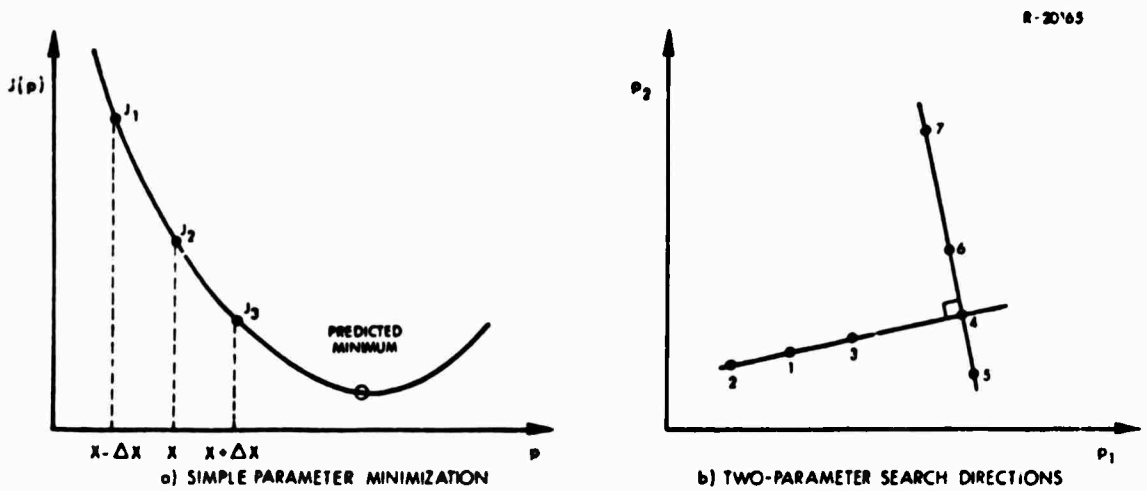

Figure 7 Parametric Minimization Concepts

A two-dimensional parametric optimization is depicted in Fig. 7b. The basic concepts are the same as for the single parameter case, but more function evaluations are required. The first set of function evaluations, denoted by points 1 to 4 in the figure, represents the three trial points (1-3) and the predicted minimum (4) in the p_1 - p_2 parameter space. Function evaluations 5 and 6 are again trial steps; however, they are performed along a direction which is orthogonal to the initial search direction. Function evaluation 7 is performed at the predicted minimum of this new search direction.

As in the single parameter optimization, successive iterations enable the optimum point to be approached as closely as desired. The program which is used for the parametric optimization procedure, EXTREM, is a modified version of a program presented in Ref. 40. This program also modifies the magnitude of the search steps to improve convergence, and it is capable of handling parametric optimizations of any dimension.

Parametric techniques have been shown to have the capability to define optimal segments and complete trajectories. These trajectories are optimal in that they are the best trajectories which follow the profiles determined by the specified parameters. Variational optimization methods determine optimal trajectories which are not confined to pre-specified profiles (e.g., constant IAS and Mach number climb modes). The parametric-optimal flight paths, however, facilitate the use of variational optimization methods by providing a good starting trajectory for the exact optimal solution.

3.6 VARIATIONAL OPTIMIZATION OF FLIGHT PATHS

Variational optimization methods determine the "best" trajectory profiles subject to any number of desired terminal conditions and in-flight constraints. Although variational techniques are more difficult to implement than parametric algorithms, they are applicable in those cases where the proper choice of parameters is not obvious. Thus, the resultant optimal profiles are not constrained to follow a parametrically defined (e.g., constant Mach number) profile.

The particular variational technique employed here combines a steepest-descent algorithm with the direct search used for parametric optimization. It is a first-order gradient algorithm which iteratively modifies the aircraft control history to improve overall trajectory performance. The control perturbations are chosen to <u>maximize the reduction in trajectory cost per unit change in control history</u>, i.e., the controls are applied along projections of the gradient. Thus, the technique used here is a <u>modified</u> steepest-descent approach which retains the essential features of many accelerated gradient methods.

The steepest-descent gradient algorithm is derived by specifying a cost function similar to that of Eq. (3.5-1):

$$J = \Phi(\underline{x}(R_f)) + \int_{R_0}^{R_f} \left\{ L(\underline{x},\underline{u},R) + \underline{\lambda}^T \left[(\underline{f}(\underline{x},\underline{u},R) - \underline{x}' \right] \right\} dR \tag{3.6-1}$$

where $\underline{\lambda}$ is the costate (or adjoint) vector of the state, $\underline{x}$. Because the state derivatives with respect to path length are given by

$$\underline{x}' = \underline{f}(\underline{x},\underline{u},R) \qquad (3.6\text{-}2)$$

the magnitude of the second term under the integral in Eq. (3.6-1) is zero. Adjoining the dynamic equations to the cost function, however, enables consideration of the effects of state perturbations at R_f, caused by control perturbations applied at previous values of the independent variable (R_0, for example), on the trajectory cost. The relationship between the state and costate variables is defined by the following differential equation:

$$\underline{\lambda}'(R) = - \underline{f}_{\underline{x}}^{T}(R)\, \underline{\lambda}(R) - L_{\underline{x}}^{T}(R) \qquad (3.6\text{-}3)$$

Here, the matrix $\underline{f}_{\underline{x}}^{T}$ is the transpose of the partial derivative of the vector, $\underline{f}$, with respect to $\underline{x}$. The vector, $L_{\underline{x}}^{T}$, is the partial derivative of L (a scalar) with respect to $\underline{x}$. This differential equation is integrated backwards from R_f to R_0, as only the terminal values $\underline{\lambda}$ are immediately available. The terminal values are defined by the sensitivity of the terminal cost to state variations:

$$\underline{\lambda}(R_f) = \partial\Phi(\underline{x}(R_f))/\partial\underline{x} \qquad (3.6\text{-}4)$$

The Hamiltonian, H, is a scalar function defined as

$$H(\underline{x},\underline{u},\underline{\lambda},R) = L(\underline{x},\underline{u},R) + \underline{\lambda}^{T}\underline{f}(\underline{x},\underline{u},R) \qquad (3.6\text{-}5)$$

It is shown in Ref. 39 that the Hamiltonian has the property that its partial derivative with respect to control perturbations, $H_{\underline{u}}$, is zero at locally stationary points. This is a necessary condition for a trajectory to be optimum. When $H_{\underline{u}} \neq 0$, it indicates which way to adjust the controls to reduce total cost.

The gradient, $H_{\underline{u}}$, at a non-optimum point indicates the direction of control perturbation which effects a reduction in total cost. It can be computed, using the costate vector, as

$$H_{\underline{u}}(R) = -\left[L_{\underline{u}}(\underline{x},\underline{u},R) + \underline{f}_{\underline{u}}^{T}(\underline{x},\underline{u},R)\ \underline{\lambda}^{T}(R)\right] \qquad (3.6\text{-}6)$$

where the vector $L_{\underline{u}}$ is the partial derivative of L with respect to the controls $\underline{u}$, and $\underline{f}_{\underline{u}}$ is the partial derivative matrix of $\underline{f}$ with respect to $\underline{u}$.

Having determined the direction of control perturbation, actual perturbations can be generated as

$$\delta\underline{u}(R) = C\ H_{\underline{u}}(R) \qquad (3.6\text{-}7)$$

where the matrix C contains unspecified gain values. In order to accelerate the convergence of the gradient algorithm to the optimal trajectory, the present study makes use of the parametric optimization tools described in Section 3.5. This is accomplished by specifying a diagonal form for C, with the diagonal elements being independent parameters. For a two-dimensional case, the gain matrix would be defined as

$$C = \begin{bmatrix} c_1 & 0 \\ 0 & c_2 \end{bmatrix} \qquad (3.6\text{-}8)$$

and the resultant control perturbations are given by

$$\begin{bmatrix} \delta u_1(R) \\ \delta u_2(R) \end{bmatrix} = \begin{bmatrix} c_1\ H_{u_1}(R) \\ c_2\ H_{u_2}(R) \end{bmatrix} \qquad (3.6\text{-}9)$$

where the terms δu_1, δu_2, H_{u_1}, H_{u_2}, are the components of

the control perturbation and gradient vectors respectively. The new control history, $\underline{u}_{i+1}$, is computed as

$$\underline{u}_{i+1}(R) = \underline{u}_i(R) + \delta\underline{u}(R) \qquad (3.6\text{-}10)$$

where $\underline{u}_i$ is the previous control history and the control perturbations are those specified in Eq. (3.6-9). The iteration is complete when no further significant reduction of the cost function can be obtained.

The gain values, c_1 and c_2, can be chosen through the parametric optimization process. Once the gradient, $H_{\underline{u}}$, is determined, the changes in the cost function are only dependent upon the choice of gain parameters. This use of parametric optimization in the variational technique enhances the convergence characteristics of the first-order algorithm, thereby permitting the optimal trajectory to be determined with fewer steepest-descent iterations. As the computation of trajectory partials ($L_{\underline{x}}$, $L_{\underline{u}}$, $\underline{f}_{\underline{x}}$, $\underline{f}_{\underline{u}}$) can be burdensome, the reduction of iterations results in a substantial reduction of computer time.

The execution of a steepest-descent optimization iteration consists of performing a series of mathematical operations. In order to clarify the technique, this section is concluded with an ordered list of these operations:

- Generate an initial trajectory, $\underline{x}_0(R)$, given an arbitrary initial control history, $\underline{u}_0(R)$, using open-loop guidance commands.
- Compute trajectory and cost function partial derivatives: $\underline{f}_{\underline{x}}, L_{\underline{x}}, \underline{f}_{\underline{u}}, L_{\underline{u}}$.
- Integrate (backwards) the costate differential equation to determine $\underline{\lambda}(R)$.

- Evaluate the gradient, $H_{\underline{u}}(R)$, in order to determine control perturbations, $\delta\underline{u}(R)$.

- Parametrically optimize the control perturbation gains, C, to obtain the lowest trajectory cost, J.

- Either terminate execution or repeat, starting at the second step and using the best trajectory as the new initial point.

This section has presented the basic concepts of variational optimization. The results of applying these concepts to the fuel-minimization problem are shown in the following chapters of this report.

3.7 CHAPTER SUMMARY

The optimization and trajectory analysis techniques brought to bear on the C-141A fuel-minimization problem have been presented in this chapter. The equations of motion applicable to the current study and the mathematical aircraft model serve to define trajectory state response as a function of the input controls. By working within the vehicle model framework, the optimal trajectories generated are physically realizable, i.e., they can be flown by actual aircraft.

The key points and significant advantages of the current trajectory analysis can be summarized as follows:

- Two-degree-of-freedom equations are employed to simplify fuel-minimization analysis in the vertical plane.

- The C-141A vehicle model includes all the major factors which influence aircraft trajectory characteristics.

- A scalar cost is assigned to each trajectory. This enables the relative comparisons of trajectory performance.

- Parametric techniques provide for computationally efficient trajectory segment optimization.

- Steepest-descent optimization methods are used to generate fully optimal flight profiles and vehicle control histories. Parametric methods are employed to enhance the convergence characteristics of the steepest-descent algorithm.

The analysis tools described in this section provide flexible and accurate means for trajectory shaping and analysis. The results of applying these tools to the fuel-minimization problem are presented in the following chapters.

IV. AIRCRAFT PERFORMANCE ON FLIGHT PATH SEGMENTS

4.1 OVERVIEW

In this chapter, C-141A performance on individual flight path segments is considered. The flight profile is divided into the three natural flight modes: climb, cruise, and descent. The climb segment typically is flown with maximum throttle setting (Refs. 32 and 47), and during this phase, the aircraft increases altitude and velocity until cruising flight conditions are achieved. Cruising flight is characterized by a constant, or slowly varying, altitude and velocity profile. The descent mode is initiated following cruise, and it serves the purpose of reducing altitude from the cruise to landing phases of flight.

By considering these flight modes individually, simple analysis tools can be employed to optimize fuel consumption. The parametric methods described in Section 3.5 are applicable for optimizing the climb and descent flight segments, while direct search techniques are useful in determining the conditions which define fuel-optimal cruising flight.

Minimizing fuel consumption on the individual flight segments provides results which either can be implemented directly or can be used to assist in complete trajectory optimization. If, for example, the climb and descent flight modes are constrained (due to ATC considerations), at least the cruise phase may be flown in a fuel-minimal fashion. If, on the other hand, the cruising flight segment is constrained,

some fuel savings may still be achieved through optimization of the climb and descent schedules.

By piecing together the individually optimized segments, fuel-efficient complete trajectory profiles are defined. These complete trajectory profiles, however, may not be fully optimal for two reasons. First, the parametric optimization methods constrain the aircraft to fly a specific profile shape, which is defined by the parameters to be optimized. Second, by considering each flight mode separately, the optimality of the transitions from one mode to the next is ignored. Comparisons of the parametric-optimal trajectories (formed by piecing together fuel-minimal segments), and fully optimal profiles (determined by means of variational optimization), are presented in Chapter 5. There it is demonstrated that parametrically optimized flight segments provide for nearly optimal fuel minimization.

The cruise, climb, and descent flight modes are discussed in Sections 4.2, 4.3, and 4.4, respectively. The cruise segment is examined first, as the terminal conditions for the climb mode and the initiation point for the descent phase are determined by the cruising flight conditions. A summary of the chapter is then provided in Section 4.5.

4.2 CRUISING FLIGHT PARAMETERS

A straightforward method of examining the fuel efficiency of a trajectory is to divide the trajectory path length by the amount of fuel consumed. The resultant value, commonly called specific range, SR, indicates the nautical miles flown per pound of fuel. The instantaneous value of specific range at any point on the trajectory is given approximately as

$$SR = \frac{V}{\omega} \qquad (4.2\text{-}1)$$

where V is the aircraft's velocity in knots and ω is the fuel flow rate in pounds per hour.

The expression in Eq. (4.2-1) is approximate, in that it assumes that the velocity vector is parallel to the ground i.e., that the flight path angle is zero. This is the same approximation that is made in deriving the maximum range flight defined by the Breguet equations (Ref. 52). As the flight path angle during optimal cruise is on the order of a few hundredths of a degree, the approximation is a good one.

Fuel-optimal cruising flight can be achieved by flying at conditions such that the aircraft's instantaneous value of specific range, as given by Eq. (4.2-1), is maximized. The maximum value of specific range is determined by the point at which V/ω attains a maximum, as shown in Fig. 8.

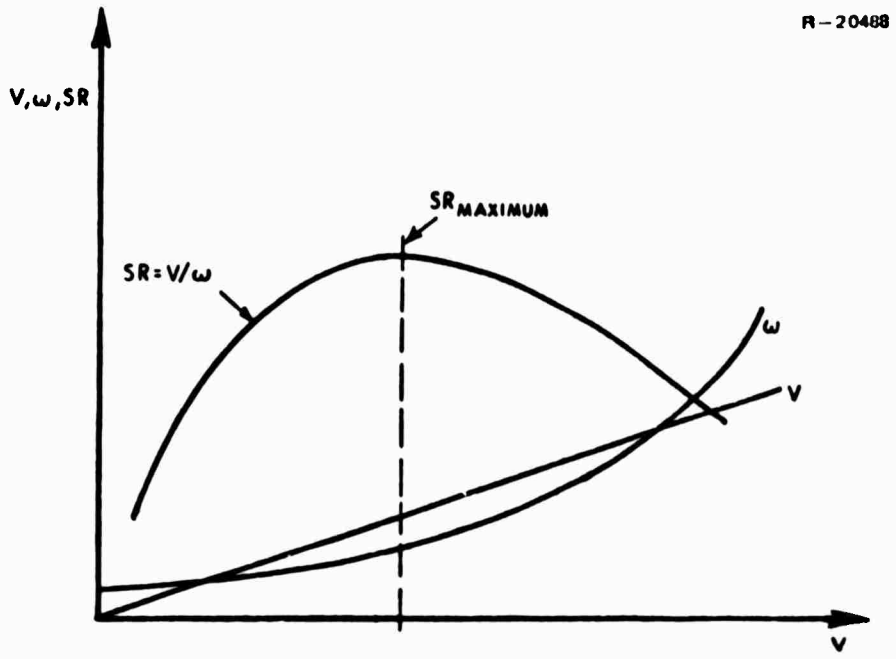

Figure 8 Specific Range Evaluation

It is shown in Refs. 1 and 2 that maximum specific range for a turbojet aircraft can be achieved by flying at constant values of W/δ (weight over atmospheric pressure ratio) and Mach number. A plot of pressure ratio (δ) vs. altitude is presented in Fig. 9a (Ref. 33). At sea level, δ equals one. As altitude increases to 50,000 ft, atmospheric pressure decreases, and δ is approximately 0.09. As the aircraft burns fuel, weight decreases, and altitude must be increased to keep W/δ constant. Profiles of altitude versus weight for three constant levels of W/δ are shown in Fig. 9b.

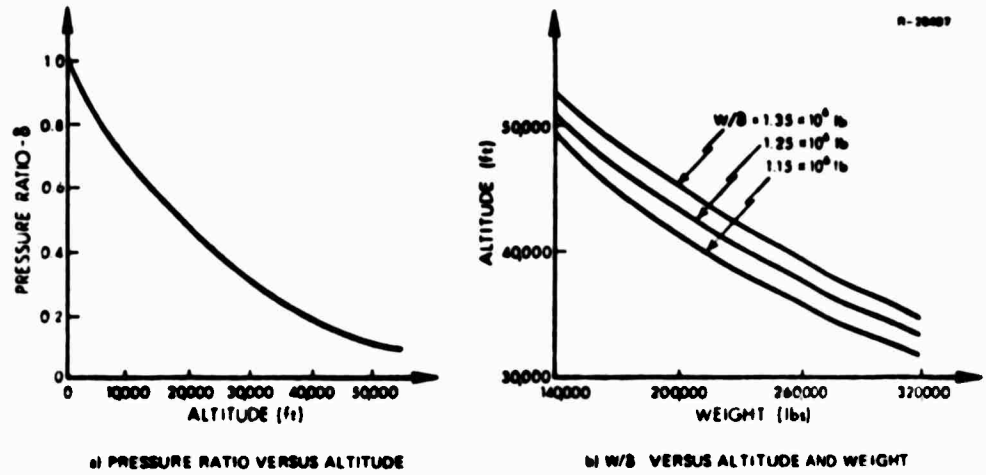

Figure 9 Optimal Cruise Parameters

These values of W/δ are typical of the optimal values for the C-141A aircraft. At a vehicle weight of 320,000 lb (the maximum C-141A weight), the W/δ profiles indicate that the fuel-minimal cruise altitude is on the order of 33,000 ft. At a weight of 140,000 lb, the optimal cruise altitude is near 50,000 ft. It is for this reason that typical aircraft trajectories include climb and descent phases. The climb segment brings the vehicle near the

minimum-fuel cruise altitude, and the descent segment returns the aircraft to low altitude prior to landing.

Sections 4.2.1 through 4.2.2 present the optimal cruise parameters, W/δ and Mach number, for the C-141A. Nominal parameter values and the effects of non-standard atmospheric conditions and vehicle configurations on these parameters are discussed.

4.2.1 Nominal Configuration

Specific range contours for the C-141A aircraft model employed in this study are shown in Fig. 10a. These contours are based upon a nominal aircraft center of gravity (c.g. = 0.241 MAC), a vehicle weight of 180,000 lb, standard atmospheric temperatures, and zero wind velocity. The specific range values presented in this figure neglect trim drag, as outlined in Appendix B.

The maximum value of specific range occurs for the following cruise conditions:

- Mach number = 0.727
- W/δ = 1.24×10^6 lb

At a vehicle weight of 180,000 lb, the maximum specific range is seen to be 0.0565 nm/lb. For other vehicle weights, the maximum specific ranges are presented in Fig. 10b. Also plotted here are the altitudes which correspond to maximum specific range for W/δ equal to the optimum value, 1.24×10^6 lb.

The maximum specific-range numbers quoted in this report are based upon the horizontal flight path assumption described in Section 4.2; however, in order to follow a

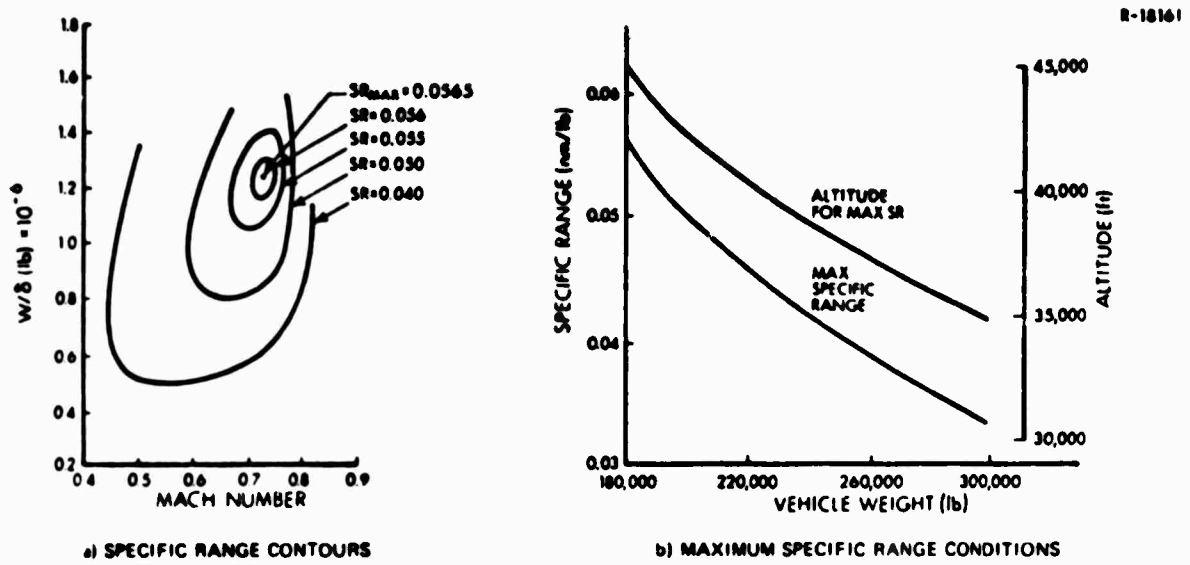

Figure 10 C-141A Nominal Specific Range Parameters

cruise-climb (constant-W/δ) profile, typical values of flight path angle for the C-141A are on the order of 0.02 deg. At a vehicle weight of 229,000 lb, the horizontal-cruise specific range is 0.04432 nm/lb, while the climbing-cruise is 0.04401 nm/lb. Thus, the horizontal flight instantaneously has a value of specific range which is 0.7 percent greater than that of the cruise-climb. This percentage is equal to the percentage increase in energy which must be expended to gain altitude on the climbing trajectory. If the horizontal flight path is maintained, however, the aircraft will no longer be flying at the optimal cruise conditions, and specific range will fall far below that obtained on the climbing profile.

4.2.2 Center-of-Gravity Shift Effects

As the vehicle center-of-gravity (c.g.) moves aft, the pitching moment supplied by the aircraft tail for trim is decreased. Thus, the magnitude of negative lift supplied by the tail is decreased, and the wing lift required for level flight is reduced by an equal amount. As the lift of the wing decreases, so does the wing's contribution to total aircraft drag. In order to examine the effects of specific range caused by c.g. location shifts, the vehicle model which incorporates tail-lift effects (see Appendix B) is employed for the present and all ensuing off-nominal specific range evaluations.

The optimal value of W/δ to maximize specific range is shown in Fig. 11 as a function of aircraft c.g. location. The values of $(W/\delta)_{opt}$ have been computed at forward (18 percent MAC), mid (24 percent MAC), and aft (34 percent MAC) center-of-gravity locations. As the specific range computations are performed at discrete altitudes (2,500 ft increments) and vehicle weights (10,000-lb increments), there is some uncertainty in the resultant mean value of $(W/\delta)_{opt}$. For this reason, the standard deviation associated with the data points is indicated. The variation in $(W/\delta)_{opt}$ is small ($W/\delta_{opt} = 1.18 \times 10^6$ lb at forward c.g., 1.22×10^6 lb at aft c.g.) and is within the uncertainty of the estimates. Thus, for most practical purposes, the variation in $(W/\delta)_{opt}$ with c.g. location shifts can be neglected. Also, the optimal cruising Mach number remains constant at a value of 0.73 (a slight increase from the 0.725 computed without trim drag effects).

A plot of maximum specific range vs. aircraft weight is presented in Fig. 12. These specific ranges are

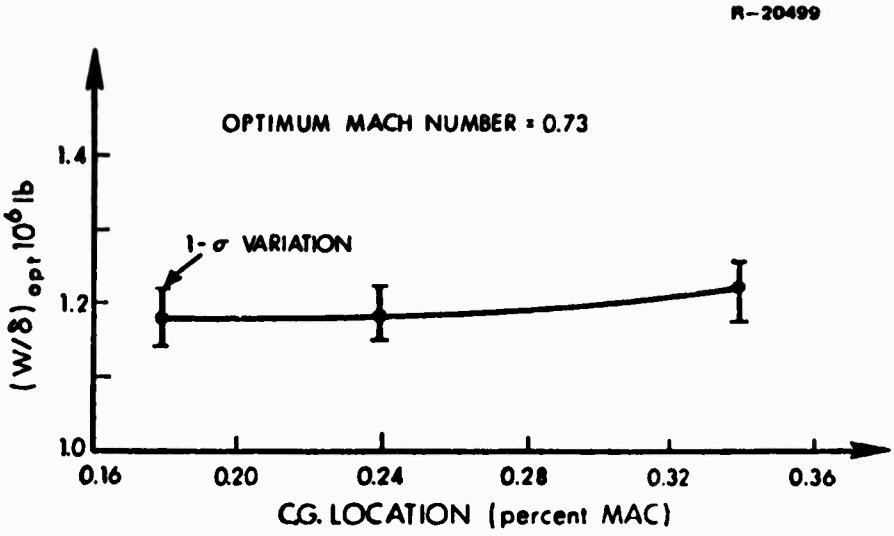

Figure 11 Effects of c.g. Location on Optimal Cruise Parameter, $(W/\delta)_{opt}$

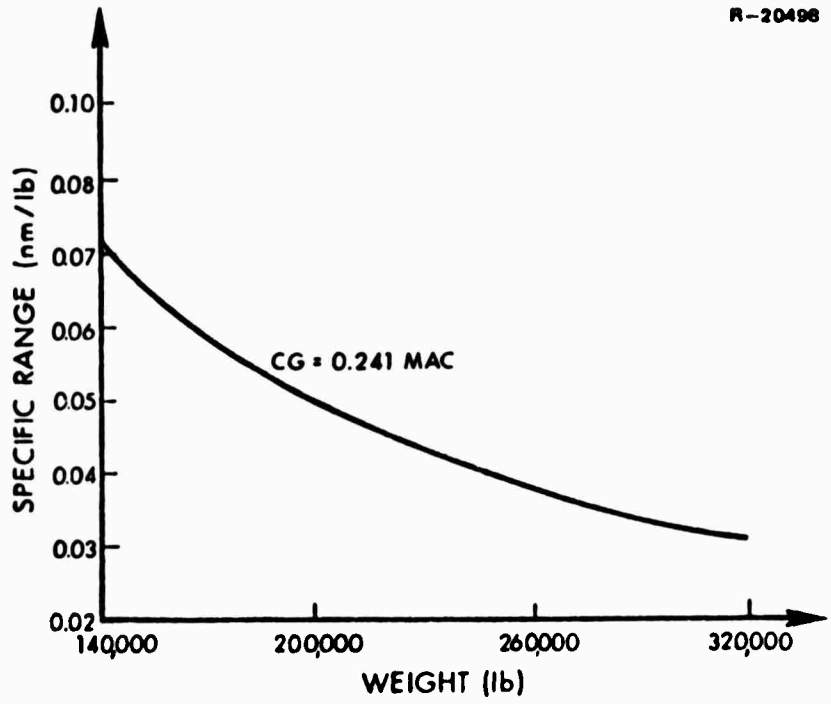

Figure 12 Maximum Specific Range -- Nominal c.g. Location

derived from the aerodynamic model which incorporates the trim lift/drag effects. Changes in these values of specific range with variation in c.g. location are shown in Fig. 13. These percentage deviations from the nominal values are independent of aircraft weight. Also, the percentage variations in specific range are seen to be linear with c.g. location shifts. The maximum deviation in specific range, as the center of gravity moves from the forward to aft location, is about 5.7 percent.

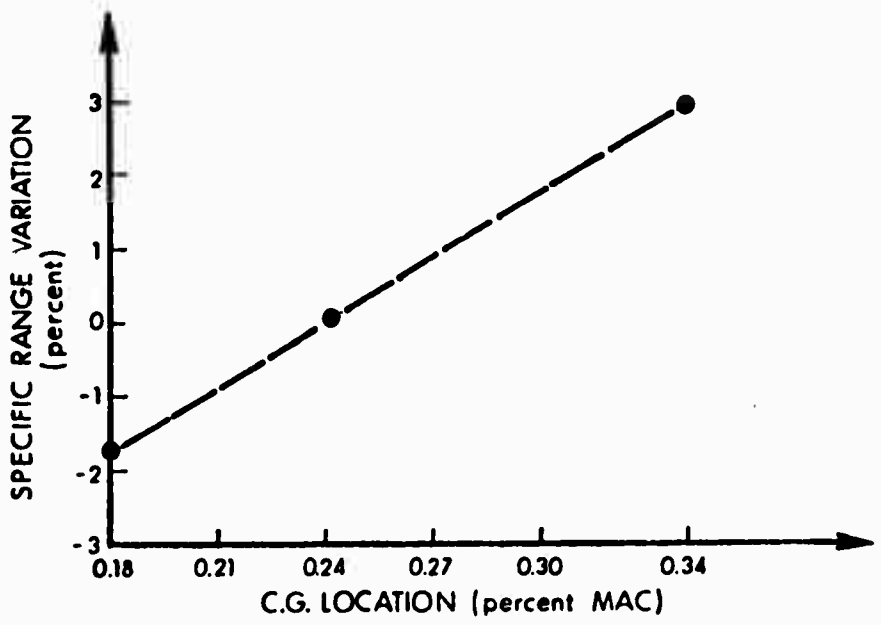

Figure 13 Effects of c.g. Location on Specific Range

4.2.3 Aircraft Drag Coefficient Effects

The major emphasis of this study is concentrated on trajectory profile shaping to minimize fuel consumption. Aircraft configuration alterations also could reduce fuel use. In particular, reduced aircraft drag serves to increase the vehicle's specific range. Each aircraft in the C-141A fleet has values of C_D which, in all probability, are not

exactly equal to the model values of this study. The effects of these individual drag variations on fuel performance can be determined from the following results.

As part of the proposed C-141A fleet "stretching" operations, aircraft modifications also would be undertaken to reduce total drag. Current projections suggest a drag reduction of up to 6 percent for the stretched version, the C-141B (Ref. 53). The effects of ± 10 percent variations in C_D on the cruise-phase specific range determined in this section can be used, therefore, to estimate the improvement in performance associated with the stretching modifications.

As vehicle drag is reduced, the engine thrust required for cruising flight is lowered by an equivalent amount. Because fuel consumption is monotonically increasing with thrust (see Fig. B-1), this in turn lowers the aircraft's fuel consumption rate. The cruising flight parameters, W/δ and Mach number, are presented in Table 1 as functions of C_D variations.* The optimum Mach number change for ± 10 percent drag variations is small (presumably because the transonic drag-rise Mach number is not changed significantly by uniform changes in C_D). However, the values of W/δ for optimum specific range indicate a definite decrease with increasing C_D. Thus, as drag increases, the cruising altitudes associated with maximum specific range are lowered. Conversely, as C_D is improved, maximum specific range is achieved by flying at higher altitudes.

*Percentage variations in C_D correspond directly to percentage variations in thrust (at a fixed fuel flow rate) of opposite sign.

TABLE 1

OPTIMUM CRUISE PARAMETERS VS.
AIRCRAFT DRAG COEFFICIENT (C_D)

C_D Variations	$(W/\delta)_{opt}$	$(\text{Mach Number})_{opt}$
-10 percent C_D	1.28×10^6 lb	0.74
Nominal	1.19×10^6 lb	0.73
+10 percent C_D	1.10×10^6 lb	0.72

The changes in fuel performance caused by drag variations are presented in terms of the aircraft's maximum specific range, Fig. 14. A reduction in drag of 10 percent produces an increase in specific range of approximately 10 percent for all vehicle weights. Increases in C_D demonstrate corresponding decreases in fuel economy. The predicted 6 percent reduction in the value of C_D for the stretched C-141B would, therefore, significantly improve the vehicle's fuel efficiency.

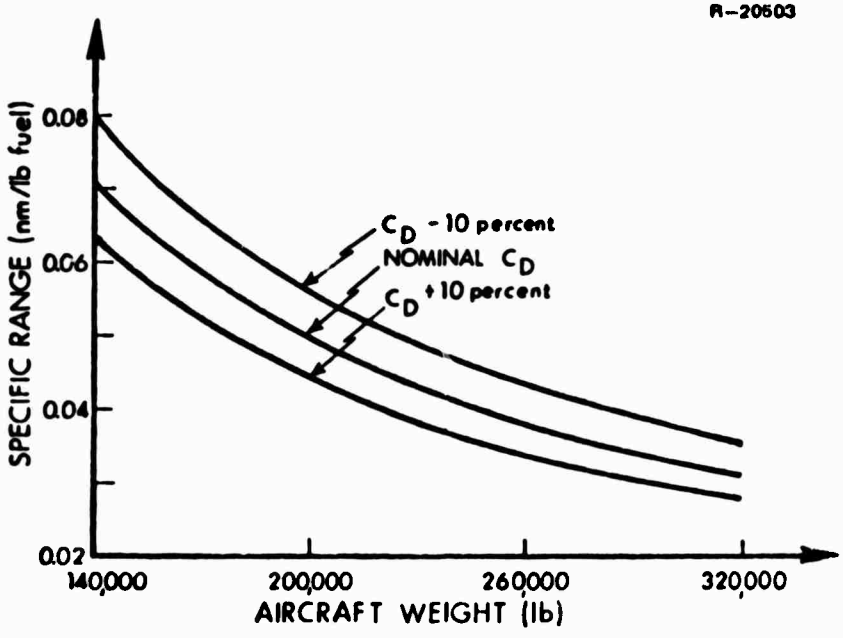

Figure 14 Specific Range as a Function of C_D Variation

4.2.4 Atmospheric Effects

In this section, the effects of variations in atmospheric conditions on fuel-optimal cruising flight are described. The atmospheric variations which are of interest here are the deviations in temperature (from the 1962 Standard Atmosphere Model) and non-zero wind velocities. It is reasonable for these parameters to change over the course of a single mission; by accounting for known variations, fuel-optimality can be assured along the cruise profile. The effects of temperature variations on cruise are found to be small compared to the vehicle configuration effects discussed in the previous sections. Table 2 presents the optimal cruise parameters associated with atmospheric temperature variations of $\pm 20^{o}F$. The effect of these variations on fuel performance (specific range) also is shown here. The optimal cruise altitudes, as defined by the parameter, W/δ, change insignificantly with temperature variations, while the "best" Mach number decreases with increasing temperature. The resultant variation in maximum specific range caused by the temperature variations is on the order of only 1 percent.

TABLE 2
EFFECTS OF TEMPERATURE DEVIATIONS ON CRUISE PARAMETERS

Temperature Variations (^{o}F)	$(W/\delta)_{opt}$ (lb)	$(\text{Mach Number})_{opt}$	Specific Range Variation (percent)
-20	1.18×10^{6}	0.74	+0.81
Nominal	1.19×10^{6}	0.73	–
+20	1.19×10^{6}	0.72	-1.02

Atmospheric winds, on the other hand, have a large effect on optimal cruise conditions. In this study, wind

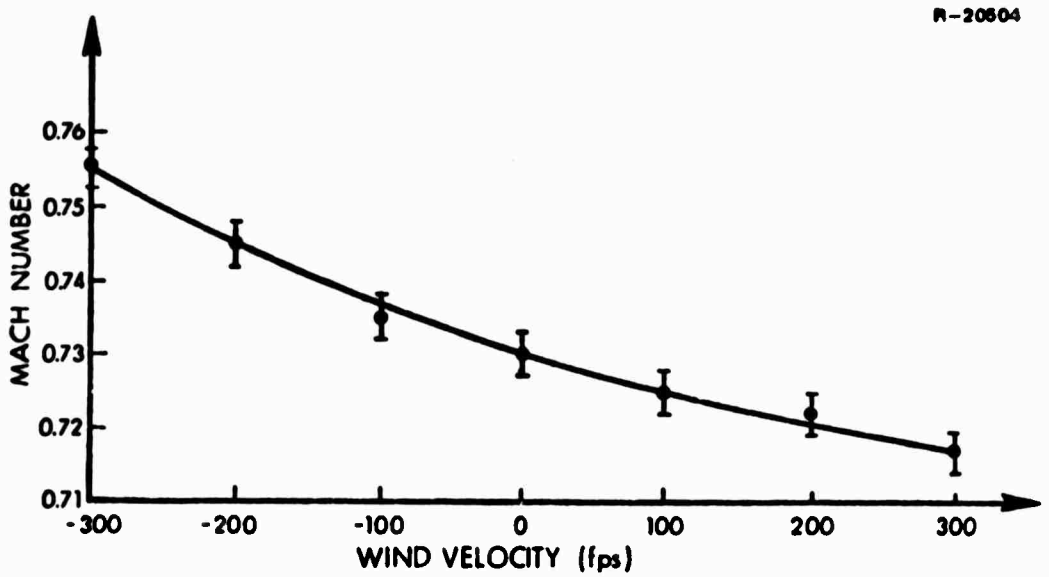

Figure 15 Optimal Cruise Mach Number vs. Wind Velocity

values of -300 fps (head wind) to +300 fps (tail wind) are examined. Optimal cruise-phase Mach numbers are presented as a function of wind velocity in Fig. 15. For a head wind, the best cruise Mach number increases from its nominal value of 0.73. With a tail wind, the desired Mach number is reduced, but the optimal value of (W/δ) for all wind velocities remains constant at a value of about 1.19×10^6 lb.

The observed optimal Mach number trends with wind variation can be explained as follows. In a tail wind environment, vehicle ground-relative speed increases if Mach number is not changed. Therefore, a reduction in Mach number to reduce fuel flow rate can be accomplished while still maintaining good ground speed. In a head wind case, ground speed is reduced. Mach number is increased in this situation, in order that the total fuel consumption for the flight is minimized.

Figure 16 presents the maximum values of specific range for the C-141A aircraft for several wind environments. Specific range curves for wind speeds between -300 and +300 fps are plotted for wind speed increments of 100 fps. In the maximum wind speed variation cases, the specific range variations are as large as 40 percent. Because the variations are this large, it would be reasonable (in some situations) to increase trajectory path length in order to maximize tail winds and minimize head winds along the flight path. Trade-offs would have to be performed to insure that the fuel reductions afforded by increasing specific range are not offset by the increase in fuel needed to fly the longer path length. In all cases, however, the cruise profile should be flown at optimal values of the cruise parameters to provide the maximum specific range for the wind conditions encountered.

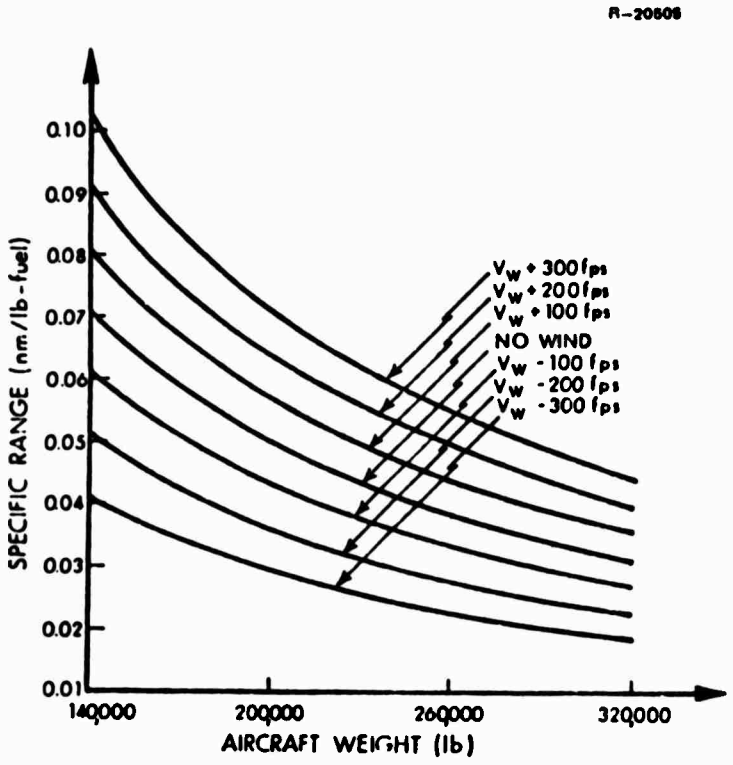

Figure 16 Specific Range as a Function of Wind Velocity

4.3 CLIMB PROFILES

During the climbing segment of flight, the aircraft's altitude and Mach number are changed from their takeoff values to the values which define the initiation of the cruise phase. Thus, the vehicle's total energy (kinetic plus potential) is greatly increased in this flight mode. In this section, flight profiles which minimize the fuel used to accomplish these energy changes are determined.

The conditions defining the end of the climb segment are obtained from the optimal cruise parameters described in Section 4.2.1. When these cruise conditions (W/δ and Mach number) are met, the aircraft profile switches from the climb to the cruise phase. In this study, the aircraft altitude at the beginning of climb is chosen to be 2,000 ft, and the initial velocity is 340 fps true airspeed. At the 2,000-ft initial altitude, this corresponds to a value of 195 KIAS. These conditions are similar to those of Ref. 32, for a vehicle which has completed takeoff and has fully retracted the flaps. Thus, the climb profiles simulated in this study assume a clean vehicle configuration and well-defined initial and terminal cruise conditions.

A conventional C-141A climb profile is described in Section 4.3.1. Optimal (minimum-fuel) climb segments for a range of initial vehicle weights are presented in Section 4.3.2. The utility of flying minimum-fuel climb modes also is demonstrated in Chapter 5, where complete trajectory climb, cruise, and descent fuel consumption is discussed.

4.3.1 Conventional Profiles

The conventional C-141A climb profiles simulated in this study closely approximate the handbook schedules documented in Ref. 32. The climb profiles consist of two constant-IAS modes followed by a climb at constant Mach number. The values of climb IAS and Mach number, as well as the mode switching points, are summarized in Table 3. All the climb modes are flown with throttle set for normal rated thrust (NRT). This corresponds to full throttle setting in this study.

TABLE 3
CLIMB SCHEDULE FOR CONVENTIONAL PROFILES

Mode Condition	Mode Termination Point	Throttle Setting
1. IAS = 250 kt	h = 10,000 ft	1.0 (NRT)
2. IAS = 280 kt	Mach Number = 0.720	1.0
3. Mach Number = 0.720	$W/\delta = 1.24 \times 10^6$ lb	1.0

A plot of altitude vs. range for a conventional climb is presented in Fig. 17. The profile is generated for a C-141A vehicle with an initial weight (at 2,000-ft altitude) of 260,000 lb. The climb trajectory has a path length of 228 nm and consumes 10,691 lb of fuel. During the constant-IAS climb modes, the aircraft's altitude rate decreases from 3,000 to 750 ft/min. Altitude rate during the constant-Mach number phase is on the order of 1,000 ft/min.

The climb profile is shown to change slope at the switch point between the constant-IAS and constant-Mach number modes. This change in slope at the IAS/Mach number switch point also is found to occur in the fuel-optimal climb profiles described in the following section.

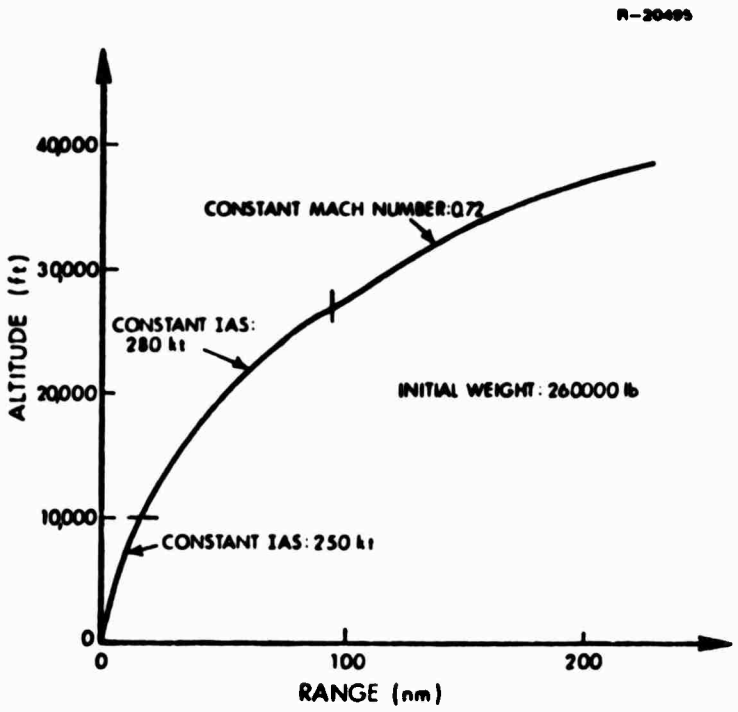

Figure 17 Conventional Climb Profile

4.3.2 Optimal Profiles

Conventional climb profiles are defined in terms of constant-IAS and constant-Mach number modes, in order to ease the task of piloting the aircraft. In the present study of fuel-minimal climbs, these same flight modes are preserved, so that flying a fuel-efficient climb will be no more difficult than following a conventionally defined profile.

The parameteric optimization techniques described in Section 3.5 have been employed for improving fuel consumption during climb. Rather than using two constant-IAS climb modes, only one constant-IAS mode followed by a constant-Mach number mode is presumed for the generation of optimal climb profiles. This enables the use of two-parameter parametric

optimization methods to determine fuel-minimal climbs. The parameters which are to be optimized are the constant values of IAS and Mach number to be flown during climb.

Parametric-optimal climb profiles have been generated for C-141A aircraft with initial weights of 200,000, 260,000, and 320,000 lb. The "best" values of airspeed and Mach number, as a function of these initial aircraft weights, are presented in Fig. 18a. A Mach number of 0.721 provides fuel-minimum climbs for all the trajectories simulated. Best indicated airspeed increases, however, with increasing initial weight. For an initial weight of 200,000 lb, the "best" constant value of airspeed is 191 kt. This value increases to 245 kt for a 320,000-lb vehicle. Also shown on the figure are the altitudes at which the switch from constant-IAS to constant-Mach number is performed.

Although the heavy aircraft terminates the climb phase at a lower altitude than does a lighter weight vehicle, it consumes more fuel in the climb segment. This is demonstrated by the plot of climb-phase fuel consumption vs. initial vehicle weight of Fig. 18b.

Altitude-vs.-range profiles for the three optimal climb trajectories are presented in Fig. 19. It is seen here that as initial aircraft weight increases, both the total climb range and the portion of flight spent in the constant-Mach number mode increase. However, the general profile shapes are similar to the conventional profile pictured in Fig. 17.

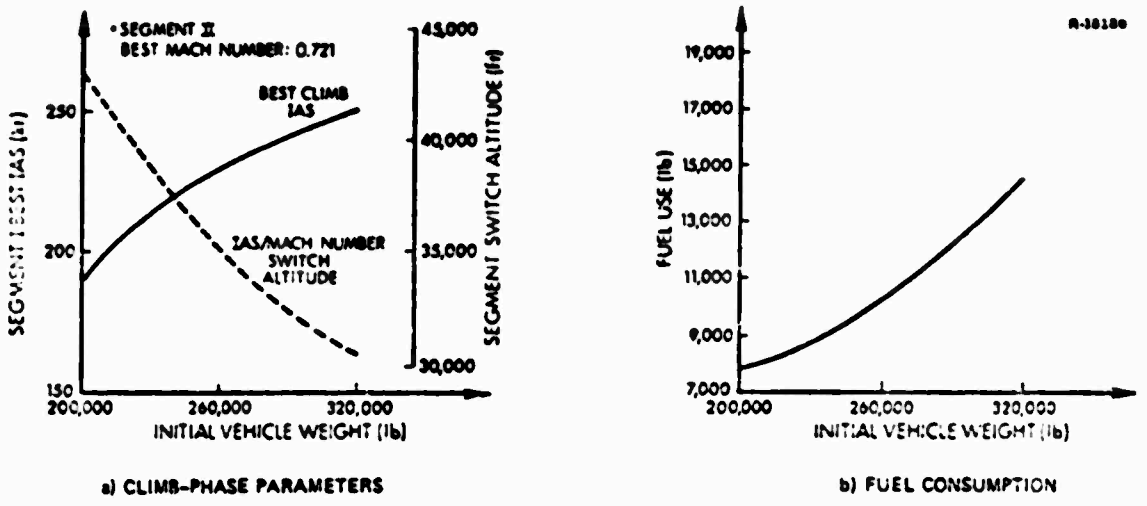

Figure 18 Optimal Climb Conditions

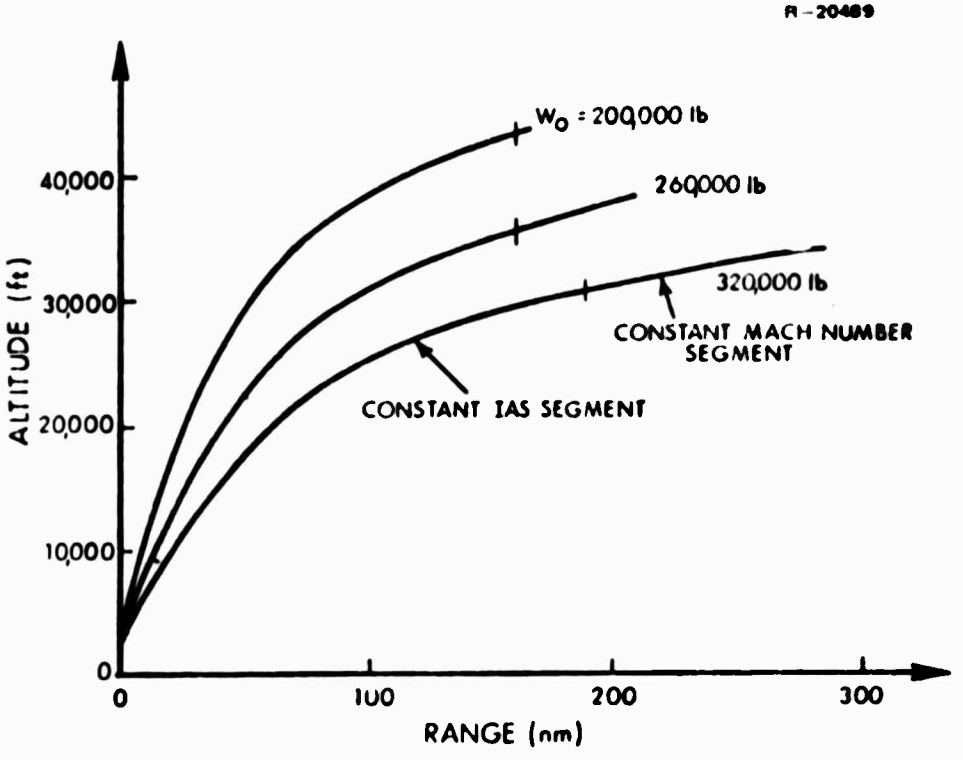

Figure 19 Parametric-Optimum Climb Profiles

The optimal climb profile for the 260,000-lb aircraft traverses a range of 211 nm during climb and consumes 10,277 lb of fuel. This is 414 lb less than the fuel needed for the conventional climb schedule. However, the conventional profile travels 17 nm further in the climb segment. Thus, the specific range (nm traveled/lb fuel consumed) is nearly identical for the fuel-optimal and conventional trajectories. The major advantage of fuel-optimal climbs is demonstrated by the short-range trajectories where the fuel minimal profiles do not contain a cruise phase. The fuel savings afforded by optimal-climb profiles for these trajectories are discussed in detail in Section 5.2.

4.4 DESCENT PROFILES

The results of the fuel-minimum cruise phase analyses, Section 4.2, demonstrate that the best C-141A cruising altitudes are typically greater than 30,000 ft. The descent flight segment serves to reduce altitude from the cruise levels to a value at which the landing phase can be initiated. In this study, the altitude at which the descent phase terminates is chosen to be 2,000 ft above sea level. This is the same value of altitude that has been used to initiate the climb phase analyses. The three fuel-optimal trajectory segments--climb, cruise, and descent--can be pieced together, therefore, to provide complete trajectories which begin and end at a 2,000-ft altitude.

As in the case of the C-141A climb profiles, both conventional and fuel-optimal descent profiles are examined in this section. The fuel-optimal descent profiles are shown to have longer flight path ranges than their conventional counterparts. This extra descent range reduces

the duration of the cruise segment for a given mission, and results in a lower value of net fuel consumption. A description of the conventional descent profiles is given in Section 4.4.1, and the fuel-optimal descents are reviewed in Section 4.4.2.

4.4.1 Conventional Profiles

The conventional C-141A descent profiles simulated in this study are representative of the "Enroute Descent" schedules of Ref. 32; however, the descents simulated here employ zero thrust (idle) throttle settings. Actual C-141A descents are typically flown with positive throttle settings, and pilots frequently increase Mach number on descent in order to begin the scheduled constant-IAS mode more quickly. Thus, the simulated conventional descents, by which the fuel-optimal profiles of this study are judged, are themselves optimistic.

The descent profiles each consist of a constant-Mach number mode followed by two constant-IAS modes. Thus, the descent schedule contains the same modes as the climb schedule, but they are flown in reverse order for descent. The values of IAS and Mach number flown on the conventional descent schedule are presented in Table 4.4-1. Also included in the table are the mode switching points and the descent phase throttle settings.

TABLE 4

DESCENT SCHEDULE FOR CONVENTIONAL PROFILES

Mode Condition	Mode Termination Point	Throttle Setting
1. Mach Number = 0.725	Mach Number $\leq$ 0.725	0 (Idle)
2. IAS = 300 kt	h = 10,000 ft	0
3. IAS = 250 kt	h = 2,000 ft	0

During descent, the throttle is set to the idle position, providing zero thrust. This does not imply, however, that fuel flow is also zero, as a certain amount of fuel is required just to keep the powerplants operating. The fact that fuel flow rate is not zero at idle throttle setting is demonstrated by the fuel flow-vs.-thrust curves of Fig. B-1. At the zero-thrust level, the fuel flow curves demonstrate positive values of flow rate which increase with increasing Mach number.

A plot of altitude vs. range for a conventional descent is presented in Fig. 20. The profile represents a simulated descent for a C-141A vehicle cruising at Mach 0.740 at an altitude of 35,000 ft. At the initiation of the descent, the aircraft weight is 232,537 lb, and the descent path length is approximately 95 nm. Descent rate during the constant-Mach number phase reaches a maximum value of about 4,000 ft/min and reduces to approximately 1,500 ft/min during the constant-IAS modes.

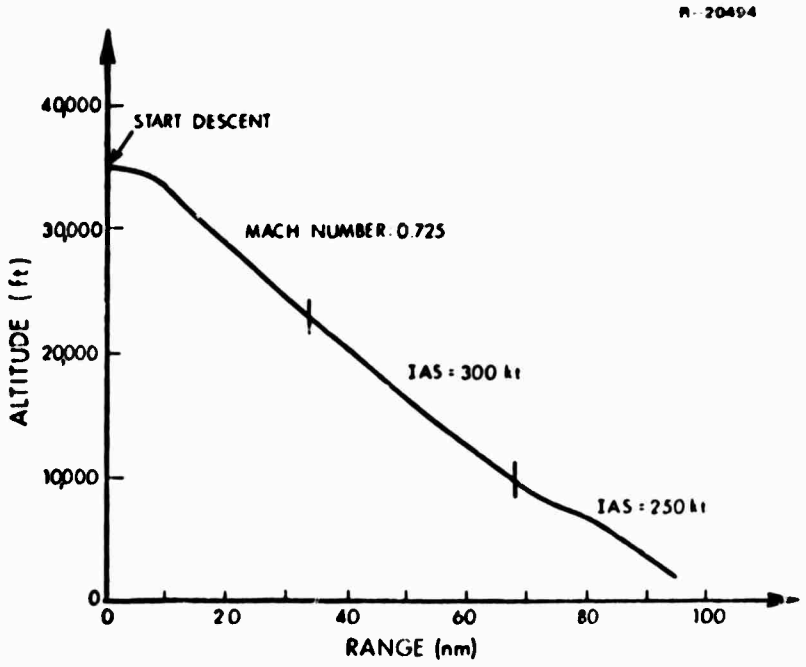

Figure 20 Conventional Descent Profile

Time of flight and fuel consumption values for this descent are shown in Fig. 21. These variables are plotted as functions of initial altitude on the descent profile. For example, at an altitude of 20,000 ft, approximately 9.5 min of flight time and 800 lb of fuel will be expended along the remainder of the descent profile. The larger increase in flight time for altitudes above 33,000 ft occurs on this profile because of the transition between the cruise and descent segments of flight. This transition period is also discernable on the altitude profile of Fig. 20. The transition between cruise and descent spans the first 10 nm of the descent profile and contributes an altitude decrease of about 2,000 ft.

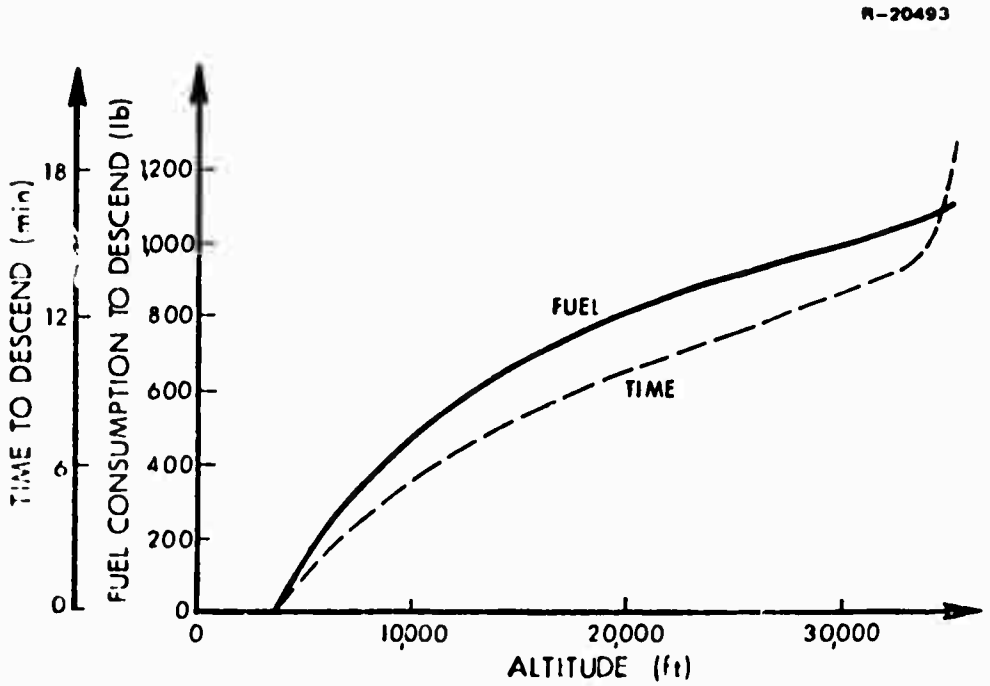

Figure 21 Conventional-Descent Fuel Consumption and Flight Time

Although most of the performance results concerning complete trajectory profiles are discussed in Chapter 5, the effects of using non-zero throttle setting during descent on total fuel consumption are presented here. Total fuel consumption for four different 1,000-nm missions are shown in Table 5. (Initial weight of the vehicle is 260,000 lb.) The missions are classified according to the constant altitude and constant Mach number flown during the cruise flight segment. The two columns of fuel consumption data correspond to flying each mission with either idle throttle or 20-percent throttle setting during descent. For both types of descent, the Mach number and indicated airspeed profiles flown are those of Table 3.

TABLE 5

MISSION FUEL CONSUMPTION FOR 1,000-NM FLIGHT PATHS WITH IDLE AND 20-PERCENT THROTTLE SETTING DESCENTS*

Cruise Conditions		Fuel Consumption (lb)	
Altitude (ft)	Mach Number	Idle Throttle	20-percent Throttle
31,000	0.740	30,032	30,956
35,000	0.740	28,452	29,520
31,000	0.767	31,199	32,022
35,000	0.767	29,233	30,237

Use of 20-percent throttle setting on the descent profiles causes an increase in fuel consumption of about 800 to 1,100 lb for these 1,000-nm missions. Thus, scheduling of idle throttle on descent does tend to reduce overall fuel

*The climb and cruise profiles are identical, however, the idle descents begin later in the flight than do the 20 percent throttle descents.

consumption on conventional trajectories. In the following section, it is demonstrated that idle throttle setting also is a characteristic of the fuel-optimal descent profiles. These results also suggest that the "conventional" profiles using idle-throttle descents, which are compared with optimal profiles in the next chapter, actually are optimistic.

4.4.2 Optimal Profiles

If fuel flow rate at idle throttle setting were zero, an optimal descent profile would be one which maximizes gliding path length. By providing maximum range during descent, the duration of the cruise phase of flight would be reduced, resulting in a minimum value of fuel consumption for the complete mission. Although fuel use is not zero at idle throttle, it is substantially lower than the values experienced for typical cruising flight. For this reason, the investigation of near-optimal descent profiles described in this section concentrates on determining maximum path-length, idle-throttle descents.

It is well known that maximum path length of a gliding aircraft is achieved by flying at the vehicle's maximum value of lift-to-drag ratio (L/D). At idle throttle, the net thrust of the C-141A is zero, so the aircraft is, in effect, flying as a glider. The problem of determining near-optimal descent profiles is to find the maximum L/D gliding flight path.

The conventional descent profiles described in Section 4.4.1 are not difficult for a pilot to fly because they are defined in terms of constant-Mach number and constant-IAS modes. Near-maximum L/D descent profiles for the C-141A can be achieved by maintaining a constant aircraft

pitch angle (θ). For the C-141A aircraft modeled in this study, a pitch angle of 0.935 degrees provides a near-maximum average value of L/D, equal to about 19.5 along the descent profiles. The validity of the assumptions (small fuel flow rate at idle throttle setting and near-maximum L/D at constant pitch angle) is demonstrated in Chapter 5 of this report. It is shown that the descent portion of the fully optimal trajectory profiles, as determined by complex variational optimization methods, is nearly identical to the simple near-optimal profiles described here.

The increased glide range afforded by the constant-θ, maximum-L/D descent schedule over the conventional descent schedule is demonstrated by Fig. 22. Both descent profiles are initiated at an altitude of about 40,000 ft with an initial vehicle weight of approximately 234,000 lb. The optimal descent traverses a path length of 143 nm, while the

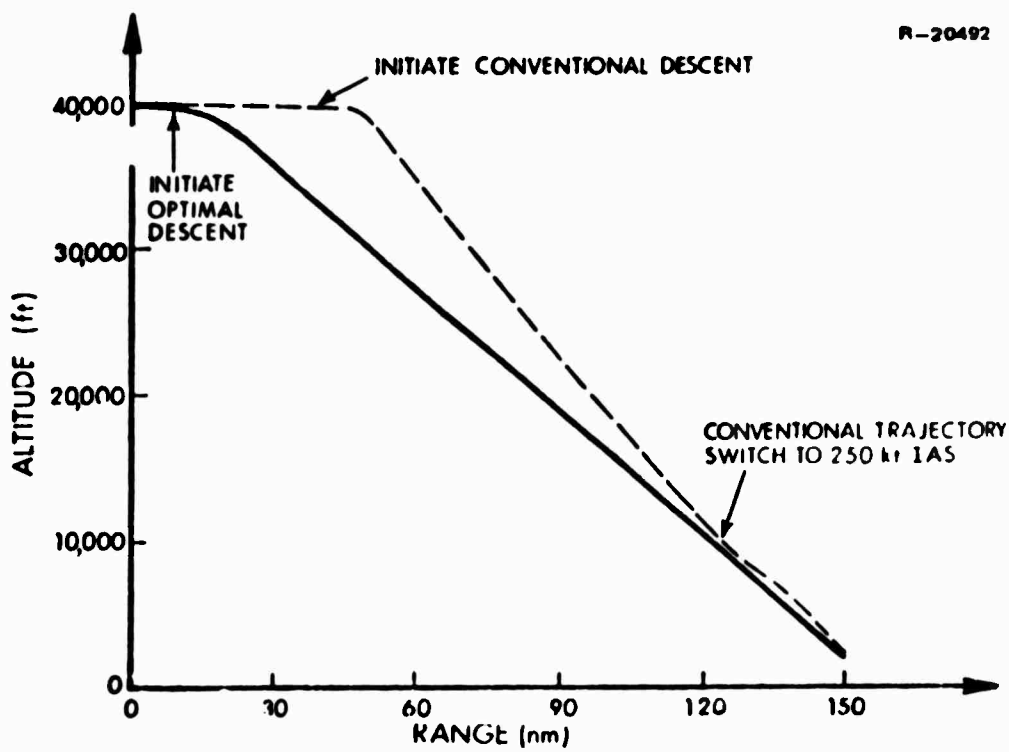

Figure 22 Comparison of Optimal and Conventional Descent Profiles

conventional descent flies only 108 nm. Thus, the trajectory which incorporates a conventional descent must fly 35 nm longer in the cruise phase.

The fuel consumption for the 150-nm profiles plotted is 1,552 lb for the optimal descent and 2,161 lb for the conventional descent. For a 1,000-nm mission with a typical total fuel requirement of 30,000 lb, this descent profile's savings of 609 lb represents a net reduction in total fuel use of about 2 percent. Thus, flying optimal descent profiles is an excellent means of reducing fuel consumption for the C-141A fleet.

4.5 CHAPTER SUMMARY

In this chapter, fuel consumption along the three major flight path segments -- climb, cruise, and descent -- has been examined. By applying the optimization techniques described in Chapter 3, minimum-fuel profile shapes are determined for these flight segments. These fuel-minimal profiles are shown to provide significant fuel-use reductions compared to currently flown, conventional flight paths.

The fuel-optimal cruise profile is found to be characterized by constant values of Mach number and W/δ (weight over atmospheric pressure ratio). As fuel is burned, aircraft weight decreases, and altitude must be increased to maintain constant W/δ. For this reason, the optimal cruise trajectories slowly climb along the mission profiles.

The effects of off-nominal vehicle and atmospheric conditions on the optimal cruise profiles also are presented in this chapter. The changes in fuel efficiency are

indicated by the specific range (nm/lb fuel) associated with the cruise profiles. As the center of gravity of the aircraft is moved aft, the cruise-phase specific range increases; however, the optimal values of Mach number and W/δ are insensitive to these c.g. location shifts.

Head winds are found to decrease specific range while increasing optimal cruise Mach number, and the opposite effects are true of tail winds; however, wind variations have no effect on the best value of W/δ. Atmospheric temperature variations have only a small effect on cruising specific range. Temperature variations of $\pm 20^{o}F$ cause a 2 percent change in the aircraft's specific range.

Decreases in aircraft drag coefficient, C_D, are shown to increase both the cruise specific range and the optimal value of W/δ. The opposite effects result for increasing values of drag coefficient.

The examination of fuel-minimal climb profiles consists of determining the best values of indicated air speed (IAS) and Mach number to fly during climb. The results of this analysis indicate that the optimal climb Mach number, 0.721, is the same for all vehicle weights. The best IAS varies, however, as a function of vehicle weight from 191 kt for a 200,000-lb aircraft to 245 kt for a 320,000-lb aircraft. The fuel consumed during the climb also increases substantially with increasing vehicle weight.

The optimal descent profiles generated in this chapter are based upon flying near-maximum L/D glides. It is shown that these fuel-efficient gliding descents can be achieved with idle throttle setting and constant aircraft pitch angle. For a typical descent from 40,000 ft to 2,000 ft,

the optimal descent profile provides a fuel consumption value 609 lb less than that obtained by flying a conventional enroute descent.

The optimal flight segments defined in this chapter can be utilized individually to provide some reduction in overall fuel consumption or they can be pieced together to provide near-optimal integrated trajectory profiles. The efficiency of these near-optimal profiles as compared to fully optimal complete flight paths is determined in the following chapter.

V. COMPARISON OF OPTIMAL AND CONVENTIONAL INTEGRATED FLIGHT PATHS

5.1 OVERVIEW

The results presented in Chapter 4 demonstrate the potential for reducing aircraft fuel consumption on individual flight segments. By simply piecing optimized flight segments (climb, cruise, and descent) together, trajectory profiles which are more fuel-efficient than current handbook profiles can be generated. There is no guarantee, however, that the resulting piecewise-optimal trajectories will be fully optimal.

Fuel consumption comparisons for conventional (handbook defined), piecewise-optimal, and fully-optimal C-141A flight profiles are presented in this section. For convenience, the trajectories are categorized according to path length: short range (0-500 nm), medium range (500-2,000 nm) and long range (2,000-5,600 nm). These trajectories are presented as Sections 5.2, 5.3, and 5.4, respectively. The comparisons in all categories demonstrate that the piecewise-optimal trajectories provide fuel consumption values which are very nearly fuel-optimal. Piecewise-optimal trajectories tend to use one to two percent more fuel than do the fully optimal flight paths. The conventional trajectory fuel usage is approximately 10 to 20 percent greater than the optimum values. These percentages vary as a function of total trajectory length and handbook cruise conditions (altitude and Mach number).

In addition to the fuel consumed, the duration, in hours, is recorded for all trajectories. The current optimization efforts are directed toward reducing total fuel usage, not total cost in dollars. The actual costs associated with each profile, are tabulated assuming a fuel cost of 45¢/gallon and a time-related cost of $400/hr. In addition, a range of fuel and time costs is considered. With this choice of numbers, some of the conventional trajectories which appear to consume excessive amounts of fuel provide for total dollar costs which are not significantly different from the fuel-minimum profiles. As fuel costs appear to be increasing more rapidly than personnel and other time-related expenses, trajectory fuel-optimality is becoming increasingly significant. The computer tools and optimization techniques employed for fuel minimization (see Chapter 3 and Appendix A) can easily handle the "dollar-optimization" problem. The means by which this can be done and the present fuel-time tradeoffs are discussed in Section 5.5. A summary of the chapter is presented in Section 5.6.

5.2 SHORT-RANGE FLIGHT PATHS

In the current study, flight profiles with ranges of 500 nm or less are considered to be "short-range." These short-range profiles are characterized by the fact that the optimal trajectories contain only little or no cruise segment. Almost all fuel-use reduction for these trajectories is achieved during the climb and descent flight modes.

The parametric-optimum altitude-vs.-range profile for a 200-nm trajectory is presented in Fig. 23a.

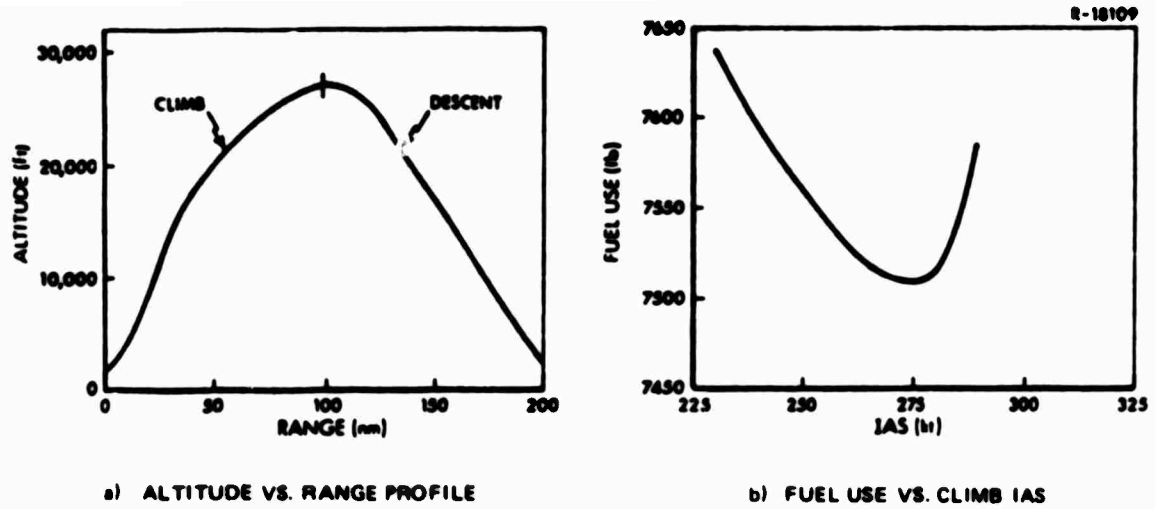

a) ALTITUDE VS. RANGE PROFILE

b) FUEL USE VS. CLIMB IAS

Figure 23 Minimum-Fuel 200-nm Trajectories

The initial aircraft weight is 260,000 lb, and the trajectory begins and ends at an altitude of 2,000 ft. Not only does the profile contain no cruise segment, but the constant-Mach number phase of the parametric-optimum climb segment (see Section 4.3.2) also is absent. Because the trajectory shape is different, the constant-IAS climb profiles for the short-range case may be different from the values obtained by optimizing the climb segment alone.

In order to determine the parametric-optimum 200-nm range profile, fuel use vs. indicated air speed (IAS) during climb is determined. Fuel use as a function of climb IAS for this short-range case is plotted in Fig. 23b. The minimum total fuel use, 7,515 lb, is obtained with a climb speed of 279 kt.

The utility of parametric optimization techniques for determining minimum-fuel trajectories is demonstrated by the comparison of fuel consumption for conventional, parametric-optimal, and fully optimal (steepest-descent)

technique) profiles. The short-range conventional profile is characterized by handbook climb and descent schedules and a one-third path-length constant-altitude cruise (h = 23,000 ft). Fuel consumptions for the three trajectories are presented in Table 6. The parametric results are within 1.3 percent of the steepest-descent defined optimal, while the conventional profile uses 12.5 percent more fuel.

TABLE 6

FUEL CONSUMPTION FOR 200-NM TRAJECTORIES

Trajectory	Fuel Use (Lb)	Percent Over Minimum
Steepest Descent Optimum	7,420	-
Parametric Optimum	7,515	1.3
Conventional (1/3 Level Flight)	8,347	12.5

Throttle-vs.-range and throttle-vs.-altitude profiles for the three 200-nm trajectory types are plotted in Figs. 24a and 24b, respectively. The steepest-descent throttle profile starts to throttle-down from maximum at the 25-nm range point. Thus, this reduction occurs during the climb segment of the trajectory. The initial conventional profile throttle reduction occurs, however, at the initiation of the cruise flight mode. By reducing throttle setting during climb, the steepest-descent profile burns less fuel than does the parametric trajectory.

Both the parametric and steepest-descent optimal trajectories reduce throttle setting to idle at a range of

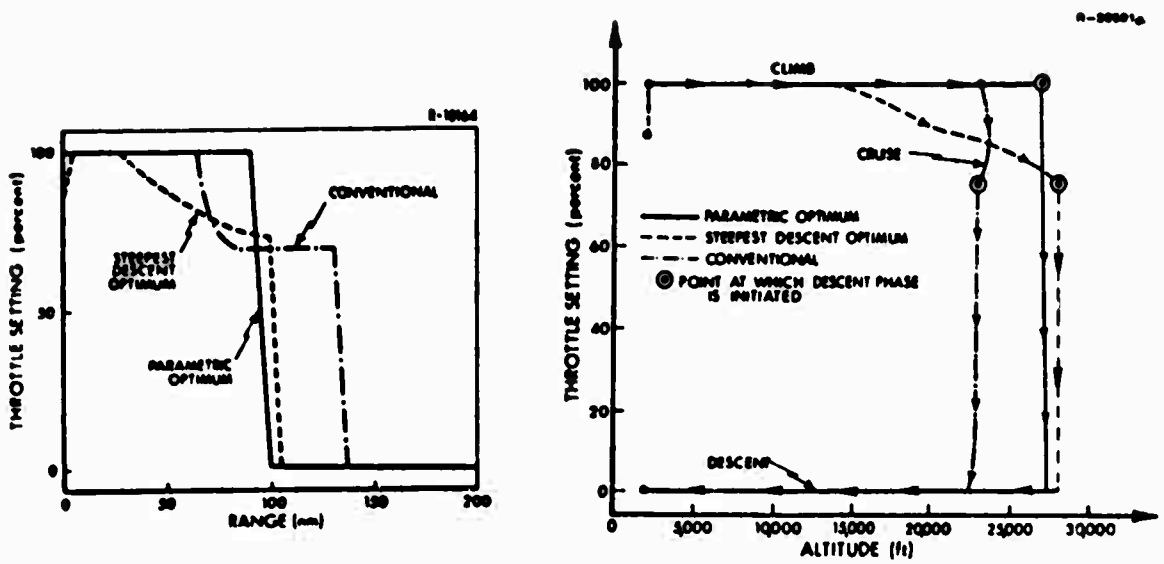

a) a) THROTTLE VS. RANGE

b) THROTTLE VS. ALTITUDE

Figure 24 Short-Range-Trajectory Throttle Profiles

approximately 100 nm. The conventional trajectory does not employ idle throttle until about 135 nm have been traversed. By following a near maximum L/D descent schedule, the optimal trajectories have a greater glide range, which contributes to their lower fuel usage. Although the steepest-descent profile provides a 1.3 percent fuel savings over the parametric trajectory, the on/off nature of the parametric throttle setting may be simpler for a pilot to fly. On the other hand, the reduced-throttle climb of the steepest-descent optimum may be advantageous from the standpoint of minimizing engine maintenance costs. In either case, the throttle profile should be accompanied by the proper altitude-Mach number profile, shown in the following figure.

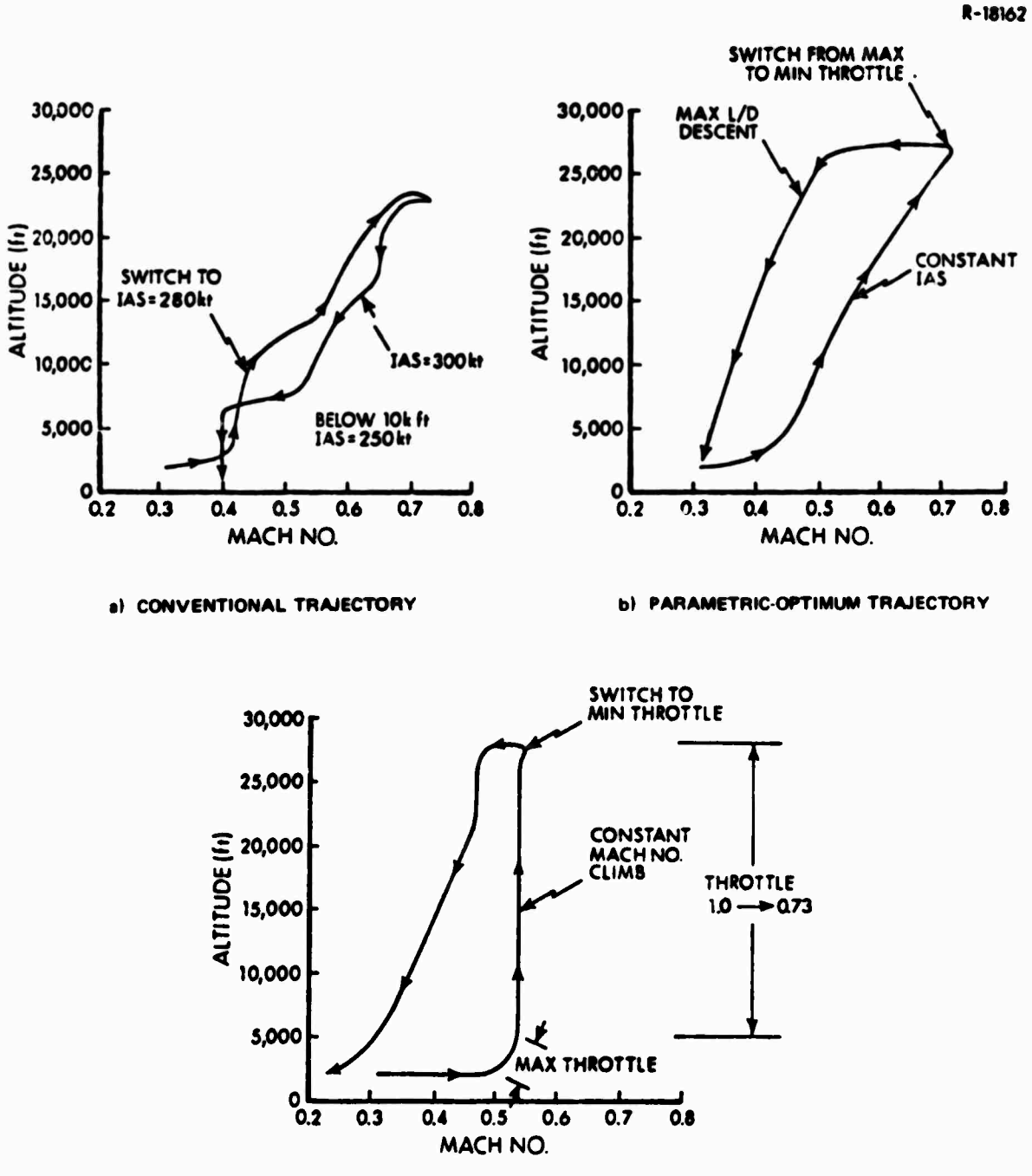

Figure 25 200-nm Altitude vs. Mach Number Profiles

The altitude-vs.-Mach number profile of the conventional trajectory, Fig. 25a, is not as smooth as those of the optimal profiles. The "bumps" in the profile are due to the numerous changes in IAS and Mach number which define the handbook climb and descent schedules. The parametric profile, Fig. 25b, follows the constant 279-KIAS climb and the maximum L/D descent segments. The fully optimal trajectory, Fig. 25c, contains a constant-Mach number climb and a near-maximum L/D descent similar to that of the parametric profile. Although the two optimal climb profiles appear to be quite different, the resultant effects on fuel reduction are not that dissimilar.

The effectiveness of parametric optimization in determining fuel-minimum flight profiles also is evident from the 500-nm, 260,000-lb vehicle, trajectory analyses. Fuel consumption values for this path length, as determined by parametric and variational optimization methods, are shown in Table 7. In this case, the parametric optimum provides for fuel consumption within 1.1 percent of the true minimum. This parametrically defined flight path consists of segments (constant-IAS climb, constant-Mach number climb, constant-altitude cruise, and constant-pitch angle descent) which can be <u>easily</u> flown or monitored by the pilot of the aircraft. Thus, the parametric optimal path embodies both fuel-optimality and ease of flying characteristics.

TABLE 7

FUEL CONSUMPTION FOR 500-NM TRAJECTORIES

Trajectory	Fuel Use (Lb)	Percent Over Minimum
Parametric Optimum	15,418	1.1
Steepest-Descent Optimum	15,248	-

The effects of increasing range on optimal flight paths are demonstrated in Fig. 26. Here, altitude-vs.-Mach number profiles for the 200-nm and the 500-nm fully optimal (steepest-descent) trajectories are compared. Although 500 nm is classified as a short trajectory range, this profile demonstrates the same characteristics as longer range, fully optimal profiles. The climb schedule consists of a nearly constant-IAS path followed by a constant-Mach number phase. Again, the descent profile is flown with the vehicle near its maximum value of lift-to-drag ratio. The 200-nm trajectory is characterized by a constant-Mach number climb schedule, i.e., the constant-IAS speed segment of climb disappears as the trajectory range decreases.

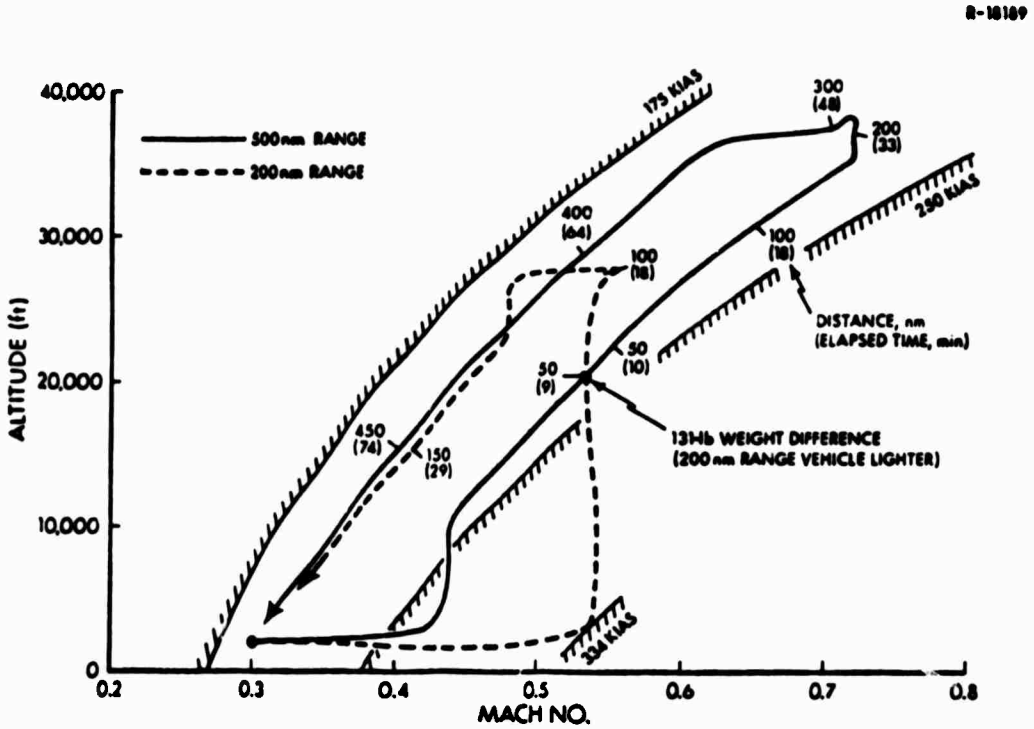

Figure 26 Short-Range Altitude-vs.- Mach Number Profiles (Steepest-descent trajectories)

Elapsed flight time, in minutes, and values of fuel consumption for the two short-range trajectories are indicated at various points on the profiles. The two profiles intersect during the climb modes at an altitude of about 20,000 ft and a Mach number of approximately 0.53. This intersection denotes the point at which the aircraft's specific total energy (kinetic plus potential energy divided by weight) is the same for both flight paths. At this equal energy point, the 200-nm vehicle has burned more fuel and has flown further than its longer-range counterpart. This occurs because the aircraft which is flying the short-range trajectory is maximizing the range travelled during the climb. On the other hand, the 500-nm vehicle maximizes energy gained during the climb and maximizes specific range during the cruise. In this manner, total fuel use for the mission is minimized.

As trajectory range becomes greater than 500 nm, the cruising flight mode takes on increasing significance. Fuel consumption and optimal profile shapes for longer range trajectories are discussed in the following sections.

5.3 MEDIUM-RANGE FLIGHT PATHS

Fuel-minimal trajectory profiles for medium-range (1,000 to 2,000 nm) flight paths are presented in this section. As in the case of the short-range trajectories, optimal trajectory shaping provides significant reductions in aircraft fuel consumption.

As trajectory range increases, the duration of the cruising segment of flight increases more quickly than that of the climb and descent modes. The predominance

of the cruise for these longer path lengths is demonstrated in Fig. 27. As path length varies between 500 to 4,000 nm, the percentage of the trajectory distance which is flown in the cruise mode increases from about 28 to 90 percent. Because the cruise mode is efficient in terms of the nautical miles flown per pound of fuel consumed (specific range), the longer range trajectories result in larger values of total specific range.

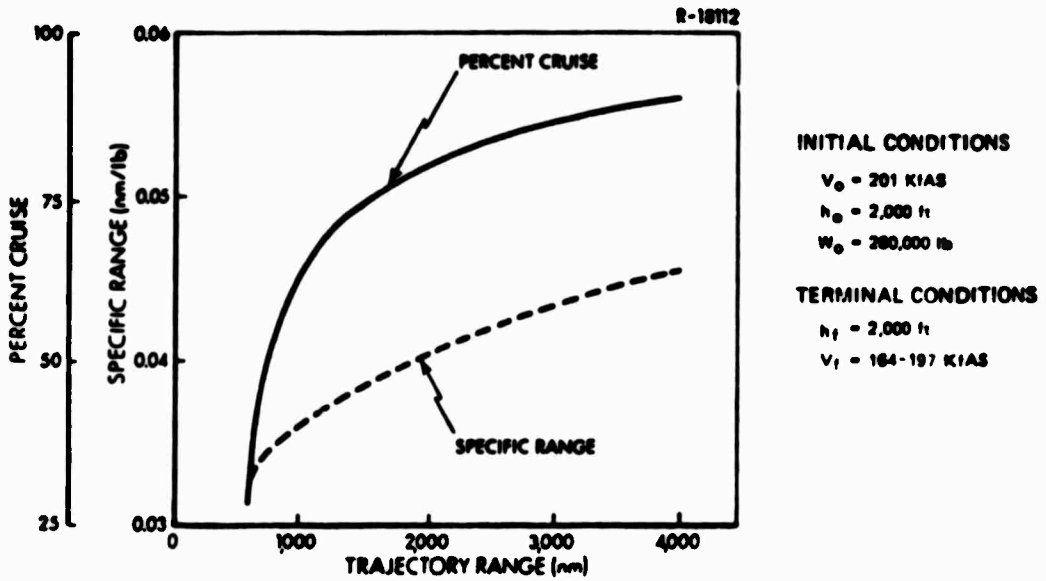

Figure 27 Cruise Duration as a Percentage of Path Length

The parametric-optimum and the steepest-descent-optimum profiles are similar for the medium-range trajectories. Plots of altitude versus range for these two optimal profiles are presented in Fig. 28. The profiles are indicative of a 1,000-nm trajectory for an initial vehicle weight of 260,000 lb. The major difference between the trajectories occurs during the transition from the climb to the cruise phase of flight. The fully optimal (steepest-descent) profile performs a more gradual transition than

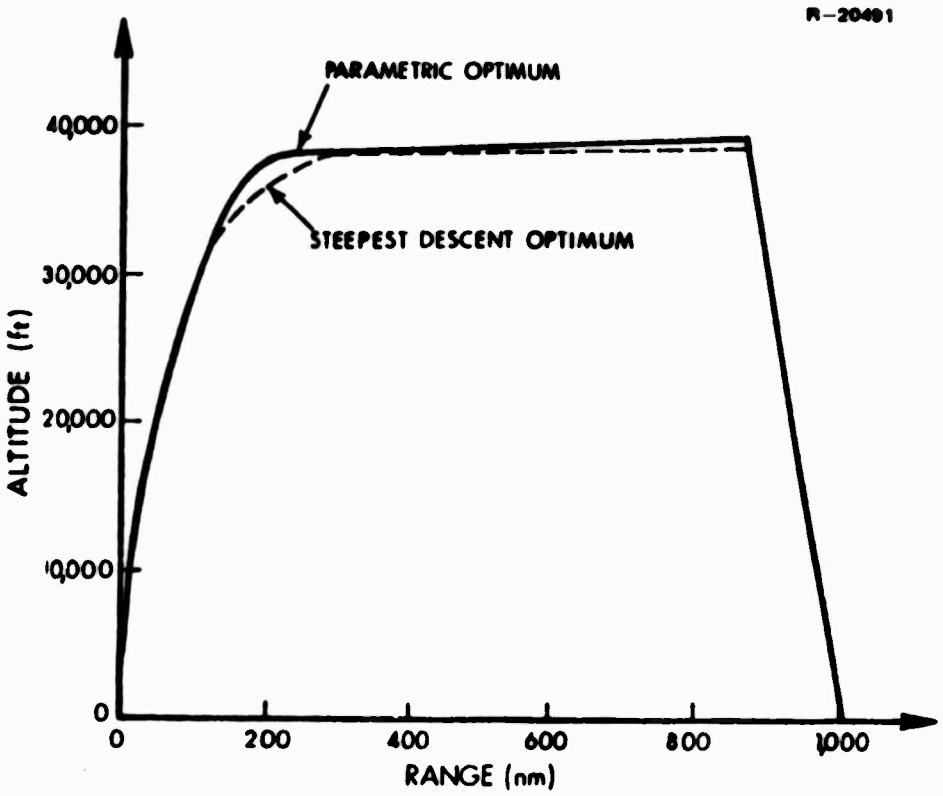

Figure 28 Fuel-Minimal Medium-Range Trajectory Profiles

transition than that of the parametric optimum. Also, the fully optimal profile does not climb quite as much during cruise.

Conventional trajectory profiles include cruise at constant altitudes and Mach numbers due to air traffic control regulations (Refs. 30 and 32). Because an optimal cruise increases altitude as vehicle weight decreases, the conventional constant-altitude cruise is clearly sub-optimal. The Mach numbers flown on conventional trajectories also differ from the C-141A optimal value of approximately 0.725. Comparisons of fuel consumption for the two optimal 1,000-nm profiles and four conventional trajectories are presented in Table 8. In addition to flying at constant altitude

during cruise, the conventional flight paths also include the handbook climb and descent schedules described in Sections 4.3.1 and 4.4.1.

TABLE 8

FUEL CONSUMPTION FOR 1,000-NM TRAJECTORIES

Trajectory Type 1,000-nm Range 260,000-lb Initial Weight		Fuel Use (Lb)	Percent Over Optimum
Steepest-Descent Optimum		26,932	-
Parametric Optimum		27,274	1.3
Conventional			
Altitude (h)	Mach Number (M)		
31,000 ft	0.740	30,032	11.5
31,000 ft	0.767	31,199	15.8
35,000 ft	0.740	28,452	5.6
35,000 ft	0.767	29,233	8.5
Constant-Altitude Optimum h = 39,114 ft		27,293	1.3

Also included in the above table is the fuel consumption required for a 'constant-altitude optimum" profile. This profile follows the same climb and descent schedule as the parametric optimum, and M = 0.725, but the cruise mode is flown at a constant altitude. The altitude is chosen to be the average value of the initial and final cruise altitudes experienced by the parametrically defined optimum cruise.

The parametric-optimum flight path provides for fuel consumption within 1.3 percent of the fully optimal trajectory. This performance is significantly superior to the results obtained with the handbook profiles (5.6 to 15.8 percent above

optimum). The "constant-altitude-optimum" fuel consumption is basically the same as that of the parametric optimum. Since constant altitude cruise is easily specified and is the method currently employed, it is reasonable to suggest this profile as a convenient means of obtaining substantial fuel savings.

Table 9 presents fuel consumption values for trajectories with path lengths of 2,000 nm. Here, the parametric-optimum profile, which has demonstrated fuel consumption values extremely close to the fully optimal profiles, is chosen as the point for comparison. As with the 1,000-nm case, the parametric-and constant-altitude-optimum trajectories yield fuel consumption values significantly lower than those of the conventional profiles.

TABLE 9

FUEL CONSUMPTION FOR 2,000-NM TRAJECTORIES

Trajectory Type 2,000-nm Range 260,000-lb Initial Weight		Fuel Use (Lb)	Percent Over Optimum
Parametric Optimum		49,291	--
Conventional			
Altitude (h)	Mach Number (M)		
31,000 ft	0.740	56,184	14.0
31,000 ft	0.767	58,918	19.5
35,000 ft	0.740	52,223	5.9
35,000 ft	0.767	54,153	9.9
Constant-Altitude Optimum h = 40,147 ft		49,539	0.5

The fuel consumption data presented in Tables 8 and 9 demonstrate the utility of trajectory optimization in reducing fuel consumption for varying path length missions. In all cases, however, the initial vehicle weight is 260,000 lb. The effects of differences in initial weight on fuel consumption are shown in Fig. 29. In this figure, fuel consumption is plotted for a 2,000-nm trajectory flown by aircraft with initial weights of 200,000, 260,000 and 320,000 lb. For each vehicle weight, the fuel consumption represents the amount of fuel used in flying the parametrically-defined optimal profiles. The cruise altitudes for each of the profiles also are indicated on the figure. Over the range of initial vehicle weights examined, the increase in fuel for each pound of initial weight is linear, with a slope of 0.19 lb-fuel/lb-initial weight. The penalty paid for carrying excess fuel on this 2,000-nm trajectory is equal, therefore, to 19 percent of the extra fuel. This points up the desirability of <u>not</u> loading the vehicle with more fuel than is required to carry out the mission with a reasonable degree of safety.

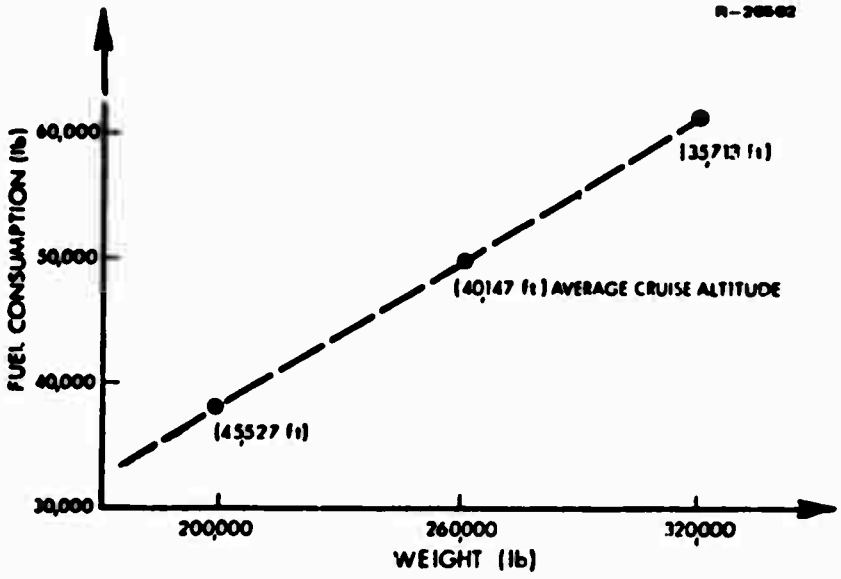

Figure 29 Effects of Initial Aircraft Weight on Total Fuel Consumption (Parametric-optimum profiles)

5.4 LONG-RANGE FLIGHT PATHS

Potential fuel reduction for a long-range mission is even greater than that of the short- and medium-range flight paths. In this study, trajectory ranges of more than 2,000 nm are categorized as "long-range."

Many of the results previously presented here are determined for an intermediate value of initial C-141A aircraft weight (260,000 lb). The aircraft weight and maximum fuel-loading data for a C-141A aircraft indicate that at a vehicle weight of 316,000 lb, the maximum amount of fuel which can be loaded for flight is 148,000 lb. Thus, for an initial weight of 260,000 lb, about 92,000 lb of fuel is available to fly a mission.

The parametric-optimum 4,000-nm trajectory consumes 87,285 lb of fuel for an initial 260,000-lb total aircraft weight. This value is close to the limit of fuel which can be loaded for this initial weight. Thus, a 4,000-nm range is approximately the maximum range of a C-141A with this loading. Fuel consumption values for this parametric-optimum, four handbook profiles, and the constant-altitude optimum are presented in Table 10. Note that all the handbook profiles require more than the 92,000 lb of fuel available. The relative percentage fuel savings indicated in the table are, however, indicative of the potential fuel reductions which can be achieved with trajectories of this range. Also, the constant-altitude-optimum profile again provides performance which is nearly equal to that of the parametric-optimum profile.

The maximum range capability of the modeled C-141A aircraft (see Appendix B), is 5,600 nm. This long-range

TABLE 10

FUEL CONSUMPTION FOR 4,000-NM TRAJECTORIES

Trajectory Type 4,000-nm Range 260,000-lb Initial Weight		Fuel Use (Lb)	Percent Over Optimum
Parametric Optimum		87,285	--
Conventional			
Altitude (h)	Mach Number (M)		
31,000 ft	0.740	105,850	21.3
31,000 ft	0.767	111,605	27.9
35,000 ft	0.740	96,219	10.2
35,000 ft	0.767	100,511	15.2
Constant-Altitude Optimum h = 42,215 ft		88,636	1.5

profile, Fig. 30, has been generated by performing a parametric optimization for a vehicle with an initial weight of 320,000 lb. The aircraft burns 138,328 lb of fuel, only 10,000 lb less than the maximum which can be loaded, on this maximum range mission.

The important characteristics of long-range fuel-optimal trajectory profiles are highlighted by the 5,600-nm flight path. About 9 percent (500 nm) of the trajectory is flown during the climb and descent segments. Thus, by optimizing fuel consumption during cruise, significant reductions in fuel use are achieved. The increasing altitude characteristic of the optimal, constant-W/δ climb also is clearly demonstrated on this trajectory. The initial cruise altitude is approximately 34,500 ft, and the cruise phase terminates at an altitude of about

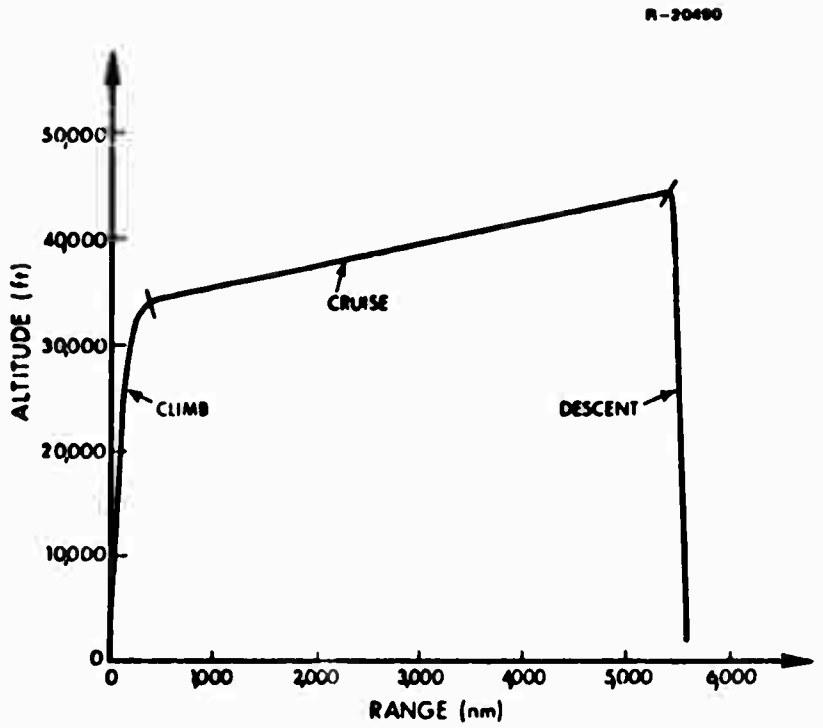

Figure 30 5,600-nm Optimal Trajectory Profile

44,500 ft. While this 10,000-ft increase in altitude during cruise is larger than that which would be experienced on shorter length profiles, the climbing-cruise characteristic of the optimal profiles is the same.

5.5 FUEL/TIME/COST TRADEOFFS

The trajectory shaping efforts of this study are directed toward minimizing aircraft fuel consumption. By lowering the quantity of fuel used on any given flight, the dollar costs associated with fuel are reduced. Many aircraft mission costs can be related to the time duration of the flight. Personnel costs, frequency of aircraft overhaul, and equipment life expectancy are among those factors which contribute to time-related costs. It is

demonstrated in this section that trajectories which are fuel-optimal may not be optimal in terms of minimizing total costs; however, as fuel costs increase, the minimum fuel trajectories do provide the lowest total costs.

A major factor influencing the interest in fuel-use reduction is the current dramatic price increase for petroleum products. USAF total aircraft fuel consumption and fuel (JP4) costs per gallon for the years 1972 through 1976, as obtained from Ref. 25, are shown in Fig. 31. It is seen here that while fuel consumption is expected to remain relatively constant, fuel costs are expected to be about four times higher in 1976 than they were in 1973. As the rise in fuel costs is more rapid than the increase in time-related costs, fuel reduction becomes an increasingly important objective in reducing total mission expenses.

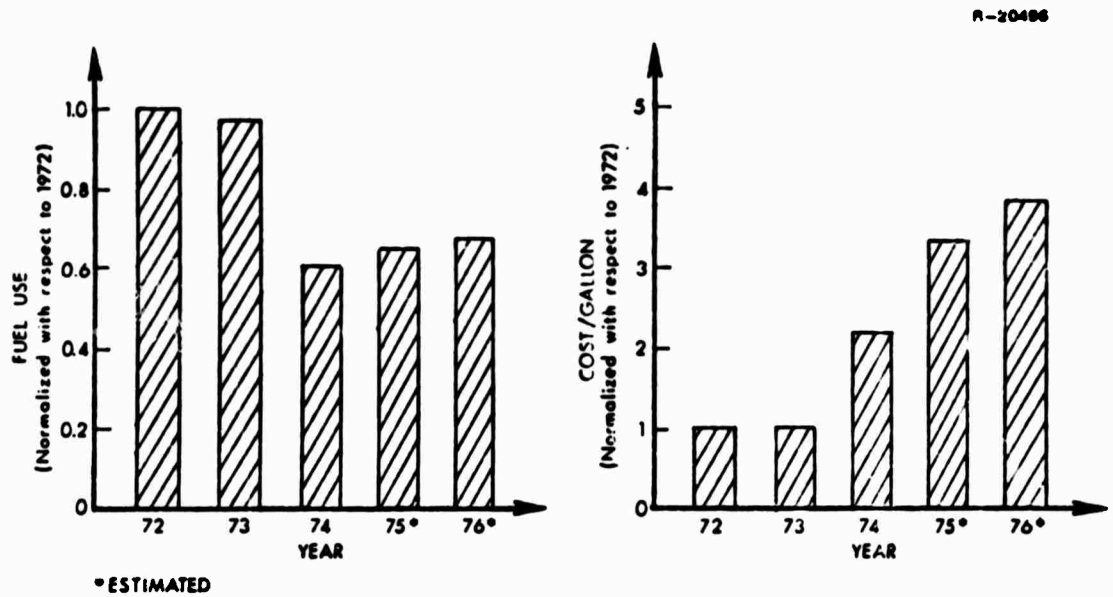

Figure 31 Yearly Fuel Consumption and Fuel Costs

The tradeoff between fuel-based costs and time-based costs is exemplified by the comparison of the 200-nm parametric-optimum and conventional trajectories. The fuel consumed and the elapsed time for these trajectories are presented in Table 11. Also shown is the total cost (in dollars) for each trajectory, assuming a fuel cost of 45¢/gallon, 6.55 lb per gallon, and a time-based cost of $400/hr. The minimum-fuel parametric-optimum trajectory uses 932 lb less fuel than the conventional trajectory, but its flight time is 0.11 hr longer. This results in a nearly equal value of total cost for the two trajectories.

TABLE 11
TOTAL TRAJECTORY COSTS --
200-NM FLIGHT PATH

Trajectory Type	Fuel Use (Lb)	Time (Hr)	Total Cost ($)
Parametric Optimum	7,515	0.664	782
Conventional (1/3-Level)	8,347	0.554	795

The effects of increased fuel prices on the cost-optimality of minimum-fuel trajectories are demonstrated in Table 12. Here, total costs for the 200-nm parametric-optimum and conventional trajectories are shown for a variety of fuel and time-based costs. With an increase in fuel prices, the optimal trajectory provides minimum total cost as well as minimum fuel performance.

TABLE 12
TRAJECTORY COSTS VS. FUEL/TIME PRICE COMBINATIONS --
200-NM PATH LENGTH

Trajectory Type	Cost I ($)	Cost II ($)	Cost III ($)	Cost IV ($)
Parametric Optimum	782	1,126	1,413	1,545
Conventional	795	1,178	1,496	1,606

- COST I 45¢/gallon, $400/hr
- COST II 75¢/gallon, $400/hr
- COST III $1.00/gallon, $400/hr
- COST IV $1.00/gallon, $600/hr

Trajectory fuel consumption, time duration and total costs for 1,000-, 2,000-, and 4,000-nm missions are presented in Table 13. As before, the total costs are based on a rate of 45¢/gallon for fuel and $400/hr for time. Total trajectory expense for other values of fuel and time costs can be computed from the fuel-consumption and time data contained in the table. For each trajectory range, parametric-optimum, constant-altitude optimum, and four handbook trajectory results are shown. The handbook trajectories are denoted as HB1 through HB4, and the constant altitudes (h) and constant Mach numbers (M) which describe their cruise conditions are as follows:

- HB1 : h = 31,000 ft, M = 0.74
- HB2 : h = 35,000 ft, M = 0.74
- HB3 : h = 31,000 ft, M = 0.767
- HB4 : h = 35,000 ft, M = 0.767

TABLE 13

TRAJECTORY COST AS A FUNCTION OF PATH LENGTH AND FLIGHT PROFILE

Trajectory Range	Trajectory Type	Fuel (Lb)	Time (Hr)	Total Cost ($)	Excess Cost (Percent)
	† Parametric Optimum	27,274	2.671	2,943	-
	Constant-Altitude Optimum	27,293	2.671	2,943	0.0
1,000 nm	HB1	30,032	2.400	3,023	2.7
	* HB2	28,452	2.434	2,927	-0.5
	‡ HB3	31,199	2.336	3,078	4.6
	HB4	29,233	2.358	2,951	0.3
	*† Parametric Optimum	49,291	5.104	5,428	-
	Constant-Altitude Optimum	49,539	5.104	5,445	0.3
2,000 nm	HB1	56,184	4.701	5,741	5.8
	HB2	52,223	4.790	5,504	1.4
	‡ HB3	58,918	4.554	5,876	8.3
	HB4	54,153	4.635	5,574	2.7
	*† Parametric Optimum	87,285	9.970	9,987	-
	Constant-Altitude Optimum	88,636	9.978	10,080	0.9
4,000 nm	HB1	105,850	9.286	10,986	10.0
	HB2	96,219	9.453	10,391	4.0
	‡ HB3	111,605	8.988	11,262	12.8
	HB4	100,511	9.147	10,564	5.8

*Lowest Total Cost
†Minimum Fuel
‡Minimum Time

For all trajectory ranges, the parametric-optimum profile provides the lowest value of fuel consumption. In the 2,000- and 4,000-nm profiles, the parametric optimum also results in the lowest trajectory costs. As fuel prices continue to rise, the savings available from these trajectories will become even more pronounced.

In the case of the 1,000-nm trajectory, the lowest cost is obtained with a conventional profile, HB2. Although this profile consumes 1,178 lb more fuel than does the parametric optimum, the flight time is reduced by 0.237 hr. At a rate of $400/hr, this is enough to offset the increased fuel costs. Trajectory costs for other fuel price combinations are presented in Table 14. As fuel prices increase, the minimum-fuel trajectories also are the minimum-total-cost profiles.

TABLE 14

TRAJECTORY COSTS FOR A VARIETY OF FUEL/TIME PRICES

Trajectory Range	Trajectory Type	Cost I ($)	Cost II ($)	Cost III ($)	Cost IV ($)
1,000 nm	Parametric Optimum	2,943	4,192	5,233	5,767
	Constant Altitude Optimum	2,943	4,193	5,234	5,770
	HB1	3,023	4,399	5,545	6,025
	HB2	2,927	4,231	5,317	5,804
	HB3	3,078	4,507	5,698	6,165
	HB4	2,951	4,290	5,406	5,878
2,000 nm	Parametric Optimum	5,428	7,686	9,567	10.587
	Constant-Altitude Optimum	5,445	7,714	9,605	10,625
	HB1	5,741	8,314	10,459	11,399
	HB2	5,504	7,896	9,889	10,847
	HB3	5,876	8,574	10,823	11,727
	HB4	5,574	8,055	10,122	11,049
4,000 nm	Parametric Optimum	9,987	13,985	17,317	19,307
	Constant-Altitude Optimum	10,080	14,139	17,523	19,519
	HB1	10,986	15,834	19,874	21,732
	HB2	10,391	14,798	18,471	20,362
	HB3	11,262	16,374	20,634	22,432
	HB4	10,564	15,168	19,004	20,833

- COST I 45¢/gallon, $400/hr
- COST II 75¢/gallon, $400/hr
- COST III $1.00/gallon, $400/hr
- COST IV $1.00/gallon, $600/hr

Tables 13 and 14 demonstrate fuel-use trends for vehicles whose initial total weights are equal. The results of comparing trajectories with equal final weights, reflecting decreased "tankering" of excess fuel, is even more dramatic. Assuming that the weight ratio, μ, defined by

$$\mu = \frac{W_0}{W_0 - \Delta W_{fuel}} \qquad (5.5\text{-}1)$$

is unchanging for each mission length and trajectory type, the fuel savings obtained by flying parametric-optimum trajectories instead of minimum-time conventional trajectories are compared, with the following results:

- 1,000-nm trajectory:
  Fuel saved = 4,419 lb (14 percent)
- 2,000-nm trajectory:
  Fuel saved = 11,865 lb (20 percent)
- 4,000-nm trajectory:
  Fuel saved = 36,666 lb (33 percent)

In this case, the fuel saved is fuel which is not loaded on the aircraft, so the initial weights of the aircraft which fly the parametric-optimum trajectories are 223,334 to 255,571 lb. The minimum-time aircraft begins at 260,000 lb in each case.

Another interesting comparison is payload weight improvement for fixed initial weight (260,000 lb). Comparing the parametric-optimum profile to the minimum-fuel conventional profile indicates the following percentage increases in available payload weight, assuming 10 percent fuel reserve:

- 1,000-nm trajectory: 1.5 percent
- 2,000-nm trajectory: 5.2 percent
- 4,000-nm trajectory: 69.4 percent

The latter figure is seen to have significant implications for the strategic airlift mission, because it says that the same payload could be moved with 41 percent fewer flights. Since the fuel used on each flight also is 9 percent less, equal total payload weight would be moved with 46 percent less fuel.

On an actual strategic mission, the aircraft would operate closer to its maximum gross weight on takeoff, carrying more payload and fuel in both the optimum and conventional cases, and the above results do not account for volumetric limitations on specific payloads. Consequently, the percentage payload gain could be reduced. The gain would be further reduced by the fact that the average altitude of the optimal trajectory would be lower for higher weights and, therefore, nearer the HB2 flight path. Nevertheless, the 260,000-lb result indicates the proper trends for the benefits obtained from fuel-optimal flight.

Rather than determining trajectory profiles to minimize fuel consumption, the analysis tools employed in this study could be used to determine cost-optimal profiles. Determination of a cost-efficient cruise phase might proceed in a fashion similar to that of Section 4.2. However, instead of maximizing specific-range (nautical miles travelled per pound of fuel), a specific-cost factor (nautical miles per dollar) would be substituted. The dollar costs associated with each nautical mile of path length are the price of the fuel consumed plus the costs associated with the time duration for flying each nautical mile.

Fully optimal minimum-cost trajectories can be determined by variational means, as described in Section 3.6.

The cost function of Eq. (3.6-1) need simply be modified to include a terminal penalty on time as well as on fuel consumption. Thus, the present fuel-optimal program development (see Appendix A) also is capable of handling the minimum-cost trajectory problem.

5.6 CHAPTER SUMMARY

This chapter has demonstrated the utility of flying optimized (fuel-minimal) trajectory profiles in order to reduce total fuel consumption. The optimized flight segments described in Chapter 4 serve as the starting point for the current complete trajectory optimization. By combining these piecewise optimal segments, parametric-optimum profiles are constructed. These profiles are found to provide excellent fuel economy when compared with the fully optimal (steepest-descent) flight paths.

The potential for fuel use reduction by means of trajectory shaping has been shown to exist for short-, medium-, and long-range trajectories. The optimal short-range trajectories demonstrate a maximum fuel savings of about 12 percent. This percentage increases (with increasing path length) to approximately 28 percent for the long-range flight paths.

Constant-altitude-optimal flight paths also have demonstrated fuel efficiency close to that of the fully optimal trajectories. These constant-altitude-optimal profiles are characterized by parametrically defined climb and descent segments, while the cruise phase is flown at a constant altitude. The altitude is chosen to be the midpoint value defined by a fuel-minimal, constant W/δ flight path.

The final point emphasized in this chapter is that fuel-minimal profiles are not necessarily cost-minimal profiles. As costs associated with flight time are factored into the problem, it is found that some conventional trajectories are competitive, in terms of total trajectory cost, with the fuel-optimal flight paths. As fuel costs increase at a dramatic rate (they have quadrupled in four years), the fuel-optimal characteristics of mission profiles become increasingly significant. Simple methods are presented which can be employed to minimize total (fuel plus time) costs. These methods are similar to the techniques employed for the fuel-minimization study and are, therefore, expected to provide good results with a minimum of effort.

Having generated the fuel-optimal trajectory profiles for a variety of flight segments and mission constraints, the problem remaining is to develop a means of flying these profiles. An automated method for profile following which can be implemented on actual aircraft is presented in the following chapter.

VI SYNTHESIS OF FUEL-OPTIMAL GUIDANCE ALGORITHMS

6.1 OVERVIEW

The earlier chapters have established the groundwork for fuel-optimal guidance by discussing use factors, presenting analytical tools, and developing a wide range of fuel-optimal flight paths. This chapter presents the means of using these results to define throttle/energy management algorithms which can be implemented in an individual aircraft. As introduced in Chapter 1, the basic approach is to

- Define fuel-optimal flight paths
- Compute linear-optimal guidance gain schedules
- Design a real-time system for generating the reference flight paths and following this path in the presence of disturbances.

Section 6.2 describes the separation of nonlinear and linear dynamic models which allows this approach to throttle/energy management to be used, and it presents the linear perturbation guidance law which is required for flight path following. The fuel-optimal flight path results of earlier chapters are generalized for on-board implementation in Section 6.3, and corresponding functional requirements on sub-system components are discussed in Section 6.4. The chapter is summarized in Section 6.5.

6.2 LINEAR-OPTIMAL GUIDANCE LAWS

In this section, the formulation of a guidance system designed to follow a reference trajectory is presented. Although the concepts are applicable to all trajectories, the current efforts are directed toward flying the fuel-optimal profiles previously described. The resulting algorithm provides a guidance technique which minimizes aircraft fuel consumption when used in conjunction with the fuel-optimal flight path generator described in the next section.

Linear-optimal guidance algorithms (Refs. 38 and 39) compute guidance gains to yield desired state deviation and control perturbation response. This is accomplished by determining guidance commands to minimize the following quadratic cost function:

$$J = \Delta\underline{x}^T(R_f)P_f\Delta\underline{x}(R_f) + \int_{R_o}^{R_f} \{\Delta\underline{x}^T A\Delta\underline{x} + \Delta\underline{u}^T B\Delta\underline{u}\}dR \qquad (6.2\text{-}1)$$

where the state and control vector deviations are defined by $\Delta\underline{x}(R)$ and $\Delta\underline{u}(R)$, respectively, and the matrices, A and B, are used to penalize in-flight deviations in state and control. The matrix, P_f, is used to penalize the terminal trajectory deviations, and the independent variable, R, is trajectory path length. By specifying large values for the elements of A, the cost function places emphasis on maintaining small state deviations. Large values of B, relative to A, mean that the control perturbations will remain small, even when faced with large state deviations. The choice of values used in the current study is discussed in Section 6.2.2.

If the dynamic relationship between the state and control is linear, i.e.,

$$\Delta\underline{x}'(R) = F(R)\Delta\underline{x}(R) + G(R)\Delta\underline{u}(R) \qquad (6.2\text{-}2)$$

then the control history which minimizes Eq. (6.2-1) can be specified in a feedback fashion as

$$\Delta\underline{u}(R) = -K(R)\Delta\underline{x}(R) \qquad (6.2\text{-}3)$$

(The notation $()'$ represents differentiation with respect to path length).

In the above equations, the matrices F(R) and G(R) describe the effects of state and control deviations on the state perturbation derivative, $\Delta\underline{x}'(R)$, and the elements of K(R) are the desired perturbation feedback gains.

The control perturbations, $\Delta\underline{u}(R)$, of Eq. (6.2-3) are linear functions of the state deviations, $\Delta\underline{x}(R)$, and they provide the minimum (optimal) cost for Eq. (6.2-1). Thus, the descriptor "linear-optimal" truly applies to the guidance algorithm, as long as perturbations from the reference flight path are described adequately by Eq. (6.2-2). The method of determining these guidance gains is presented in the following section.

6.2.1 Design Fundamentals

The aircraft equations of motion derived in Section 3.2 are nonlinear functions of the state and control variables. The trajectory perturbations can be expressed in the linear form of Eq. (6.2-2) by performing a Taylor series expansion of the exact equations and retaining only first-order terms.

The perturbed trajectory equations can be derived by substitution in Eq. (3.6-2):

$$(\underline{x}_D+\Delta\underline{x})' = \underline{f}[(\underline{x}_D+\Delta\underline{x}),(\underline{u}_D+\Delta\underline{u})] \tag{6.2-4}$$

where $\underline{x}_D$ and $\underline{u}_D$ are the state and control vectors which describe the desired flight path, and $\Delta\underline{x}$ and $\Delta\underline{u}$ represent trajectory perturbations. The first-order Taylor series expansion of Eq. (6.2-4) results in

$$\underline{x}_D' + \Delta\underline{x}_D' = \underline{f}(\underline{x}_D,\underline{u}_D) + \underline{f}_{\underline{x}}\Big|_D \Delta\underline{x} + \underline{f}_{\underline{u}}\Big|_D \Delta\underline{u} \tag{6.2-5}$$

where $\underline{f}_{\underline{x}}$ and $\underline{f}_{\underline{u}}$ are the motion equation partial derivative matrices with respect to the state and control variables, respectively, evaluated along the desired trajectory.

By definition, the desired trajectory satisfies the nonlinear equations of motion, i.e.,

$$\underline{x}_D' = \underline{f}(\underline{x}_D,\underline{u}_D) \tag{6.2-6}$$

Subtracting Eq. (6.2-6) from Eq. (6.2-5), it can be seen that the dynamics of small variations from the nominal flight path are described approximately by

$$\Delta\underline{x}' = F\Delta\underline{x} + G\Delta\underline{u} \tag{6.2-7}$$

where the partial derivative matrices, $\underline{f}_{\underline{x}}$ and $\underline{f}_{\underline{u}}$, have been denoted simply as F and G. Equation (6.2-7) has the required linear form of Eq. (6.2-2).

The determination of a perturbation control history to minimize Eq. (6.2-1) (Refs. 38 and 39) is accomplished by integrating the following matrix Riccati equation from R_f to R_o:

$$P' = -PF - F^T P + PGB^{-1}G^T P - A \qquad (6.2\text{-}8)$$

subject to the boundary condition

$$P(R_f) = P_f \qquad (6.2\text{-}9)$$

Solving this matrix equation is analogous to determining the costate variables in the variational optimization problem described in Section 3.6. The optimal perturbation guidance gains then are defined in terms of the Riccati solution matrix, P, the control partial derivative matrix, G, and the control penalty matrix, B, as follows:

$$K(R) = [B(R)]^{-1} G^T(R)P(R) \qquad (6.2\text{-}10)$$

The solution of Eq. (6.2-8) by means of numerical integration techniques is a computationally expensive task. The matrix Riccati equation used to compute guidance gains accounts for time variations in aircraft dynamics as fuel is burned and as altitude and velocity are varied. These dynamic variations are slow compared to the natural frequencies of the system. Small time steps are required in the Riccati differential equation solution as a consequence of these natural frequencies, and this results in an excessive number of computations to analyze the gains for a single mission.

In order to surmount these numerical difficulties, use is made of the fact that the partial derivative matrices, F and G, are slowly varying along the aircraft trajectories. Rather than integrating Eq. (6.2-8) backwards along the complete trajectory profile, only steady-state gain values (for constant values of F and G) at discrete trajectory points (e.g., every 50 nm) are computed. Because of the slowly varying nature of these gains, the resulting

steady-state gains are essentially identical to those obtained from the complete numerical integration of the Riccati equation.

The computation of steady-state gains is significantly simpler than the determination of the time-varying values. Transition matrix solutions (the "Kalman-Englar Method") are used to replace the numerical integration methods (Ref. 54). Because the partial derivative matrices (F and G) are assumed to be constant at each steady-state gain computation point, the necessary transition matrix need be calculated only once at each of these points. The Kalman-Englar method employed in this study reduced the computational effort required for direct numerical integration gain evaluations by a factor of about one hundred.

6.2.2 Weighting Matrices for System Design

The perturbation guidance technique presented in this chapter employs guidance gains which yield desired state deviation and control perturbation response. These gains are computed to minimize the following scalar cost function:

$$J = \int_{R_o}^{R_f} (\Delta \underline{x}^T A \Delta \underline{x} + \Delta \underline{u}^T B \Delta \underline{u}) dR \qquad (6.2\text{-}11)$$

This quadratic cost function is essentially the same as that of Eq. (6.2-1). The present version does not include a terminal penalty (the term outside the integral in Eq. (6.2-1)), as only the steady-state gain values are of interest.

In order to insure that the cost function has a minimum, the penalty weighting matrices, A and B, must be positive semi-definite and positive definite, respectively (Ref. 54). This means that for any state or control deviations, the following relationships must hold:

$$\Delta\underline{x}^T A \Delta\underline{x} \geq 0 \qquad (6.2\text{-}12)$$

$$\Delta\underline{u}^T B \Delta\underline{u} > 0 \qquad (6.2\text{-}13)$$

A simple technique for insuring positive definiteness is to choose the A and B matrices to be of diagonal form with positive or zero elements along the diagonal. For a diagonal matrix, Eq. (6.2-12) can be evaluated as

$$\Delta\underline{x}^T A \Delta\underline{x} = a_{11}\,\Delta x_1^2 + a_{22}\,\Delta x_2^2 + \ldots a_{nn}\,\Delta x_n^2 \qquad (6.2\text{-}14)$$

where the quantities, a_{ii}, are the diagonal elements of the A matrix, and the terms, Δx_i, are the elements of the state perturbation vector. Because of its quadratic form, Eq. (6.2-14) is guaranteed to be greater than or equal to zero as long as the coefficients, a_{ii}, are greater than or equal to zero.

If the values of the elements of the A matrix are chosen to be large compared to those of B, the state deviations are penalized more heavily than are the control perturbations. This, in turn, leads to large guidance gain values, whereby large values of control would be used to null even small deviations from the reference-trajectory states. Conversely, if the B matrix elements are chosen to be large compared to those of A, the control variables are more heavily penalized, and only small control perturbations will be employed to bring the vehicle state close to the reference values.

The choice of values for A and B in the current fuel optimization study were derived from information concerning desired trajectory state and control response obtained from USAF personnel (Ref. 25). This information was provided in terms of the maximum trajectory deviations that one could allow in an actual flight and the typical control perturbation which would be exercised to null them. The current analyses considered velocity, ΔV, altitude, Δh, and flight path angle, $\Delta\gamma$, perturbations as the state variables to be controlled. $\Delta\gamma$ corresponds to an altitude rate perturbation, since $\Delta\gamma \approx \Delta\dot{h}/V$. Pitch angle, $\Delta\theta$, and throttle setting, ΔT, are the available perturbation control variables. The maximum desired values of these quantities are presented in Table 15.

TABLE 15

DESIRED PERTURBATION GUIDANCE CHARACTERISTICS

Maximum State Deviations	Maximum Control Perturbations
Velocity (ΔV): 10 kt (17 fps)	Pitch Angle ($\Delta\theta$): 1.5 deg
Flight Path Angle ($\Delta\gamma$): 0.17 deg	Throttle Setting (ΔT): 10 percent
Altitude (Δh): 100 ft	

Specifications of A and B penalty matrices to reflect the maximum trajectory deviations of Table 6.2-1 is accomplished by a straightforward procedure. The diagonal elements of the penalty matrices are set equal to the square of the inverse of the maximum allowable perturbations, i.e.,

$$a_{ii} = 1/(\Delta x_{i_{max}})^2 \qquad (6.2\text{-}15)$$

$$b_{ii} = 1/(\Delta u_{i_{max}})^2 \qquad (6.2\text{-}16)$$

where the variables $\Delta x_{i_{max}}$ and $\Delta u_{i_{max}}$ are the specified maximum allowable state and control deviations, respectively. This method assures that the penalties associated with each maximum trajectory deviation contribute an <u>equal</u> amount to the total cost function of Eq. (6.2-11). For example, a 10-kt velocity deviation causes the same increase in the cost function as a 100-ft altitude deviation or a 10-percent throttle perturbation.

Using the values presented in Table 6.2-1 and Eqs. (6.2-15) and (6.2-16), the A and B weighting matrices for the current study are given as

$$A = \begin{bmatrix} 3.46\times10^{-3} & 0 & 0 & 0 \\ 0 & 1.11\times10^{5} & 0 & 0 \\ 0 & 0 & 1.\times10^{-4} & 0 \\ 0 & 0 & 0 & 0 \end{bmatrix} \qquad (6.2\text{-}17)$$

$$B = \begin{pmatrix} 1.445\times10^{3} & 0 \\ 0 & 1.0\times10^{2} \end{pmatrix} \qquad (6.2\text{-}18)$$

In the above equations, $\Delta\gamma$ and $\Delta\theta$ penalties are scaled in radians and the ΔV penalty is scaled in fps. The fourth diagonal element of matrix A represents the penalty on vehicle mass deviations. By setting this element (a_{44}) to zero, no <u>direct</u> penalty is imposed on mass variations.* Mass values should be well controlled, however, as long as the actual trajectory closely follows the reference fuel-

*Note that positive or negative mass variations are penalized equally in Eq. (6.2-11), i.e., both cause J to increase; hence, the quadratic cost function cannot minimize fuel use directly--it can only minimize its deviation from a nominal value.

optimal profile. Dynamic coupling in the state equations given by Eq. (6.2-6) results in small gains on mass in the linear perturbation guidance law even though there is no direct penalty function applied to the mass deviations.

6.2.3 Linear-Optimal Guidance Gains

The preceding sections of this chapter have described the procedure by which linear-optimal guidance gains are computed and the numerical values of the weighting matrices which affect perturbed trajectory response. In this section, the actual guidance gains and simulated trajectory responses are presented for a typical C-141A flight profile.

For the current study, the vector perturbation controls, Eq. (6.2-3) can be written in component form as:

$$\Delta\theta = k_{11}(V_D-V) + k_{12}(\gamma_D-\gamma) + k_{13}(h_D-h) + k_{14}(m_D-m)$$
$$= \theta_D - \theta \qquad (6.2\text{-}19)$$

$$\Delta T = k_{21}(V_D-V) + k_{22}(\gamma_D-\gamma) + k_{23}(h_D-h) + k_{24}(m_D-m)$$
$$= T_D - T \qquad (6.2\text{-}20)$$

Here, the perturbed controls, pitch angle, $\theta_D-\theta$, and throttle, T_D-T, are related to the state deviations through the eight guidance gains (k_{11}, k_{12},...k_{24}). The subscript D on the trajectory states represents the values of the state variables along the desired flight path. The gain values, k_{ij}, represent the amount by which the controls are perturbed for a given value of state deviation. The gain k_{11}, for example, represents the ratio between pitch command and velocity deviation, $\Delta\theta/\Delta V$, while the gain k_{23} is the ratio of throttle perturbation to altitude, $\Delta T/\Delta h$. The remaining

gains represent similar control-to-state perturbation ratios as defined by Eqs. (6.2-19) and (6.2-20).

Actual gain values, computed at 50-nm intervals along a 525-nm trajectory, are plotted in Fig. 32. For the purposes of simulating perturbed trajectories, the gain values are linearly interpolated between computed points. For this reason, the plots of Fig. 32 present the gain histories in the form of straight-line segments.

The reference trajectory along which these gain values are evaluated consists of a climb phase (0 to 200 nm), a 200-nm cruise segment (h ≈ 39,000 ft), and a descent segment (400 to 525 nm). The six major gains -- $\Delta\theta/\Delta V$, $\Delta\theta/\Delta\gamma$, $\Delta\theta/\Delta h$, $\Delta T/\Delta V$, $\Delta T/\Delta\gamma$, $\Delta T/\Delta h$ -- are seen to be relatively constant during cruise, with major gain changes occurring during climb and descent (Fig. 6.2-1). The two gains which relate control perturbations to deviations of vehicle mass, $\Delta\theta/\Delta m$ and $\Delta T/\Delta m$, obtained average values of only 0.017 deg/1,000 lb and 0.32 percent/1,000 lb along this reference trajectory. Plots of these gains as functions of range are not included in the figure.

The guidance gain plots give an indication of the control perturbations which are employed by the guidance algorithm in reducing state deviations. For example, during the cruise segment, the plots show that a 100-ft altitude deviation will cause a pitch-angle perturbation of -1.5 deg and a throttle perturbation of approximately -1.5 percent to be commanded. The true merits of the guidance gain values can only be determined, however, by observing the perturbed trajectory response provided by the complete set of gains.

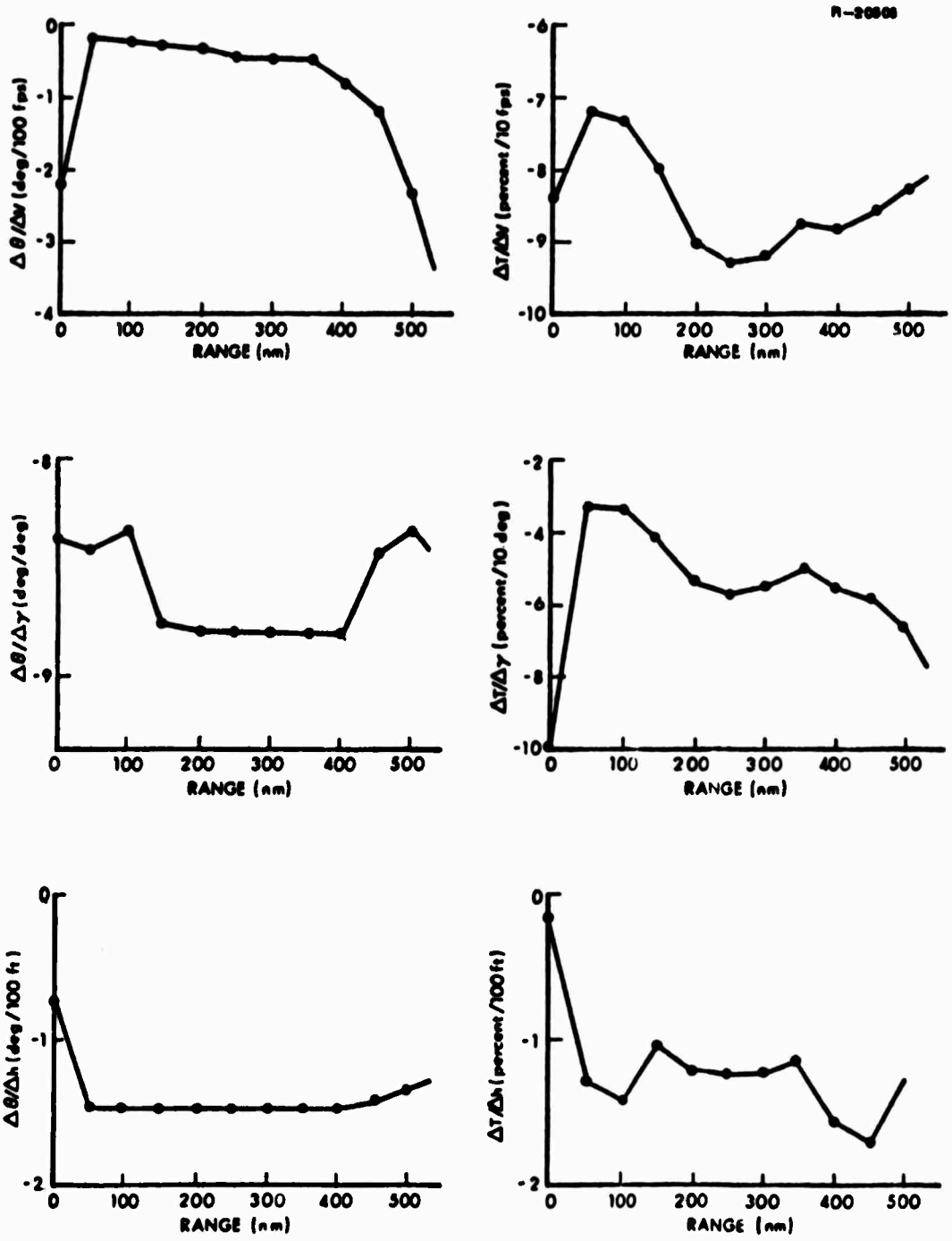

Figure 32 Linear-Optimal Guidance Gain Values

Perturbation state and control profiles for each of the major flight segments (climb, cruise, and descent) are presented in Figs. 33 through 35. In each flight segment, the effects of initial deviations in velocity (ΔV = 17 fps), flight path angle ($\Delta\gamma$ = 0.20 deg), and altitude (Δh = 100 ft) are examined individually. The initial state perturbations are set to the maximum values which define the desired guidance system response (Table 15). In addition to plots of the perturbed state profile, the control perturbations, $\Delta\theta$ and ΔT, commanded by the linear-optimal guidance algorithm to null the trajectory deviations also are depicted. An initial perturbation in a single state variable causes the other state variables also to deviate somewhat from the reference trajectory. These secondary deviations arise through the coupling of the trajectory states defined by the vehicle's equations of motion. Also, the control perturbations employed to reduce the initial trajectory deviation simultaneously affect the initially unperturbed state variable profiles. The present analysis demonstrates that the induced deviations in the originally unperturbed states are small compared to the specified trajectory response characteristics. Therefore, only profiles of the initially perturbed state variables are plotted. The maximum values of the induced deviations are noted for each perturbed trajectory simulated.

Examination of the perturbed climb profiles (Fig. 33) shows that the initial trajectory deviations in velocity and flight path angle are eliminated in a range of less than 12 nm. In particular, flight path angle deviation is eliminated in about 1 nm. The initial altitude perturbation is substantially reduced in the figure but has not yet reached a zero perturbation level in the 12-nm range.

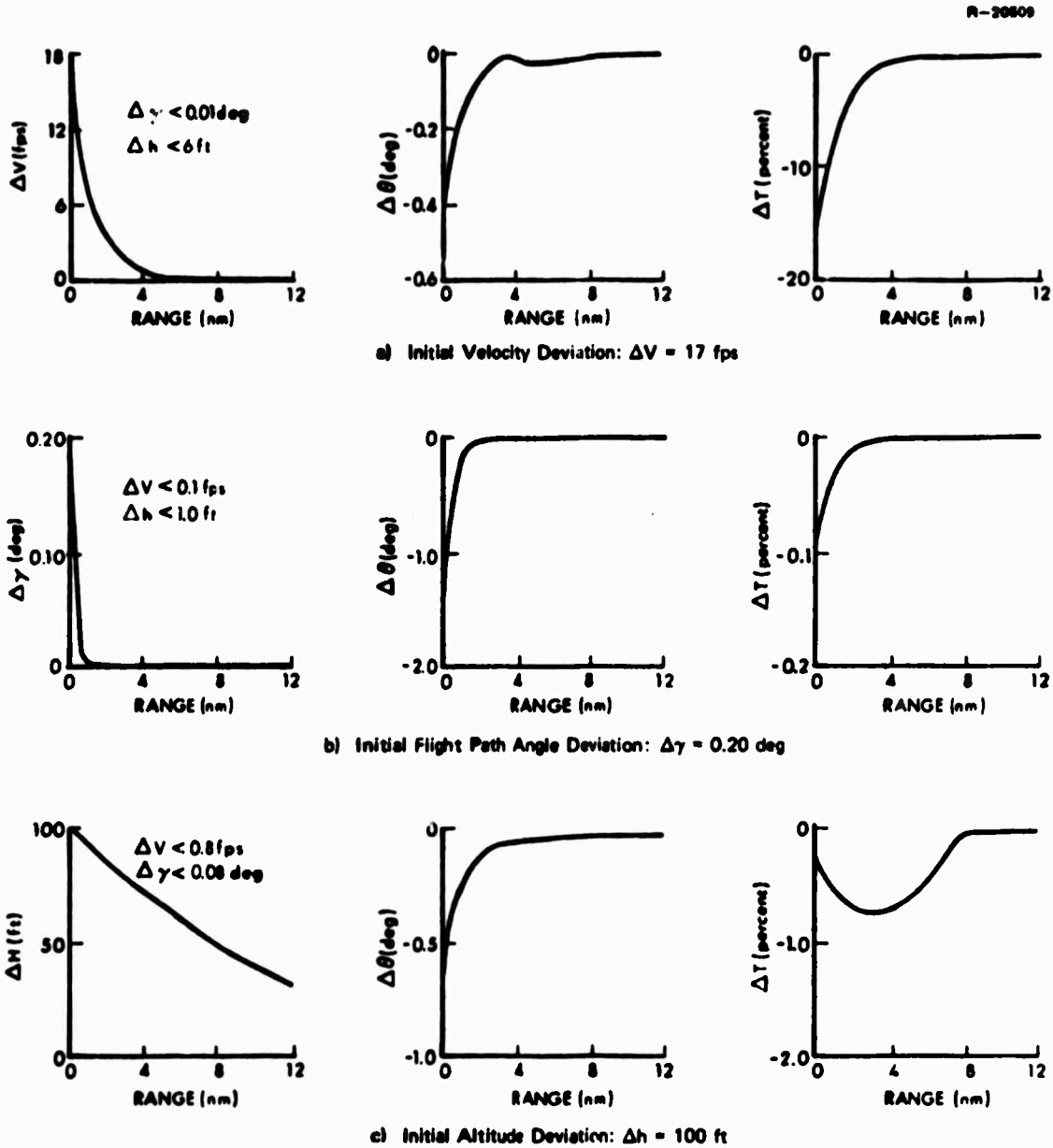

Figure 33 Climb Phase Perturbation Response

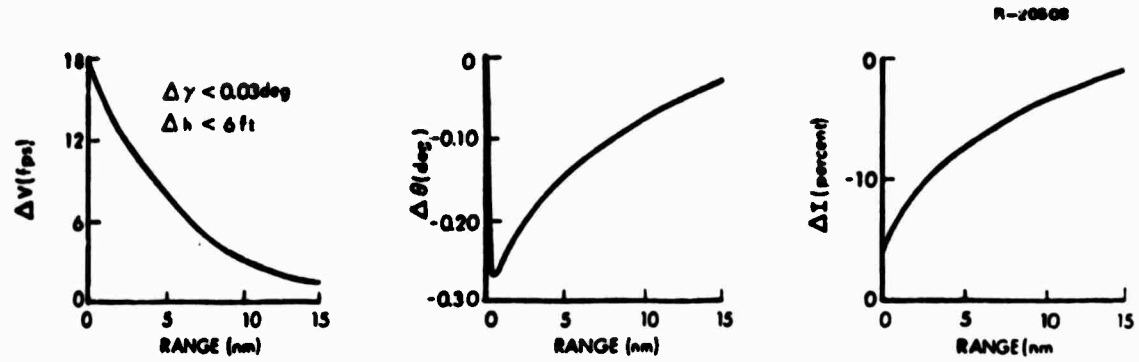

a) Initial Velocity Deviation: ΔV = 17 fps

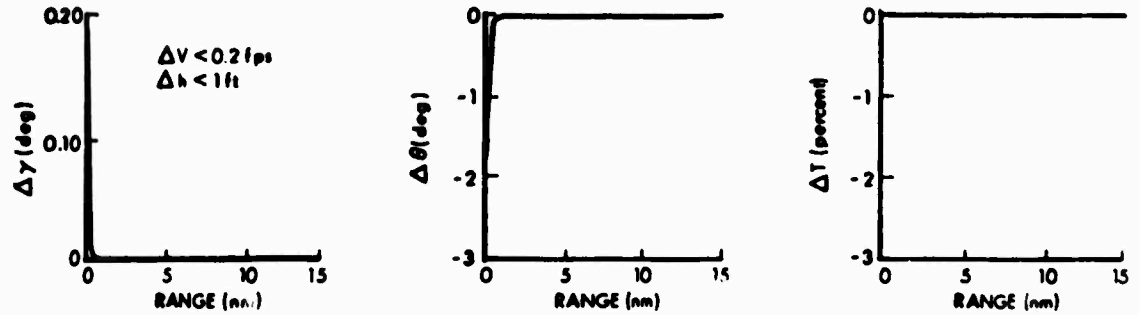

b) Initial Flight Path Angle Deviation: Δγ = 0.20 deg

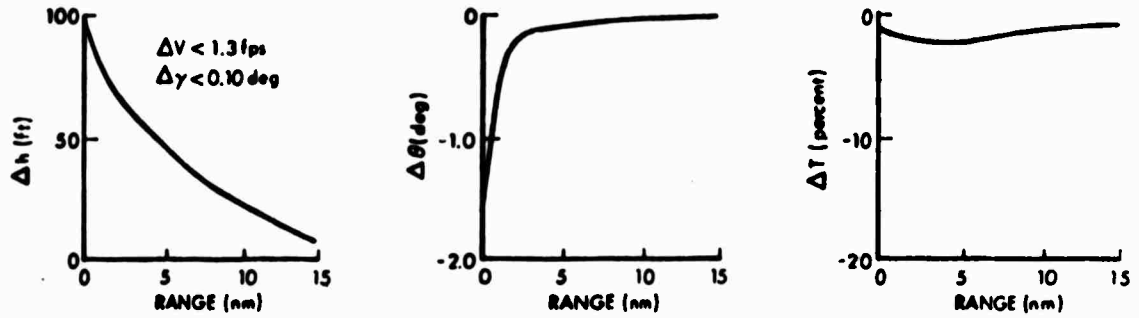

c) Initial Altitude Deviation: Δh = 100 ft

Figure 34 Cruise Phase Perturbation Response

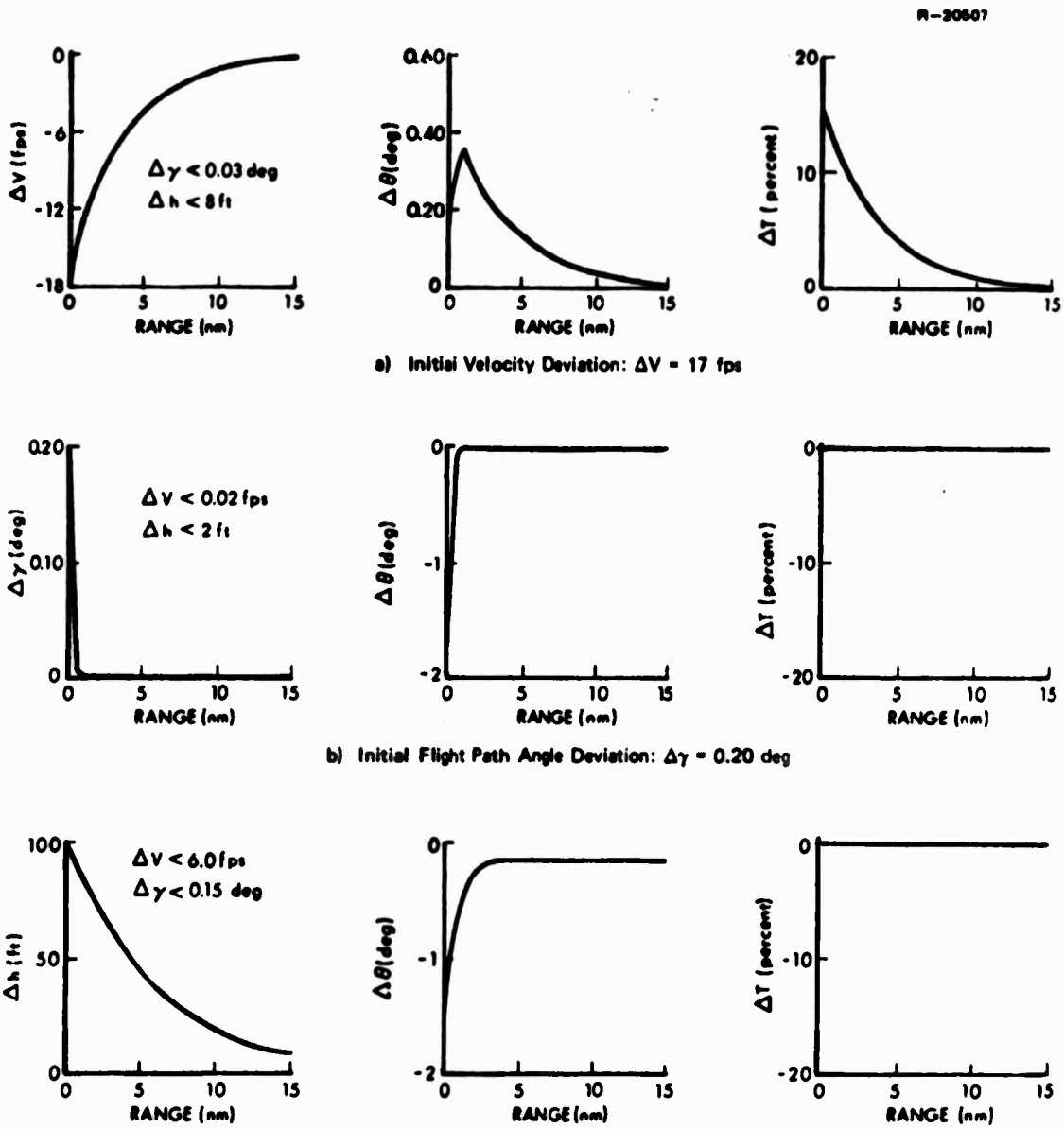

a) Initial Velocity Deviation: ΔV = 17 fps

b) Initial Flight Path Angle Deviation: Δγ = 0.20 deg

c) Initial Altitude Deviation: Δh = 100 ft

Figure 35 Descent Phase Perturbation Response

The perturbed profiles for the cruise and descent flight segments, Figs. 34 and 35, respectively, demonstrate characteristics similar to those of the climb phase. As before. initial perturbations in flight path angle are nulled almost instantaneously. The initial deviations in velocity and altitude take longer to remove but are significantly reduced over the 15-nm profiles. In all flight modes, not only are the initial perturbations reduced effectively, but the induced secondary perturbations also are small.

The perturbed flight profiles demonstrate the excellent trajectory-following capabilities of the linear-optimal guidance system. Implementing this system on an actual aircraft would necessitate some means of gain determination other than the table lookup as a function of range employed in the current simulations. Because each actual flight would be different, i.e., path length and trajectory profiles would vary, an adaptive gain determination, based upon actual flight conditions, would be needed. The following section describes an adaptive gain scheduling technique.

6.2.4 Correlation of Gains With Flight Condition

This section presents a three-step procedure for scheduling the linear-optimal guidance gains. The gains are scheduled by finding functional relationships between certain aircraft flight conditions and the control gains at these flight conditions. This results in an adaptive method of gain scheduling which could be utilized in an on-board guidance system.

Previous methods for scheduling control gains have been successful and indicate that gain scheduling is a sound approach (Refs. 55 and 56). The methodologies typically are based on single-input/single output concepts (e.g., maintaining constant loop gain); therefore, they provide inadequate insight for scheduling multivariable systems.

The method employed here (Ref. 57) is a logical extension of previous work to multivariable systems. It involves three steps and places minimum reliance on past experience and intuition. The three steps are:

- The determination of a mean/standard deviation table which aids in finding the gains that should be kept constant instead of being scheduled.
- The determination of a correlation coefficient table which aids in specifying the strongly correlated flight conditions that will be used in gain scheduling algorithms.
- The determination of relationships (or curve fits) between the chosen flight conditions and gains.

The first step in the procedure is to determine the mean and standard deviations of the optimal guidance gains over a wide range of flight conditions. The mean value of a gain, k, is given by

$$\bar{k} = \sum_{i=1}^{N} \frac{k_i}{N} \qquad (6.2\text{-}21)$$

where k_i is the value of the gain observed at flight point i, and N is the number of points at which the gain has been computed. The gain's standard deviation, $\sigma(k)$, is computed as

$$\sigma(k) = \sqrt{\frac{\sum_{i=1}^{N} (\bar{k}_i - k)^2}{N-1}} \qquad (6.2\text{-}22)$$

If both the mean and standard deviation of a gain are small, then the gain does not affect the control perturbations and need not be included in the closed-loop guidance algorithm. If the mean value is significant, but the standard deviation is small with respect to the mean, then the gain value is essentially constant over the flight conditions examined. Rather than being scheduled as a function of flight conditions, the gain should be considered constant.

The means and standard deviations of the guidance gains described in Section 6.2.3 are presented in Table 16.

TABLE 16
MEAN VALUE AND STANDARD DEVIATION OF
PERTURBATION GUIDANCE GAINS

Gain	Mean Value	Standard Deviation (Percent of Mean)
1. $\Delta\theta/\Delta V$	-7.04×10^{-3} (deg/fps)	108.8
2. $\Delta\theta/\Delta\gamma$	-8.61 (deg/deg)	2.5
3. $\Delta\theta/\Delta h$	-1.41×10^{-2} (deg/ft)	11.1
4. $\Delta\theta/\Delta m$	1.72×10^{-5} (deg/lb)	19.9
5. $\Delta T/\Delta V$	-8.43×10^{-1}(percent/fps)	10.7
6. $\Delta T/\Delta\gamma$	-5.27×10^{-1}(percent/deg)	35.8
7. $\Delta T/\Delta h$	-1.22×10^{-2}(percent/ft)	21.8
8. $\Delta T/\Delta m$	3.13×10^{-4}(percent/lb)	43.8

These values represent gain statistics for a twenty-point sample. The mean gain values for $\Delta\theta/\Delta m$ and $\Delta T/\Delta m$ are extremely small. A 10,000-lb weight deviation causes a change in pitch command of only 0.17 deg and a change in throttle setting of only 3 percent. These gains could be omitted, therefore, when implementing an on-board system.

Gains 2, 3, and 5 ($\Delta\theta/\Delta\gamma$, $\Delta\theta/\Delta h$, and $\Delta T/\Delta V$ respectively), have standard deviations equal to less than 12 percent of their mean value. Because the variation is low, it is reasonable to schedule these gains as constants in the guidance algorithm.

The remaining gains (1, 6, and 7) have significant mean values and do vary as functions of flight conditions. The second step in scheduling these gains is to determine flight conditions with which they are correlated.* The search for gain/flight variable dependencies begins by determining correlation coefficients between the gains and all available flight variables. One method of determining the correlation coefficient between a set of gains (dependent variables) and flight variables (independent variables) is given by the following (Ref. 58):

$$\rho(k,d) = \frac{|\mathrm{cov}[k,d]|}{\sigma(k)\,\sigma(d)} = \frac{\left|\sum_{i=1}^{N}(k_i-k)(d_i-\bar{d})\right|}{\sqrt{\sum_{i=1}^{k}(k_i-\bar{k})^2}\sqrt{\sum_{i=1}^{N}(d_i-\bar{d})^2}} \qquad (6.2\text{-}23)$$

*Two variables are correlated if, by observing the value of one variable, a conclusion can be drawn about the value of the other variable.

In Eq. (6.2-23), N is the number of flight conditions for which the gains are known, k_i is the value of the gain observed at flight point i, and d_i is the measured value of the flight variable at flight point i. The variable, $\bar{k}$, is the mean value of the gain, and $\bar{d}$ is the mean value of the flight variable. The closer the value of the correlation coefficient, ρ, is to one, the better the correlation between the gain and the flight variable.

The independent flight variables considered for gain correlation in the current study are true airspeed (TAS), atmospheric pressure ratio (δ), weight divided by pressure ratio (W/δ), weight divided by dynamic pressure (W/q), and angle of attack (α). While by no means an exhaustive set, these flight variables represent major dynamic variations with vehicle flight conditions.

In addition to determining the correlation coefficients for the flight variables stated, correlations between the guidance gains and functions of the flight variables such as the square, the inverse, the inverse square, etc., of each flight variable can be obtained. Also, correlation coefficients relating the gains and a <u>combination</u> of the flight variables can be determined assuming the following functional dependency:

$$\hat{k} = b_0 + b_1 d_1 + b_2 d_2 + \ldots + b_n d_n \qquad (6.2\text{-}24)$$

where $\hat{k}$ is the computed guidance gain, d_1 to d_n are the flight variables, and the coefficients, b_i, provide the "best" gain estimate as a function of the varying flight variables. The estimate provided by the b_i is "best," in that it provides a least-squares fit to the data points. That is, the $\hat{k}_i$ are computed to minimize the following cost function:

$$J = \sum_{i=1}^{N} (k_i - \hat{k}_i)^2 \qquad (6.2\text{-}25)$$

The techniques for determining the functional coefficients, b_i, as well as the correlation coefficients for the multiple flight condition relationships are detailed in Ref. 57.

A summary of the correlation coefficients for the three guidance gains ($\Delta\theta/\Delta V$, $\Delta T/\Delta\gamma$, $\Delta T/\Delta h$) of interest here is presented in Table 17. Correlation coefficients are shown for those flight variables which are highly correlated with these gains. The first gain $\Delta\theta/\Delta V$, correlates strongly with both W/q and α. Because α may be a difficult quantity to measure in flight, it would not be unreasonable to schedule $\Delta\theta/\Delta V$ as a function of W/q only. The sixth guidance gain, $\Delta T/\Delta\gamma$ also correlates most strongly with W/q. The combination of W/q and α does not, in fact, yield a larger correlation for this gain.

TABLE 17

GUIDANCE GAIN CORRELATION COEFFICIENTS

Gain	Flight Conditions			
	W/q	α	$(1/TAS)^2$	W/q, α
1. $\Delta\theta/\Delta V$	0.83	0.89	0.81	0.89
2. $\Delta T/\Delta\gamma$	0.93	0.90	0.83	0.93
3. $\Delta T/\Delta h$	0.26	0.51	0.45	0.80

The gain relating throttle commands to altitude deviations, $\Delta T/\Delta h$, has its strongest single-flight-variable correlations with α and with $(1/TAS)^2$. The correlation of $\Delta T/\Delta h$ with a linear combination of these two variables did not show any improvement; however, the correlation of $\Delta T/\Delta h$

with the combined flight variables, W/q and α, correlated significantly, with a coefficient equal to 0.80.

Employing W/q to schedule both $\Delta\theta/\Delta V$ and $\Delta T/\Delta h$ and the combination of W/q and α to schedule $\Delta T/\Delta h$ results in the following gain scheduling equations:

$$\Delta\theta/\Delta = 2.994\times10^{-2} - 2.344\times10^{-5}\ W/q \qquad (6.2\text{-}26)$$

$$\Delta T/\Delta\gamma = 0.5245 - 6.707\times10^{-4}\ W/q \qquad (6.2\text{-}27)$$

$$\Delta T/\Delta h = 0.5257\times10^{-2} - 0.1755\times10^{-4}\ W/q + 0.4386\times10^{-2}\ \alpha \qquad (6.2\text{-}28)$$

In the above equations, the coefficients of the flight variables are those obtained from the polynominal regression analysis described in Ref. 57. The gain $\Delta\theta/\Delta V$ has units of deg/fps, while the gains $\Delta T/\Delta\gamma$ and $\Delta T/\Delta h$ have units of percent/deg and percent/ft, respectively. The flight variable W/q is expressed in units of ft^2, and α is measured in degrees. The use of these coefficients provides for the correlations between the guidance gains and flight variables presented in Table 6.2-2.

This section has described a means by which the linear-optimal guidance gains can be scheduled in an adaptive fashion. This enables the use of these gains in an on-board guidance algorithm. The results presented provide reasonably good correlations between the gains and flight conditions. Better correlations could be obtained by employing more independent flight variables and using higher-order polynomial representations. The purposes of this section are served, however, by the demonstration of the application of the correlation-coefficient gain-scheduling method to the fuel-optimal perturbation guidance problem.

6.3 STRUCTURE OF THE THROTTLE/ENERGY MANAGEMENT ALGORITHM

The previous section has shown how the fuel-minimizing guidance algorithm can be separated into two parts: the generation of a desired flight path, $\underline{x}_D$, and its associated nominal guidance variable, $\underline{u}_D$; and the correction of flight path errors using a linear guidance law

$$\Delta\underline{u} = -K\Delta\underline{x} = -K(\underline{x}_D - \underline{x}) \qquad (6.3\text{-}1)$$

The total guidance command, $\underline{u}_C$, is the sum of the nominal value and the linear perturbation:

$$\underline{u}_C = \underline{u}_D + \Delta\underline{u} \qquad (6.3\text{-}2)$$

It can be seen in Eq. (6.3-2) that the guidance command has an open-loop component, $\underline{u}_D$, which corresponds to the trim values of pitch angle, θ, and throttle setting, T, plus the closed-loop component, $\Delta\underline{u}$, derived from the feedback of the difference between the desired and actual state to the pitch and throttle channels. The result is a combined autopilot/autothrottle command which provides coordinated control of altitude and velocity.

The guidance commands, θ_C and T_C, should be considered as set points for the inner-loop control law. Thus, it is assumed that the throttle/energy management logic is followed by pitch attitude and throttle setting regulators, as shown in Fig. 36. Typically, the pitch channel would use attitude and rate feedback, while the throttle channel could use Engine Pressure Ratio, EPR, and low-speed compressor RPM, N_1.

Figure 36 illustrates the basic features of the throttle/energy management structure. The desired flight

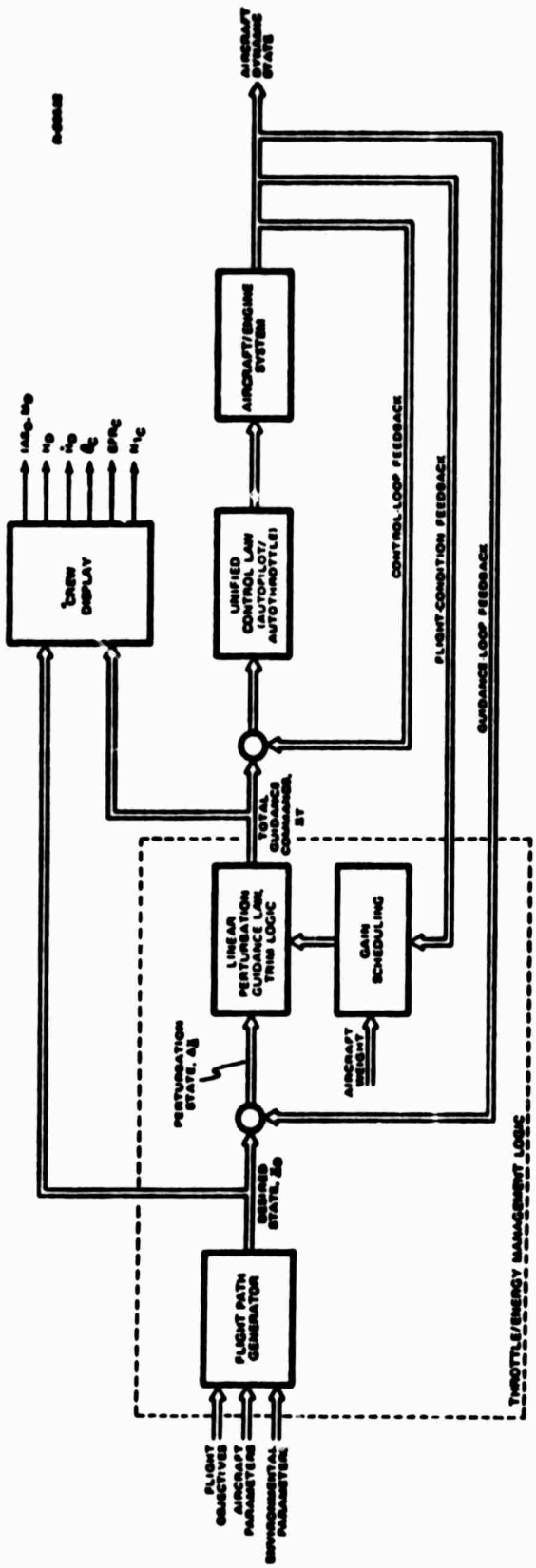

Figure 36 Fuel-Optimal Throttle/Energy Management

path is specified by the flight path generator logic, which is discussed below. The linear perturbation guidance law and gain scheduling were discussed in the previous section, and the trim logic is presented in this section. Requirements for crew display appear in a later section. The advantages of this guidance structure are that

- The system generates near-optimal flight paths;
- These flight paths are followed using reasonable commands; and
- The throttle/energy management is directly applicable to all large transport and bomber aircraft, although the present results are numerically specific to the C-141A.

It is important that this guidance structure be implemented in a practical way, if it is to be used on an operational basis. This means that fuel-optimal flight paths must be stored in an efficient manner while providing sufficient adaptability to changing flight conditions and flexibility with respect to mission constraints. Unless reasonable simplifications are made in the storage and computation of the $\underline{x}_D$ and $\underline{u}_D$ profiles, the computer burden of the throttle/energy management algorithm could be excessive. This section illustrates that partitioning each mission into flight path segments leads to efficiency in specifying $\underline{x}_D$, while using trim integrators to compute $\underline{u}_D$ is consistent with managing fuel use with a simple system.

6.3.1 Trim Computation

The ad hoc guidance logic used to generate parametric-optimum and reference flight paths (Chapter 3) provides the design algorithm for the trim logic (for those

flight conditions in which the trim settings are not defined explicitly). Integrating these rate-command guidance laws (Eqs.(3.4-1) and (3.4-2)) leads to

$$\theta_C = k_{\theta_1} \int (V_D - V)dt + k_{\theta_2}(V_D - V) \qquad (6.3\text{-}3)$$

$$T_C = k_T \int (E_D - E)dt \qquad (6.3\text{-}4)$$

The linear-optimal guidance laws derived in the previous section (Eqs.(6.2-19) and (6.2-20)) provide disturbance rejection by using proportional feedback. Dropping the proportional term in Eq. (6.3-3), the ad hoc guidance laws provide integral compensation which assures zero steady-state error in following the aircraft's velocity and specific total energy. The trim values, θ_D and T_D, corresponding to the desired flight path are computed by

$$\theta_D = k_{\theta_D} \int (V_D - V)dt \qquad (6.3\text{-}5)$$

$$T_D = k_{T_D} \int (E_D - E)dt \qquad (6.3\text{-}6)$$

where $k_{\theta D}$ and k_{T_D} are chosen to provide trim adjustment times which do not conflict with the proportional perturbation guidance. (For example, the gain $k_{\theta D}$ is chosen to be a small percentage of the value of $\Delta\theta/\Delta V$ given in Eq. (6.2-26). Since both velocity and altitude contribute to E (Eq. (3.4-3)), k_{T_D} is small compared to both $\Delta T/\Delta V$ and $\Delta T/\Delta h$ in Table 16 and Eq. (6.2-28).

The trim logic should be relatively insensitive to the oscillatory phugoid mode for several reasons. The gains in Eqs.(6.3-5) and (6.3-6) are small, and periodicities in the

integrands will be averaged out. Furthermore, the phugoid mode is a constant-energy oscillation, and it should be largely unobservable in the integrand of the throttle equation. Finally, the perturbation guidance law augments damping of the phugoid mode.

6.3.2 Fuel-Minimizing Flight Path Segments

Integrated flight profiles must be computed to determine the fuel-optimal means of flying from one point to another, but once these profiles are understood, distinct flight path segments can be identified and used as the basis for real-time implementation. The segments are useful because not every parameter is significant to fuel use in every segment; hence, efficiency is gained by using the minimum number of appropriate parameters to define each segment.

It has been shown that there are two basic flight path segments for short-range trajectories (climb and descent) and three segments for longer trajectories (climb, cruise, and descent). Figure 37 illustrates that 8 segment types can be defined for a throttle/energy management system. These are

- Takeoff-Climb Transition
- Climb
- Climb-Cruise Transition
- Cruise
- Step Climb
- Cruise-Descent Transition
- Descent
- Descent-Approach Transition

The following paragraphs describe the major features of each segment. In every case, V represents true airspeed

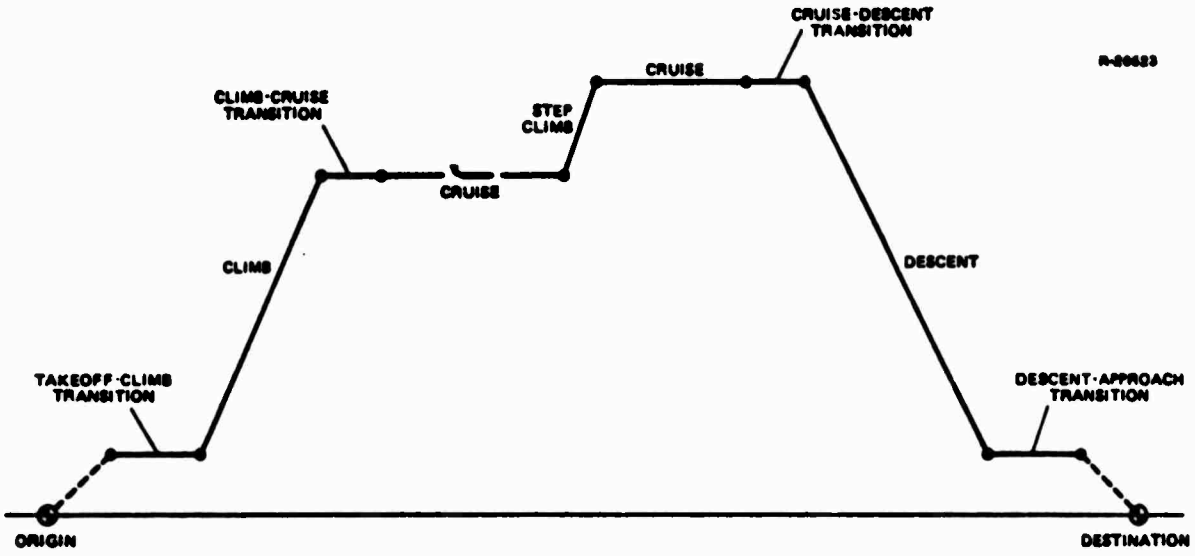

Figure 37 Flight Path Segments for the Throttle/ Energy Management System

(TAS), and h is the pressure altitude. It is assumed that estimates (or measurements) of weight, range to go, wind speed, and sea level pressure are available as each segment progresses. In many cases, indicated airspeed (IAS) or Mach number is a more useful variable than TAS; hence, V typically is a function of h. Numerical definitions which support these descriptions are given in the next section.

Takeoff-Climb Transition - This segment is initiated when the landing gear and flaps are fully retracted and when the throttle/energy management system is enabled by the crew. It lasts for approximately one minute. Desired values of the state and control variables initially are as follows:

- $V_D = V$, i.e., the current value

- $\dot{h}_D$ = Zero to current value
- h_D = Constant to current value
- θ_D = Value which provides horizontal flight (trim off)
- T_D = 1.0 (trim off)

Velocity-error feedback and perturbation throttle commands are suppressed; hence, the throttle command is entirely "open-loop", and perturbation pitch angle regulates altitude as velocity is increasing. During the initial phase of the transition, θ_D decreases as velocity increases.

During the climb phase, θ is used as a velocity control, and h is treated as an independent variable; therefore, a gradual change in the function of θ must be accomplished as the climb speed is approached. The change process is called "fade out/fade in", and it is obtained by interpolation of V_D, $\dot{h}_D$, and h_D. Assume that the fade-out/fade-in time is t_{F_c} sec and that the vehicle is accelerating at a rate of $\dot{V}$. The change begins at time, t_c, when the measured velocity is

$$V(t_c) = V_{D_{CLIMB}} - \dot{V}(t_c)t_{F_c} \tag{6.3-7}$$

At the beginning of the change, V_D is $V(t_c)$, $\dot{h}_D$ is zero, and h_D is the altitude at the beginning of the transition. During the transition, θ_D is fixed at $\theta_D(t_c)$, and

$$V_D(t) = V(t_c) + \dot{V}(t_c)\ \Delta t/t_{F_c} \tag{6.3-8}$$

$$\dot{h}_D(t) = \dot{h}(t)\ \Delta t/t_{F_c} \tag{6.3-9}$$

$$h_D(t) = h_D(t_c) + [h(t)-h_D(t_c)]\Delta t/t_{F_c} \tag{6.3-10}$$

where

$$\Delta t = t - t_c \tag{6.3-11}$$

In other words, the desired velocity gradually takes its climb value, and $\dot{h}_D$ and h_D gradually become the current values (nullifying the errors in the perturbation guidance equations). The transition is complete when $\Delta t = t_{F_C}$.

Climb - This segment begins when the IAS has reached its initial climb value, and it lasts for 15 to 40 min (depending on vehicle weight), the initial cruising altitude (for long-range flight paths), and the transition to descent (for short-range flight paths). Desired values of the state and control variables are the following:

- V_D = Value which yields constant IAS or M, as defined below
- $\dot{h}_D$ = Current value of h
- h_D = Independent variable
- $\theta_D = k_{\theta D} \int (V_D - V) dt$ (trim on)
- T_D = 1.0, or piloted-selected reduced setting (trim off)

V_D is a function of vehicle weight, throttle setting, altitude, air temperature, mission range, and air traffic control constraint. At most, there are three sub-segments of the velocity profile:

- V_D provides 250 KIAS below 10,000-ft altitude.
- V_D provides optimal IAS until M = 0.721.
- V_D provides M = 0.721 until cruise condition is reached.

The first segment is absent if ATC approval for higher speed is obtained, or if the optimal IAS is less than 250 KIAS (as is the case for light vehicles). The third segment is absent on short-range missions which do not reach cruising conditions. As shown in Chapter 4, the optimal IAS during

climb increases as vehicle weight increases, and the climb IAS is increased for short-range missions without cruise segments; the desired value is computed taking these factors into account. It also can be shown, using energy-state methods, that climb IAS is approximately proportional to the square root of engine thrust; therefore, a 10-percent thrust reduction should be accompanied by a 5-percent speed reduction. Climb thrust reduction increases fuel use but may be selected for reasons of reduced engine wear or in an engine-out condition. In addition, the crew should have the option of specifying desired values of IAS and M for comparative testing.

Initialization logic in the throttle/energy management system must determine whether or not each mission contains a cruise segment. If cruise is absent, the descent-initiation prediction procedure described in Section 6.3.3 must be executed during the climb segment. If cruise is present, the decision to switch to climb-cruise transition is made in the climb segment. The switch is made when the time to climb to cruise altitude (either computed from W/δ or specified by the crew) equals the desired transition time, assuming that the climb proceeds at $\dot{h}_D$. If cruise is absent, the climb-cruise transition is immediately followed by cruise-descent transition, and it is selected on the basis of range to go.

Altitude and altitude-rate errors are suppressed in the linear $\Delta\theta$ and ΔT controllers because altitude is used as the independent variable for climb; therefore, the present altitude <u>is</u> the desired value, and the error is zero. Throttle commands are limited to 1.0 or less. When climbing at normal-rated thrust ($T_D = 1.0$), negative ΔT commands are executed, but positive ΔT commands are not. For $T_D < 1.0$, perturbation

commands of both signs are issued up to the point that $T_C = 1.0$.

Climb-Cruise Transition - This segment begins when the climb-segment prediction indicates that cruise is imminent. The dominant features of this segment are the adjustment of velocity to cruise value, the reduction of climb rate, and the achievement of the desired initial altitude for cruising flight. The principal functions of this segment are to "fade out" climb desired values and to "fade in" cruise desired values using transition interpolation; therefore, the cruise option selected by the crew (described below) must be accessible during this segment and should be used to compute initial values of the desired cruising flight variables. Given this information plus the range to the final destination, the desirability of step climbs during cruise should be evaluated. The transition segment is complete when velocity and altitude reach their respective cruise values.

Assuming a transition time of t_{F_k}, the desired velocity changes from the climb value, $V_{D_{CL}}$, at time, t_k, to the cruise value, $V_{D_{CR}}$:

$$V_D(t) = V_{D_{CL}} + (V_{D_{CR}} - V_{D_{CL}})\Delta t/t_{F_k} \qquad (6.3\text{-}12)$$

where

$$\Delta t = t - t_k \qquad (6.3\text{-}13)$$

while the altitude-rate and altitude errors are established by fading in the desired cruise values, $\dot{h}_{D_{CR}}$ and $h_{D_{CR}}$:

$$\dot{h}_D(t) = \dot{h}(t) + [\dot{h}_{D_{CR}} - \dot{h}(t)]\Delta t/t_{F_k} \qquad (6.3\text{-}14)$$

$$h_D(t) = h(t) + [h_{D_{CR}} - h(t)]\Delta t/t_{F_k} \qquad (6.3\text{-}15)$$

The transition should begin early enough to prevent an altitude overshoot with the established climb rate and closed-loop guidance response. Section 6.2 indicates that $\Delta\gamma$ response (which is equivalent to $\Delta\dot{h}$ response) of the perturbation controller is rapid; therefore, t_k can be chosen on the basis of load factors required to reduce $\dot{h}$ from the climb value to the cruise value.

On a short-range flight, the climb-cruise transition is followed immediately by the cruise-descent transition. In this case, the primary function of the climb-cruise transition is to arrest the climb rate and to begin throttle reduction. A nominal reduction in desired velocity should be specified for $V_{D_{CR}}$, along with zero value for $\dot{h}_{D_{CR}}$ and current altitude for $h_{D_{CR}}$.

Cruise - Three options are implemented in the cruise segment logic:

- Breguet Climbing Cruise
- Constant-Altitude Cruise With Optimal (Varying) Velocity
- Constant-Altitude Cruise with Constant Velocity

In the first option, h_D increases to maintain W/δ at its optimal value, and V_D is chosen to maintain optimal M. Optimal W/δ is a function of c.g. location, drag coefficient, and air temperature, while optimal M is a function of air temperature and wind speed. Mach number decreases in constant-altitude cruise for the second option, providing a relative-optimum condition as fuel is burned and W/δ varies. The third option allows a conventional cruise segment to be flown automatically for comparative purposes.

Subject to these options, the desired values of the state and control variables are as follows:

- V_D = Value which yields desired IAS or M, as defined above
- $\dot{h}_D$ = 0, or function of V_D and h_D in climbing cruise (Section 6.3.3)
- h_D = Value which provides optimal W/δ, or constant, as defined above
- $\theta_D = k_{\theta_D} \int (V_D - V)dt$ (Trim on)
- $T_D = k_{T_D} \int (E_D - E)dt$ (Trim on)

The full perturbation guidance algorithms (Eq. (6.2-19) and (6.2-20)) are implemented for altitude and velocity control during the cruise phase.

A particular cruise segment can end in one of two ways: a step climb (followed by another cruise segment) or a descent. Background computations to predict when either segment change could occur should be conducted during the cruise segment. The step climb prediction is computed only during constant-altitude cruise, and it is assumed that the climb must occur in a 4,000-ft increment. The current aircraft weight, c.g. location, air temperature (adjusted to account for standard lapse rate), and any known variation in the particular aircraft's drag coefficient, are used to compute the optimal W/δ and the corresponding pressure altitude. A step climb is indicated when the optimal altitude is 2,000 ft above the current h_D. Prediction of the descent initiation is carried out by estimating the range increment during descent plus the range increment during cruise-descent transition and subtracting the result from the range to go (Section 6.3.3).

Although each prediction is individually useful, the two can be used together to decide whether or not a step climb is desirable. Following the 4,000-ft climb, the aircraft will be 2,000 ft above its optimal altitude. The step climb produces measurable fuel savings if the aircraft spends enough time at the higher altitude for the fuel burnoff to make the new altitude optimal. Otherwise, the fuel consumed in gaining potential energy is not offset by the improved specific range. If the range to be flown to descent initiation (computed for the higher altitude) would not require sufficient fuel burnoff, then the step climb should not be made.

Step Climb - The procedures followed during the step climb are similar to those of the earlier climb segment. Altitude again is the independent variable, full throttle is used, and pitch trim is engaged. Referring to Fig. 10, it can be seen that the optimal Mach number on the higher constant-altitude cruise segment will be greater than it was on the lower cruise segment (since the relative-optimal M is defined by the zero-slope tangencies on the constant-specific range contours, Fig. 10); therefore, V_D should increase linearly during the step climb to match the relative-optimal cruise points at the beginning and end of the climb.

Cruise-Descent Transition - This important flight path segment is a near-constant-altitude, minimum-throttle deceleration from the cruise Mach number to the IAS required for $(L/D)_{max}$ descent. The primary objective of this segment is to provide a smooth transition which does not excite the phugoid mode. (The latter would lead to velocity-altitude oscillations, which would be perceived as load-factor oscillations by passengers and the crew.) Unlike the takeoff-climb and climb-cruise transitions, the distance

travelled during the transition is important for flight path management. The descent initiation point, i.e., the start of the cruise-descent transition, must be predicted for maximum fuel savings, so the transition range increment should be designed to be easy to compute. This infers that the transition velocity profile, which is integrated to obtain wind-relative distance travelled, should be well-defined and followed closely.

Desired state and control variables for the cruise-descent transition are the following:

- V_D = Cruise V_D to descent V_D
- $\dot{h}_D$ = Zero to descent value
- h_D = Cruise altitude to descent value
- $\theta_D = k_{\theta_D} \int (V_D - V)dt$ (Trim on)
- $T_D = k_{T_D} \int (E_D - E)dt$ (Trim on)

This segment can be sub-divided into the <u>throttle-down</u> and <u>deceleration</u> phases, both of which involve fade-out/fade-in logic. In the first phase, the total throttle command is reduced linearly from its cruise setting, T_C, to the descent setting (normally idle), T_M, over a period of t_{F_t} sec. Assuming the transition begins at t_t,

$$T_C(t) = T_C(t_t) - [T_C(t_t) - T_M]\Delta t_t / t_{F_t} \qquad (6.3\text{-}16)$$

where

$$\Delta t_T = t - t_t \qquad (6.3\text{-}17)$$

T_D is ignored during the throttle reduction and reinitialized to zero at the end of the phase. During the throttle-down

there is a nominal decrease in V_D to the value V_{D_t}, $\dot{h}_D$ is zero, and h_D is the cruise altitude. During the deceleration the desired velocity decreases from V_{D_t} to V_{D_d} and $\dot{h}_D$ and h_D are faded to the initial descent values over a period of t_{F_d} sec using Eq. (6.3-9) and (6.3-10).

Descent - Guidance during the descent is analogous to guidance during the climb, but there is an additional function to be conducted: range control. If the descent has been initiated at the proper point, then the vehicle will arrive at the terminal altitude and range with no error; however, it is more likely that disturbances would cause the vehicle to miss the terminal condition in an open-loop descent. It is necessary, therefore, to minimize position errors as well as fuel use during this trajectory segment. By reducing flight path errors early in the descent, range control allows operational constraints to be satisfied with a minimal fuel penalty.

The basic descent profile is a maximum lift-to-drag ratio flight path with throttle set at idle. (Reference 47 indicates that air conditioning and pressurization can be maintained at idle throttle, so there is no need to consider powered descent.) This is a maximum-range glide path; in the absence of wind, the corresponding constant flight path angle, γ_{opt}, is

$$\gamma_{opt} = -\cot^{-1}(L/D)_{max} \qquad (6.3\text{-}18)$$

which is independent of aircraft weight. Consequently, there is a straight-line relationship between altitude and range on the optimal descent path, and it, too, is independent of weight. Calling the range to go (to reach the destination), R_{GO}, and the terminal altitude, h_{GO}, the desired altitude is

$$h_D = h_{GO} - R_{GO} \tan \gamma_{opt}$$

$$= h_{GO} + \frac{R_{GO}}{(L/D)_{max}} \qquad (6.3\text{-}19)$$

The associated altitude rate is a function of weight, as is the time to go, t_{GO}, because the dynamic pressure (and, therefore, the indicated airspeed) required to maintain "1-g" flight varies. The desired altitude rate is

$$\dot{h}_D = -V_D \sin\gamma_{opt} \qquad (6.3\text{-}20)$$

where

$$V_D = \sqrt{\frac{2W\cos\gamma_{opt}}{C_{L_{opt}} \rho S}} \qquad (6.3\text{-}21)$$

and $C_{L_{opt}}$ is the lift coefficient at $(L/D)_{max}$. Note that the specific total energy during descent is fully defined by Eq. (6.3-19) and (6.3-21).

The descent flight path must be adjusted for wind effects. The air-relative variables are unchanged, but the effective flight path angle, γ_E, is made shallower by tail winds ($V_w>0$) and steeper by head winds ($V_w<0$). Since $\tan \gamma_E = -\dot{h}/\dot{R}$,

$$\gamma_E = -\tan^{-1}[\dot{h}_D/(V_D\cos\gamma_{opt}+V_w)] \qquad (6.3\text{-}22)$$

and, assuming a constant wind profile,

$$h_D = h_{GO} - R_{GO}\tan\gamma_E \qquad (6.3\text{-}23)$$

The desired state and control variables are then defined by

- V_D = Eq. (6.3-21)
- $\dot{h}_D$ = Eq. (6.3-20)

- h_D = Eq. (6.3-23)
- $\theta_D = k_{\theta_D}\int(V_D-V)dt$ (Trim on)
- $T_D = k_{T_D}\int(E_D-E)dt$ (Trim on)

There are two choices for descending through a varying wind profile: either update γ_E as the variations occur or use an average value of V_w to compute a fixed descent path. The first approach is more nearly fuel-optimal, but the second produces a more predictable path and is, therefore, more compatible with air traffic control.

The full perturbation guidance algorithms are employed during descent. For the most part, it can be assumed that pitch control will be used when the vehicle is flying "long" (i.e., above or faster than the nominal flight path) and that throttle control will be used when the vehicle is flying "short" (the opposite). In the first case, $E > E_D$, which normally would decrease T_D: however, T_D is nominally zero and cannot become smaller, so θ_D will increase to lower the specific kinetic energy ($V^2/2g$). In the second case, $E < E_D$, and the vehicle does not possess sufficient energy to glide to its destination. T_D will increase to provide the necessary energy.

Descent-Approach Transition - Once the vehicle has descended from altitude, the sink rate must be arrested to restore the aircraft to level flight. The descent-approach transition can be regarded as establishing a low-altitude cruise condition by increasing throttle setting and pitch angle. The desired state and control variables at the end

of the transition are:

- V_D = Pilot-selected value
- $\dot{h}_D = 0$
- h_D = Pilot-selected value
- $\theta_D = k_{\theta_D} \int (V_D - V)dt$ (Trim on)
- $T_D = k_{T_D} \int (E_D - E)dt$ (Trim on)

The fade-out/fade-in logic used for the climb-cruise transition can be used here as well. The guidance algorithm enters a cruise segment at the completion of the transition.

6.3.3 Computational Details

Additional aspects of the throttle/energy management algorithm are introduced here. These include generation of the nominal flight paths, prediction of the descent initiation point, computation of descent speed, and support calculations for crew display and throttle control interface.

Nominal Profiles - In order to provide efficient storage of data, nominal flight profiles are stored in natural dimensions, and auxiliary calculations are implemented where necessary. Rather than storing true airspeed, which is only indirectly related to energy management, nominal values of indicated airspeed and Mach number are stored, as appropriate. Similarly, W/δ is stored in place of altitude. Nonzero values of altitude rate are used only in the descent and Breguet-cruise guidance algorithms. If future testing indicates the need for improved damping during

climb, the $\dot{h}_D$ required to form the feedback error can be computed from aircraft characteristics, V_D, and h_D. During a constant-IAS segment,

$$\dot{h}_D = \frac{V_D}{W}\left[\frac{F-C_D S\rho V_D^2/2}{\left(\frac{\beta h_D}{2g} V_D^2+1\right)}\right] \qquad (6.3\text{-}24)$$

where F is engine thrust, and air density (ρ) and scale height (β) are functions of h_D. During a constant-M segment, only potential energy changes (neglecting the effects of sound-speed variation on M), leading to

$$\dot{h}_D = \frac{V_D}{W}\ (F-C_D S\rho V_D^2/2) \qquad (6.3\text{-}25)$$

If the aircraft is climbing at constant M to keep W/δ constant,

$$\dot{h}_D = \frac{\dot{W}}{(W/\delta)\ \frac{\partial\delta}{\partial h}} \qquad (6.3\text{-}26)$$

Chapter 4 has indicated that IAS, M, and W/δ are smoothly varying functions of flight conditions and vehicle characteristics; therefore, these quantities are most easily stored in functional form. The algorithms used to develop gain schedules in Section 6.2 can be employed to schedule desired values of IAS, M, and W/δ as functions of the major variables.

Descent Initiation Prediction - The point at which the cruise segment ends and the descent begins must be computed precisely if maximum fuel savings are to be realized. Given the cruise conditions during medium- to long-range flight and the climb conditions during short-range flight,

the descent should be initiated when R_{GO} equals the sum of four incremental ranges:

- Climb-cruise transition range (short-range flight path only)
- Throttle-down range
- Deceleration range
- Idle thrust descent range

On a short-range mission, the descent is initiated during the climb, and the climb-cruise transition segment is used to arrest the climb rate. The range travelled during this segment is approximately

$$R_0 = [V_{w_0} + (V_{D_{CL}} + V_{D_{CR}})/2]t_{F_k} \qquad (6.3\text{-}27)$$

where V_{w_0} is the prevailing wind velocity.

The throttle-down velocity and range can be computed using an analytical expression for the deceleration which occurs during a linear decrease in throttle setting. Assuming C_D and altitude remain constant during the throttle reduction,

$$\dot{V} = -k_t \Delta t_T V^2 \qquad (6.3\text{-}28)$$

where Δt_T is defined by Eq. (6.3-17), and

$$k_t = C_D \rho S/2mt_{F_t} \qquad (6.3\text{-}29)$$

Calling the initial and final velocities, $V_{D_{CR}}$ and V_{D_t}, Eq. (6.3-28) is integrated to obtain

$$V_{D_t} = V_{D_{CR}}/(1+V_{D_{CR}} k_T t_{F_t}^2/2) \qquad (6.3\text{-}30)$$

and the corresponding ranges, R_0 and R_1,

$$R_1 = R_0 + \sqrt{\frac{2V_{D_{CR}}}{k_t}} \tan^{-1} \sqrt{\frac{V_{D_{CR}} k_t}{2}} \; t_{F_t} \qquad (6.3\text{-}31)$$

Next, the vehicle must decelerate from V_{D_t} to the desired initial velocity for descent, V_{D_d}. The deceleration model is

$$\dot{V} = -k_d V^2 \qquad (6.3\text{-}32)$$

where

$$k_d = C_D \rho S/2m \qquad (6.3\text{-}33)$$

Equation (6.3-32) is integrated once, implicitly defining the deceleration time, t_{F_d}, and again to obtain the range at the end of deceleration, R_2:

$$V_{D_d} = V_{D_t}/(1+V_{D_t} k_D t_{F_d}) \qquad (6.3\text{-}34)$$

$$R_2 = R_2 + \left(\frac{1}{k_d}\right) \ln \left(\frac{V_{Dt}}{V_{Dd}}\right) \qquad (6.3\text{-}35)$$

The range increment during deceleration, R_{w_t} due to the prevailing wind, V_{w_t}, is

$$R_{w_t} = V_{w_t}(t_{F_t}+t_{F_d}) \qquad (6.3\text{-}36)$$

The range travelled during descent is obtained from the developments of Section 6.3.2. The wind-free range increment during descent is

$$R_3 = (h-h_{GO})(L/D)_{max} \qquad (6.3\text{-}37)$$

assuming that the current altitude, h, and the altitude following deceleration are the same. The wind effect during descent is a function of the descent time as well as the wind speed. The descent (glide) time, t_g, can be approximated by

$$t_g = \frac{2}{k_g \beta} \left(e^{-\beta h/2} - e^{-\beta h_{GO}/2} \right) \qquad (6.3\text{-}38)$$

where

$$k_g = \sqrt{\frac{2W\cos\gamma_{opt}}{C_{L_{opt}} \rho_{GO} S}} \sin\gamma_{opt} \qquad (6.3\text{-}39)$$

and W is the average value of aircraft weight during the descent. Variations in atmospheric temperature and pressure can be reflected in the values of scale height, β, and air density at the destination altitude, ρ_{GO}. With an average wind of V_{w_g} during descent, the wind-induced range increment is

$$R_{w_g} = V_{w_g} t_g \qquad (6.3\text{-}40)$$

The total range increment from descent initiation to destination is

$$R = R_1 + R_2 + R_3 + R_{w_t} + R_{w_g} \qquad (6.3\text{-}41)$$

and the descent is initiated when $R \geq R_{GO}$. The descent range and range to go should be evaluated at frequent intervals so that the segment switch occurs at the proper time.

Crew-Display and Throttle Control Interface - Although throttle settings are computed (as a function of the available normal rated thrust), the principal indicators of engine thrust on the C-141A are engine pressure ratio (EPR) and low-speed compressor RPM (N_1). For the crew to exercise manual throttle/energy management or for an automatic control closure to operate most effectively, the proper values of EPR and N_1 should be computed. (The computations are optional for the

automatic system, as the throttle trim integrator provides the appropriate steady-state throttle setting with or without knowledge of EPR and N_1.) The necessary transformations are presented graphically in Ref. 32, and supplemental information is contained in Ref. 47. The two transformations can be stored as functions of air temperature and altitude, taking anti-ice and other engine bleed air requirements into account.

6.4 SYSTEM SYNTHESIS

The throttle/energy management structure has been defined for a fully automatic system, as shown in Fig. 6.3-1, but the figure also suggests alternatives for manual participation. There are four levels at which fuel-minimizing throttle/energy management can be implemented:

- Handbook/Calculator Flight Path Computation (Level 1)
- Automatic Flight Path Display (Level 2)
- Automatic Flight Path and Command Display (Level 3)
- Automatic Throttle/Energy Management (Level 4)

To implement Level 1, the functions conducted in the Flight Path Generator are assembled in handbook format, and supplemental computations are defined for a programmable electronic calculator. The crew is required to make pre-flight calculations, to read aircraft instruments in flight, to compute desired flight variables, and to follow V_D, $\dot{h}_D$, and h_D with standard piloting procedures. As in the case of current EPR setting (Ref. 47), computations should be made at 5,000-ft intervals during the climb until

the climb rate has decreased below 1,000 ft/min, when more frequent computations are warranted. A similar schedule should be followed during descent. During cruise, computations should be made at 30-min intervals (Ref. 35), with decreased intervals as the descent initiation point is approached.

The need for data lookup and computation by the crew is eliminated in Level 2 implementation, as the throttle/energy management computer generates V_D, $\dot{h}_D$, and h_D from stored data and crew inputs. The computer operates without direct input of flight data from aircraft sensors, so it is necessary for the crew to enter (manually) all mission-specific data. (Aircraft-specific data is stored within the computer.) Computer outputs occur on a continuous basis, and they are followed with standard piloting procedures. The Level 2 system provides a major reduction in crew workload, and it is independent of all aircraft systems. Conceptually, the Level 2 system can be contained in a standard minicomputer which is supported by a standard keyboard-input/alphanumeric-output terminal device.

The Level 3 system incorporates feedback information from aircraft sensors. The crew workload is reduced further, and the throttle/energy management system displays V_D, $\dot{h}_D$, h_D, θ_c, and T_c (or EPR_c and N_{1c}). Crew interaction with the Level 3 system consists of mission definition, mode switching, and standard piloting procedures (aided by suggested settings for pitch angle and throttle, which are computed by the perturbation guidance law and the trim integration). This implementation automatically performs all of the fuel-minimizing throttle/energy management functions, but it leaves the piloting to the pilot. The Level 3 logic is contained in a flight computer, which is supported by real-time peripheral input devices as well as the crew terminal.

The Level 4 system is fully coupled to autopilot/autothrottle actuators (via inner-loop regulators), although the system monitors provide a Level 3 capability as an option. As in the previous case, the crew must provide mission and mode information, but the pilot relinquishes inner-loop control to the automatic system under normal flying conditions. He retains full authority to change flight level and Mach number during cruise, to step climb, to command alternate climb and descent speeds, to modify data in flight (e.g., to change the destination location, terminal altitude, or airspeed, or to respecify aircraft weight and c.g. location following an air drop), or to assume total control in an emergency.

Although not considered in the current study, the throttle/energy management algorithm can be expanded readily to a 4-D guidance law. Lateral guidance requires the addition of heading and cross-track information, leading to roll-angle commands. Time-slot control is affected by altering V_D. Fuel-minimizing guidance is totally compatible with air traffic control and with the stringent requirements of time-based navigation.

The remainder of this section is devoted to the requirements for implementation of an experimental Level 4 throttle/energy management system, including crew interface, sensors and actuators, digital flight computer, and software development.

6.4.1 Crew Interface Requirements

At a minimum, the Level 4 system requires an alphanumeric display for crew monitoring of system performance and

a keyboard for mission data input, mode switching, and experimental procedures. Manual piloting in the Level 3 mode would be aided by a graphical or flight director display, and various control functions can be implemented with dedicated switches. The following complement would be useful in an experimental system, with P indicating location at the pilot's station and E representing the flight engineer's station:

- CRT display, or flight director/LED display (P)
- Switch panel (P)
- CRT display (E)
- Full keyboard (E)

An example of a display/keyboard panel for the pilot's station using a cathode-ray tube (CRT) and calculator-button-type input is illustrated in Fig. 38. Actual and desired values of engine parameters and pitch angle are displayed on the CRT screen with alphanumeric presentation of velocity, altitude, and mode information. The pilot can enter switching and numerical information through the keyboard, and special system status information (e.g., failure indication, request for response, and pending mode switching) can be displayed on annunciator lights. Pilot inputs are displayed on the CRT and are not incorporated until the pilot verifies their correctness and pushes "ENTER".

6.4.2 Sensor and Actuator Requirements

The throttle/energy management algorithm requires data for determining the proper nominal flight path, for perturbation guidance and trim, and for gain scheduling. Manually entered data includes

- Mission range and terminal conditions

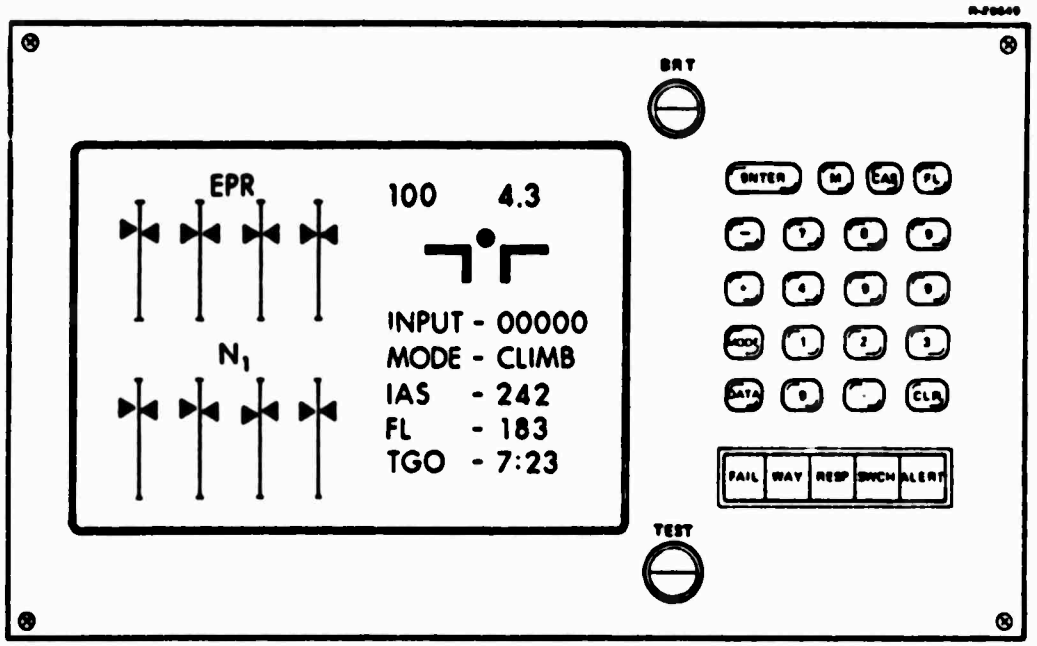

Figure 38 Display/Keyboard Panel for Throttle/ Energy Management System

- Air traffic control constraints
- Initial weight and c.g. location
- Pressure altitude calibration
- Wind data (unless derived on-board from navigation data)
- Experimental parameters

Data measurements required for primary guidance include

- Range to go
- Total temperature
- Static pressure
- Total pressure

or corresponding air data computer outputs. Measurements which are not required but which would improve performance of the primary guidance logic include

- Fuel quantity
- Fuel flow rate
- EPR, N_1, or throttle setting

- Attitude reference
- Inertial velocity
- Vertical acceleration

Section 6.2 demonstrated the use of angle of attack for gain scheduling, but this requirement can be eliminated in the flight system.

The information listed above must undergo analog-to-digital conversion at a 10- to 12-bit quantization level, which corresponds roughly to resolutions of 0.1 to 0.025 percent of full scale. While this is more than adequate for most measurements, difficulties could be encountered with the derivation of altitude from quantized static pressure measurements, particularly at the higher altitudes. For example, with 12-bit pressure quantization, and a maximum value equivalent to sea level pressure, a single bit is equivalent to an increment of 25 ft at an altitude of 40,000 ft. The problem is solved by double-word quantization -- in the present example, the altitude resolution could be improved to better than 0.01 ft by using a double word for static pressure.

There are no explicit actuator requirements for throttle/energy management system, because its outputs are assumed to command an inner-loop controller. Ultimately, the Level 4 system's commands would reach hydraulic actuators for control surface and throttle displacement, e.g., those used in the C-141A Fly-By-Wire Program (Ref. 48).

6.4.3 Computer Requirements

It is assumed that the throttle/energy management logic would be implemented in a digital flight computer for a number of reasons. The logic itself involves a number

of multiplications and nonlinear functions, and it requires precision, room for growth, flexibility, low cost, and moderate reliability. Previous experience with analog fuel management computers indicates that because they lack these traits, their value is greatly diminished in practice. Furthermore, the throttle/energy management system is compatible with navigation system requirements, and the logic could be implemented in a standard navigation computer (given sufficient memory), which almost certainly would be digital.

For maintainability, hardware and software system support, and reliability, it is desirable to use off-the-shelf equipment. The energy management function for a large jet transport does not pose stringent requirements on size, weight, or computer speed, but if the system is to be considered for fleet-wide retrofit, logistical considerations are paramount.

For an experimental Level 4 system, it is desirable that the flight computer have hardware floating-point logic and mandatory that it be supported by a higher-order algebraic programming language (i.e., that a program compiler exists). Countless recent surveys illustrate the cost savings which a compiler affords in software development. Since the higher-order language allows the program designer to specify operations as engineering equations, the full benefit of the compiler is realized only if the scaling of these operations is automatic. This is most readily accomplished by working in floating-point format. Although solution speed is a secondary consideration for fuel-minimizing guidance, the one- to two-order of magnitude improvement in execution time which the floating-point hardware provides minimizes guidance sequencing problems and improves the possibility of expanding

the logic into a full 4-D navigation system. It also allows the experimental system to execute off-line monitoring computations which can aid the testing program by providing "quick-look" analysis of system performance.

It is estimated that the throttle/energy management logic can be implemented with a memory of less than 8,192 ("8K") 16-bit words. Experience shows that the memory provided should be at least double the requirement, not only to allow for contingencies but to allow software development to proceed without the pressures of squeezing coding into the last few percent of available memory. The computer also should be supported by mass storage for program loading, data input, and logging of system outputs. Again, because speed is secondary and operational convenience is important, a cartridge or cassette tape drive is suggested for this function.

6.4.4 Software Development

The throttle/energy management structure presented in Section 6.3 can be used as a preliminary specification for software development, and the preparation of functional flow charts and coding from this section should be direct. The figures of this section illustrate the functions which remain to be accomplished in developing computer code for throttle/energy management.

Figure 39, adapted from Ref. 59, divides the software development into four phases:

- Analysis and design
- Implementation
- Evaluation and procedures
- Delivery (for flight test)

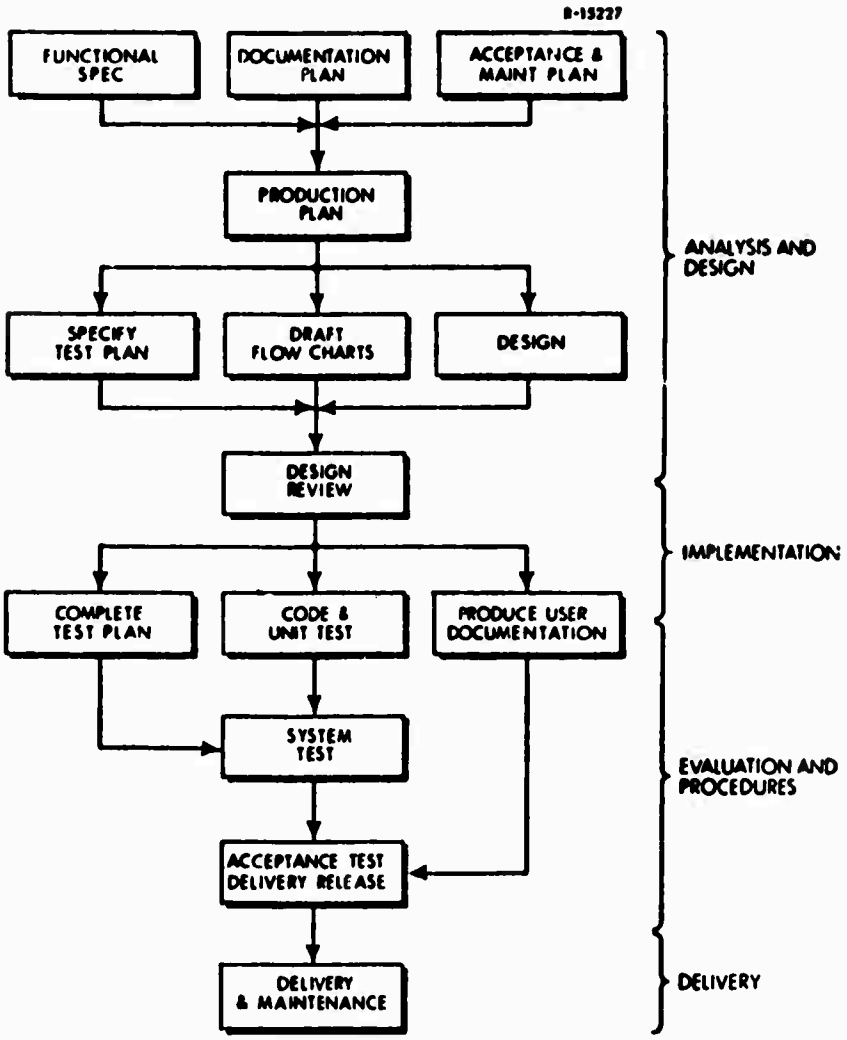

Figure 39 Phases of Software Development

The first phase translates engineering requirements into program specifications and structure. The second phase produces coding for the flight computer. The third phase involves acceptance testing and the definition of crew procedures, and the fourth phase provides system support.

The activities, documentation, and milestones which characterize this development plan are summarized in Fig. 40. It is important to identify these elements at an early stage of development and to observe certain

PHASE	ACTIVITIES	DOCUMENTATION	MANAGEMENT MILESTONES
• ANALYSIS & DESIGN	• ENGINEERING DESIGN • CONCEPT EVALUATION • FUNCTIONAL SYNTHESIS OF SYSTEM SOFTWARE	• ENGINEERING REPORTS • FUNCTIONAL SPECIFICATION OF SYSTEM SOFTWARE REQUIREMENTS	• TECHNICAL STATUS REVIEWS • SPECIFICATION OF FLIGHT TEST OBJECTIVES • PRELIMINARY DESIGN REVIEW
• IMPLEMENTATION	• DEVELOPMENT PLANNING • SYSTEM CODING • UNIT TESTING • INTERFACE TESTING	• SOFTWARE SPECIFICATION DOCUMENT • PROGRAM CHANGE REQUESTS • ANOMALY/DISCREPANCY REPORTS • PROGRAM CHANGE NOTICES • PROGRAM NOTES	• SOFTWARE STATUS REVIEWS • CRITICAL DESIGN REVIEW
• EVALUATION AND PROCEDURES	• ACCEPTANCE TESTING OF INTEGRATED SYSTEM SOFTWARE • SOFTWARE CONFIGURATION CONTROL • DEFINITION OF CREW PROCEDURES • FLIGHT TEST PLANNING	• TEST REPORTS • FLIGHT TEST PLANS • USER DOCUMENTATION	• TESTING STATUS REVIEWS • TEST EVALUATION REVIEW • SOFTWARE CONFIGURATION APPROVAL • FLIGHT READINESS REVIEW
• FLIGHT TEST	• ENGINEERING SUPPORT • SOFTWARE MAINTENANCE	• FLIGHT TEST SUMMARIES • FINAL REPORT	• FLIGHT STATUS REVIEWS

Figure 40 Elements of a Program for Throttle/Energy Management Software Development

formalities in design and documentation (e.g., anomaly reports, change notices, and test reports) even for small programs. Efficient management of available resources and assurance that milestones are accomplished requires visibility and control of the development program.

Development of fuel-minimizing throttle/energy management currently is in the first (Analysis and Design) phase. There are elements of this phase which remain to be conducted, including the preparation of flow charts and preliminary design review. The structure of the Level 4 system is defined, the preliminary software specifications are ready for flowcharting and coding, and the expected performance of the system has been estimated.

6.5 CHAPTER SUMMARY

This chapter has presented the basic information which is necessary to design and develop a fuel-minimizing guidance system for the C-141A aircraft. The throttle/energy management algorithms consist of a flight path generator which defines a fuel-minimizing reference flight path, a perturbation guidance and trim law which automatically controls the aircraft to follow the reference path, and gain scheduling functions which assure acceptable guidance response at all flight conditions. The system is synthesized for two-dimensional (vertical-plane) flight paths (Fig. 41) and can be extended to include lateral guidance and time-based navigation.

Four levels of system implementation are discussed. Handbook/Calculator Flight Path Computation (Level 1) requires no special equipment, but it imposes a large workload on the

	FLIGHT VARIABLE	TAKEOFF-CLIMB	CLIMB	CLIMB-CRUISE	CRUISE	STEP CLIMB	CRUISE-DESCENT	DESCENT	DESCENT-APPROACH
DESIRED STATE VARIABLES	TRUE AIR SPEED, V_D	V	IAS/M SCHEDULE	FADE TO CRUISE VALUE	VALUE FOR M_{opt}	FADE TO NEW VALUE	FADE TO DESCENT VALUE	VALUE FOR $(L/D)_{max}$	FADE TO SELECTED VALUE
	CLIMB RATE, $\dot{h}_D$	0 to $\dot{h}$	$\dot{h}$	FADE TO CRUISE VALUE	0	$\dot{h}$	FADE TO DESCENT VALUE	VALUE FOR $(L/D)_{max}$	0
	ALTITUDE, h_D	0 to h	h	FADE TO CRUISE VALUE	a)CONSTANT b)VALUE FOR CONSTANT H/θ	h	FADE TO DESCENT VALUE	FUNCTION OF RANGE TO GO	FADE TO SELECTED VALUE
DESIRED COMMAND VARIABLES	PITCH ANGLE, θ_D	VALUE FOR LEVEL FLIGHT	TRIM	TRIM	TRIM	TRIM	TRIM	TRIM	TRIM
	THROTTLE SETTING, T_D	1.0	1.0	FADE TO TRIM	TRIM	1.0	TRIM	TRIM	TRIM

Figure 41 Summary of Fuel-Minimizing Flight Path Segments and Associated Guidance Commands

crew, and it is likely to save less fuel than the other levels. Automatic Flight Path Display (Level 2) requires a minicomputer for data storage and computation, and it eliminates the requirements for many manual functions. The computer is independent of aircraft systems, relying on the crew for all inputs, and it could be moved form one aircraft to another with relative ease. Automatic Flight Path and Command Display (Level 3) uses direct inputs of aircraft data to compute a continuous output of state and control variables, minimizing data input by the crew and allowing the pilot to follow the fuel-optimal flight path as closely as he deems necessary. Automatic Throttle/Energy Management (Level 4) closes the guidance loop through autopilot/autothrottle actuators, relying on the crew to perform executive functions only (mission specification and choice of optional flight parameters).

Concepts for testing throttle/energy management on operational aircraft are presented in the following chapter.

VII. FLIGHT TEST CONCEPTS

7.1 OVERVIEW

The confirmation of fuel-saving flight policies by testing in the actual aircraft is made difficult by uncertainties in the environment and in the aircraft itself. To achieve the goal of reducing fuel use in practice and on a fleet-wide basis, it is necessary to consider operational constraints and preferences during test planning. The cost of testing, as well as the fuel consumed to provide conclusive results, also should be considered.

The primary objectives for flight testing are the following:

- Demonstrate fuel-optimal flight paths
- Evaluate throttle/energy management technique at four levels of implementation.
- Collect data regarding air crew and air traffic controller acceptance of fuel-saving flight policies.
- Estimate the probable impact of fuel-minimizing throttle/energy management on Air Force fuel consumption and operating costs.
- Determine the level of throttle/energy management which is most likely to provide the greatest benefits to Air Force flight operations.

This chapter presents a plan for evaluating throttle/energy management in the face of the uncertainties and limitations which are mentioned above. There are two basic tenets of the suggested flight test program:

- Fuel-saving flight policies should be demonstrated on line aircraft (using Level 1-2 implementation) and on an aircraft equipped with Level 3-4 equipment.
- Evaluation of test results will be aided materially by computerized data analysis techniques, described below.

The capital equipment required for Level 1-2 implementation is low; therefore, test results can be obtained during normal operations and at low cost. Nevertheless, fuel-minimizing guidance requires Level 3-4 instrumentation, which should be installed on at least one test aircraft. Variations in atmospheric conditions, aircraft weight, etc., will make a direct comparison of fuel used on two flights (for example, an optimal flight path and a conventional flight path) difficult; therefore, a three-way trajectory analysis procedure is developed to eliminate uncertainties in data evaluation.

Experiment descriptions, equipment and data requirements, and data evaluation are described in Sections 7.2, 7.3, and 7.4, respectively. The chapter is summarized in Section 7.5.

7.2 EXPERIMENT DESCRIPTIONS

A series of tests is suggested in this section. The tests fall into two categories: those which use minimal equipment (Levels 1 and 2) and are intended to identify operational use factors, and those which use more complete throttle/energy management equipment (Levels 3 and 4) and are devoted to system development. The first category of tests can be conducted on line aircraft performing scheduled

exercise and airlift operations. The second category of tests requires the installation of aircraft-computer interfaces and an input-display device at the pilot's and engineer's stations. This system ultimately is tested in line operations, although it must be available for flights devoted exclusively to system tests, as well.

7.2.1 Tests of Operational Use Factors

Six test routes should be chosen for these tests, two each in the short-, medium-, and long-range categories defined in Chapter 5. Where possible, the routes should be flown regularly by MAC personnel in both directions, allowing head-tail wind and flight level effects to be evaluated. They should be in areas of relatively light commercial air traffic, so that clearances for special flight paths can be obtained, as required. Conducting tests at night will increase the flexibility in choosing flight paths by reason of lighter traffic. The routes should be in areas of good Air Weather Service coverage, in order that meteorological data required for data analysis is accurate and available.

It is preferable that a limited number of aircraft (4 or less) be used in the testing program and that up to six flight crew members (in each rating) conduct the tests. Characteristics of each aircraft (by tail number) and its engines should be documented, including time since major overhaul, minor performance-related maintenance actions, and known deviations from standard configuration (e.g., actual thrust and specific fuel consumption measured at last engine overhaul, throttle and control surface rigging anomalies, etc.). Each aircraft need not fly each route segment, although it is desirable for each segment to be flown by more than one aircraft. Flight crew members should

provide a representative range of experience levels and should be able to adapt to non-standard procedures.

Two test engineers accompany each flight. One engineer is responsible for executing the Level 1-2 throttle/energy management technique and transmitting flight path information to the crew. The other engineer is responsible for logging data, verifying crew procedures, and recording the crew's comments on fuel-saving procedures. Both engineers should develop a summary of general use factors after each flight.

Ten to twenty flights should be conducted in each of the three major route lengths, with the flights being divided approximately equally between fuel-saving and conventional procedures. The former are flown to evaluate potential fuel savings, while the latter provide reference data plus sensitivities to major variables, e.g., cruise altitude and speed. Each chosen route segment should be flown at least twice: once optimally and once conventionally. Accumulated flying time (by route length) is approximately

- Short Range: 10 to 25 hours
- Medium Range: 25 to 75 hours
- Long Range: 75 to 200 hours

for Level 1-2 testing. Tests should extend over a period of six to nine months to allow time for data evaluation and incorporation of early results in final testing. It is recommended that each test flight be conducted as a unified experimental profile containing climb, cruise (if required), and descent segments that (together) form an optimal or conventional "hop," although individual flight segments can be analyzed.

Examples of flight types are given in Table 18, which shows 15 profile variations (10 conventional, 5 optimal). The optimal profiles are flown using Level 1 and 2 throttle/

energy management; hence, the flight types are equally divided. In practice, it may be necessary to repeat tests, and all 15 flight types need not be conducted in every range category.

TABLE 18

FLIGHTS FOR OPERATIONAL USE TESTING

Trajectory Type	Weight	Climb	Cruise	Descent	Comments
Conventional	Light	Standard	Standard	Standard	Cruise Mach Number = 0.74
"	Medium	"	"	"	"
"	Heavy	"	"	"	"
Optimal	Light	Optimal	Optimal	Optimal	Levels 1 and 2
	Medium	"	"	"	"
	Heavy	"	"	"	"
Conventional	Medium	Standard	Standard	Standard	Cruise Mach Number = 0.767
"	"	IAS±20 KIAS	"	"	
"	"	Standard	"	"	
"	"	"	"	Idle	Cruise Altitude ± 4000 ft
"	"	"	"	Penetration	
"	"	"	"	Standard	Head wind
"	"	"	"	"	Tail wind
Optimal	"	Optimal	Optimal	Optimal	Tail wind; Levels 1 and 2
"	"	"	"	"	Tail wind; Levels 1 and 2

Conventional profiles should be planned and executed using standard procedures. It may be desirable for these reference paths to be flown by pilots who are not familiar with the throttle/energy management program, in order to get an unbiased measure of fuel consumption on truly conventional profiles (or these flights can be conducted before the optimal flights). Repetition of optimal flight paths may improve fuel conservation by giving the pilots the opportunity to learn differences in procedures.

7.2.2 Tests for System Development

Flight tests for the development of a Level 3-4 system are similar to the Level 1-2 tests, but a greater

emphasis is placed on calibration of the aircraft. Consequently a single aircraft is used for system development. Details of fuel consumption along the flight path, as well as end-to-end consumption, are important. In addition, system checkout, i.e., the verification of proper operation and the validation of basic concepts, is a major testing goal. In this respect, Level 3-4 testing is directed at familiar goals of instrument and control system development.

The major objectives of system checkout are evaluation of

- Fuel-minimizing flight path generation
- Perturbation guidance
- Mode switching
- Command step response
- Disturbance rejection
- Human factors
- Sensor-computer interfaces
- Installation and maintenance requirements

Flight time devoted to system checkout can be minimized by judicious use of the flight computer to adapt to self-testing procedures, e.g., injecting artificial disturbances, biasing altitude inputs to simulate cruise, and accelerated sequencing through flight path segments. Prior to actual fuel-use testing, checkout functions should be completed with the equivalent of single short-range and medium-range flight paths -- about 5 to 10 flight hours.

Fuel-use testing of the Level 3-4 system can be divided into three phases:

- Concept Validation (Phase 1)
- MAC Operational Testing (Phase 2)
- Integrated Testing with 4-D Navigation (Phase 3)

Concept Validation extends for approximately 60 flight hours, allowing the throttle/energy management technique to be demonstrated and evaluated over a wide variety of mission ranges, air traffic control constraints, vehicle weights, and atmospheric conditions. To the extent possible, testing in this phase is combined with other test programs or MAC exercise flights. During MAC Operational Testing, the system is flown by Airlift Command pilots during up to 200 hours of scheduled flying. Operational use and maintenance factors are evaluated during this phase, and the system is demonstrated for appropriate personnel. Whereas Phase 1 is supported by detailed data analysis, numerical analysis is deemphasized in Phase 2, when operational factors are most important. For Integrated Testing with 4-D Navigation, the system is returned to research status.

7.3 EQUIPMENT AND DATA REQUIREMENTS

In addition to the system synthesis requirements discussed in Chapter 6, flight test equipment and reference data are required. For all tests, synoptic meteorological data should be obtained from the Air Weather Service. Standard forms used by the Airlift and Logistics Commands to document each flight stage that is part of the test program should be obtained. This information is valuable for statistical analysis of test results and for calibration of the computer analysis described in the next section.

No additional instrumentation is required for Level 1-2 testing (other than the calculator or computer used for throttle/energy management). Test engineers record necessary position and velocity from standard air data and navigation instrumentation for later use in approximate reconstruction of

the aircraft's flight path. Standard flight recorder information could be useful in this regard.

The Level 3-4 aircraft should be equipped with precision navigation and fuel-use instrumentation during Phase 1 testing to allow accurate reconstruction of the flight-path, thrust, and fuel consumption profiles. Engine condition monitoring equipment could improve calibration of the power plants.

7.4 DATA EVALUATION

Because no two flight profiles can be evaluated under identical vehicle and atmospheric conditions during flight testing, a direct comparison can only be made computationally. For example, if a given aircraft flies from A to B optimally and then returns to A on a conventional path, the winds are different and vehicle weight is decreased. Two aircraft leaving A at the same time to fly to B are subject to performance differences on the order of 5 to 10 percent due to differences in engine wear, control rigging, payload weight and distribution, and many other items (Ref. 60). As the fuel savings which the testing is supposed to demonstrate are of the same order, a single comparison may not be conclusive. The test could be repeated with the roles of the two aircraft reversed, but the desired result is obtained only by expending twice as much fuel and flight time and still is subject to atmospheric uncertainties.

Substantially more information can be obtained from each flight if the data is used in a three-way numerical comparison, consisting of computed profiles of the

- Optimal flight path
- Throttle/energy management flight path
- Conventional flight path

There are two steps in the numerical comparison:

- Model calibration to flight-test data
- Three-way comparison of flight paths

The process is illustrated in Fig. 42, assuming that the flight test result was obtained with the Level 4 throttle/ energy management system engaged.

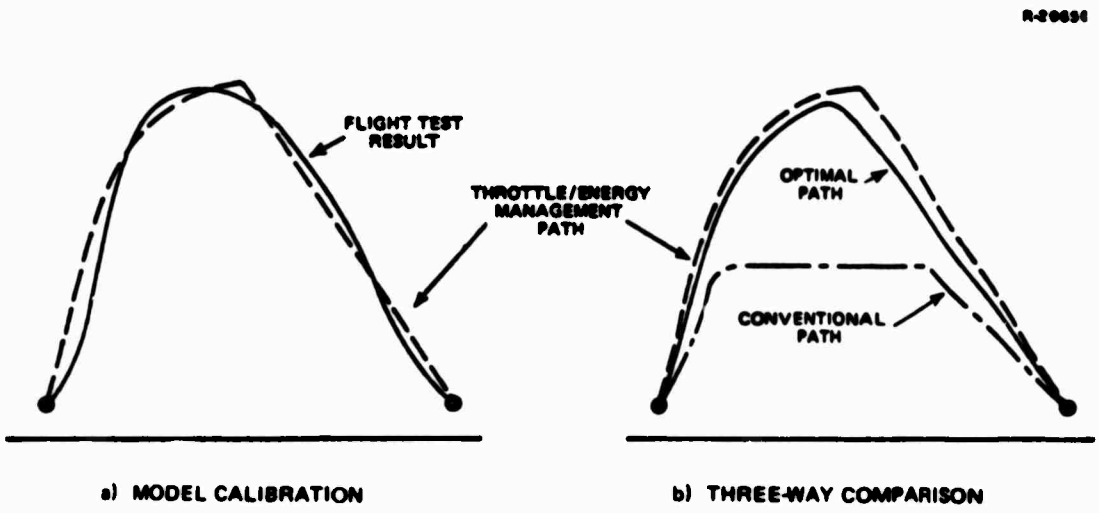

Figure 42 Computer Analysis of Flight Test Data

The basic approach uses a flight path simulation and optimization program such as ENERGY, described in Appendix A. The flight test data includes sampled time histories of the state and control variables. If the aircraft mathematical model (Appendix B) was precise, if atmospheric conditions were known, and if the measurements contained no errors, the flight path could be reconstructed exactly by integrating the equations of motion,

$$\dot{\underline{x}}(t) = \underline{f}[(\underline{x}(t),\underline{u}(t)] \qquad (7.4\text{-}1)$$

using the measured control history as an input; however, errors and uncertainties preclude an exact solution. The best that can be expected is that the reconstructed flight path minimizes an error criterion in fitting the data. For example, let the measured state be $\underline{x}_m$ and the computed state be $\underline{x}_c$. Forming the error vector

$$\Delta\underline{x} = \underline{x}_m - \underline{x}_c \tag{7.4-2}$$

a set of parameters, p_k, is chosen to minimize a quadratic cost function of the fitting error:

$$J = \Delta\underline{x}_f^T P_f \Delta\underline{x}_f + \int_{t_o}^{t_f} \Delta\underline{x}^T(t)\, A\Delta\underline{x}(t)dt \tag{7.4-3}$$

as in Section 3.5. In other words, the data fitting problem is formulated as a parametric optimization, and the parameters are <u>calibration coefficients</u> of the aircraft's mathematical model. The determination of these coefficients follows the discussion of Section 3.5 and is illustrated in Fig. A.3-1.

It is important to identify a minimal set of calibration coefficients, and in the present case, it appears that the minimal number is three. Referring to Eq. (3.2-1) to (3.2-7), it can be seen that the aircraft model enters four equations ($\dot{V}, \dot{\gamma}, \dot{\xi}, \dot{m}$) but the thrust and aerodynamic terms are identical in two equations ($\dot{\gamma}, \dot{\xi}$). For the purposes of comparing fuel used on various trajectory types, it can be assumed that the form of the aircraft model (Appendix B) is known and that the major variations from one flight to the next are contained in the relative scaling of the $\dot{V}$, $\dot{\gamma}$, and $\dot{m}$ equations. Three parameters then are necessary to describe

- Thrust-drag scaling
- Lift-weight scaling
- Fuel flow rate scaling

and these parameters account for dynamic variations due to engine parameters, weight, aerodynamics, and atmospheric effects. The disadvantage of this calibration procedure is that these parameters do not identify the source of variations. The advantage is that they provide a simple calibration of the aircraft model for comparing fuel-optimal and conventional flight operations.

The best definitions for the scaling parameters are subject to confirmation; however, the following set appears reasonable: the coefficients C_D, C_L, and ω are replaced by

$$C_D^* = p_1 C_D \tag{7.4-4}$$

$$C_L^* = p_2 C_L \tag{7.4-5}$$

$$\omega^* = p_3 \omega$$

in the equations of motion, and the p_k are chosen to minimize Eq. (7.4-3), calibrating the computer model (as shown in Fig. 42a) and completing the first step.

Program ENERGY is used to compute the remaining two flight paths in the three-way comparison using the calibrated model. If the flight test used throttle/energy management, an optimal trajectory and a conventional flight path are computed (Fig. 42b); if the test path was conventional, then the optimal and throttle/energy management paths are computed. The flight test program allows the validity of this comparison to be assessed, as both

conventional and throttle/energy management results can be used in model calibration. A single flight is thus capable of producing results which are equivalent to four test flights using the two-aircraft approach mentioned at the beginning of this section. This data analysis technique can be used with either Level 1-2 or Level 3-4 flight tests and with any number of subject aircraft, because the computer model is recalibrated for each comparison.

7.5 CHAPTER SUMMARY

Objectives for flight testing, descriptions of experiments, data requirements, and a new technique for flight path evaluation have been presented here. It is shown that tests should demonstrate not only the technical characteristics of throttle/energy management techniques but the operational use factors as well. Real fuel savings will be achieved only if fuel-saving systems are acceptable to air crews. Testing of essentially manual (Level 1-2) techniques in a MAC exercise-airlift environment requires about 100 to 300 flight hours. Testing of automatic (Level 3-4) throttle/energy management requires an equivalent amount of time. Evaluation of the true potential for saving fuel in flight operations is assisted by using a self-calibrating, three-way computer comparison method which minimizes flight testing requirements.

VIII. CONCLUSION

The objectives of this investigation have been to

- Determine fuel savings which can be realized in the flight operations of the C-141A aircraft.
- Synthesize a throttle/energy management technique which is capable of guiding the C-141A aircraft along fuel-optimal flight paths.
- Establish methods for demonstrating throttle/energy management techniques by flight testing.
- Identify fuel conservation principles which could be applied to other jet transport/bomber aircraft.

In the course of conducting this work, the fuel-optimal performance of the C-141A was defined for a wide variety of vehicle and atmospheric conditions; for climb, cruise, and descent segments; and for fully integrated flight paths with ranges of 200 to 5,600 nm. These numerical results were obtained using a newly developed computer program (ENERGY) which generates

- Conventional flight profiles
- Optimal flight profiles
- Flight profiles with closed-loop guidance
- Linear-optimal gain values for an automatic guidance (combined autopilot/autothrottle) system

This program incorporates a detailed, nonlinear model of the C-141A aircraft, as well as functions for duplicating constraints due to air traffic control and vehicle limitations. It uses new techniques for efficient computation of flight

paths and rapid convergence of optimal solutions. The program can be applied to other aircraft by changing aerodynamic, thrust, and inertial data. For jet transport/bomber/utility aircraft, e.g., C-5A, B-52, KC-135, YC-14, YC-15, B-1, T-39, and wide-bodied or conventional commercial jet transports, data conversion would be a simple and direct process. Furthermore, the program's flexibility could be of substantial benefit in comparative flight testing of fuel conservation techniques, reducing flight-hour requirements by up to 75 percent.

The throttle/energy management technique developed here has four major elements:

- Fuel-optimal flight path generator
- Perturbation guidance and trim law
- Guidance gain scheduling
- Crew input and display

The technique can be implemented at four levels of system complexity, ranging from essentially manual to fully automatic operation:

- Handbook/Calculator Flight Path Computation
- Automatic Flight Path Display
- Automatic Flight Path and Command Display
- Automatic Throttle/Energy Management

Fuel-minimizing throttle/energy management is shown to be compatible with conventional flight operations at the first level and with integrated 4-D navigation systems at the fourth level.

The suggested flight test program is divided into two parts: the evaluation of operational use factors and system development. Level 1 and 2 testing falls into the

first category, and it is conducted largely by MAC personnel. Level 3 and 4 falls into the second category, which is further subdivided into

- Concept Validation
- MAC Operational Testing
- Integrated Testing with 4-D Navigation

Uncertainties and measurement errors, which make comparative evaluation of fuel use difficult (because the levels of fuel saving and uncertainty are themselves comparable), are largely overcome by a three-way numerical comparison of flight data. The computer model is calibrated by the flight test data, and the analysis program is used to generate three flight paths which are dynamically equivalent to the measurements:

- Optimal Flight Path
- Throttle/Energy Management Flight Path
- Conventional Flight Path

It is easy to overstate the potential fuel and cost savings associated with throttle/energy management because there is so much variability in "conventional" flight paths. A high-speed, low-altitude cruise is known to use more fuel than a Breguet cruise-climb; potential savings relative to the first path are impressive, but they may be small compared to the second path. Actual fuel savings depend on actual flight policies. Taking the optimal flight profile as a base, this study has demonstrated that some "handbook" profiles use over 30 percent more fuel than the optimum, while proper choice of cruise altitude and use of idle-thrust, $(L/D)_{max}$ descent can narrow the gap to a few percent. The key to minimizing fuel use on military jet transport is to make fuel saving the "natural" way to fly the airplane. A fuel-minimizing throttle/energy management system can achieve this goal.

APPENDIX A

COMPUTER TOOLS FOR TRAJECTORY ANALYSIS

A.1 PROGRAM DEVELOPMENT

In order to develop and analyze potential fuel reducing throttle/energy management systems for aircraft, a computer program, ENERGY, has been developed. Program ENERGY provides the capability to exercise a wide variety of trajectory shaping and analysis techniques and to validate, by simulation, any proposed on-board guidance algorithms. A list of the major applications of program ENERGY include:

- Aircraft trajectory generation
- Parametric trajectory optimization
- Variational (steepest-descent) trajectory optimization
- Linear-optimal perturbation guidance gain computation
- Comparative evaluation of varying trajectory shapes and/or on board guidance algorithms.

The modular structure of program ENERGY (Fig. A-1) facilitates its modification for other types of trajectory analysis and enables each module to be used in various applications. For example, both variational optimization and linear-optimal guidance gain computations necessitate evaluating partial derivatives of the dynamic equations of motion along the aircraft's trajectory. By programming the partial derivative computations as a separate program module, duplication of effort is eliminated and program checkout and validation is simplified.

R-14791

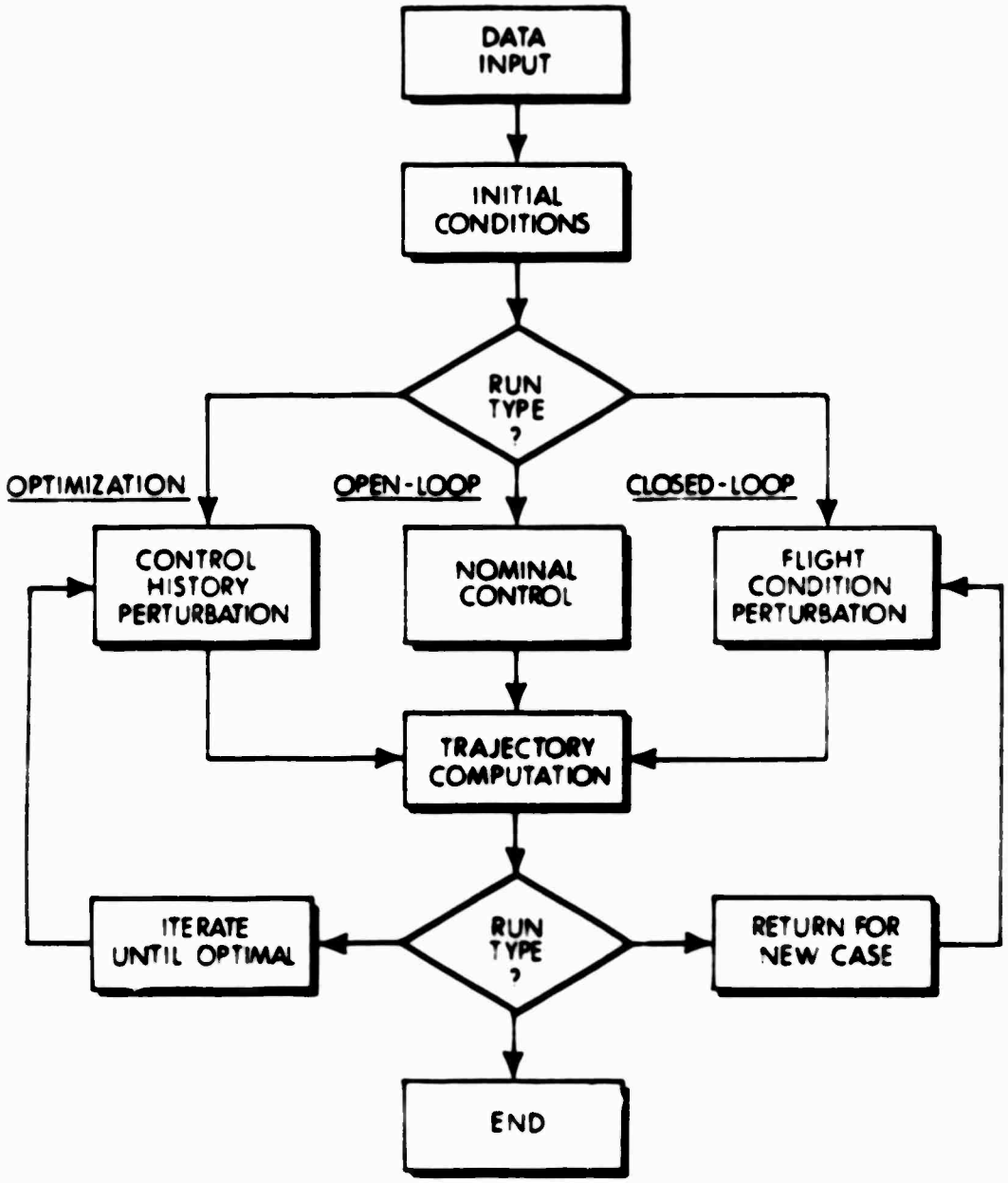

Figure A-1 Program Structure of the Engineering Simulation

The advantages of ENERGY'S modular programming structure are also demonstrated by the programs guidance algorithm options:

- Open-Loop Trajectories - Guidance commands are specified as a function of an independent variable, e.g., time or range.
- Ad Hoc Guidance - Guidance commands are generated based upon arbitrary perturbation gains.
- Optimal Perturbation Guidance - Guidance commands are generated using optimally derived perturbation gains.

These guidance options are useful for generating reference trajectories, performing trajectory optimization, and comparing guidance algorithms. These guidance techniques are by no means an exhaustive set of possible algorithms; however, the modularity of program ENERGY simplifies the addition of any options which might be of interest.

Those sections of ENERGY which define the vehicle aerodynamics also are programmed as self-contained modules. The model of the C-141A aircraft, which was the subject of the current study, is presented in Appendix B. Other aircraft can be analyzed by simply replacing the C-141A model subroutines with those that correspond to the vehicle of interest.

A.2 TRAJECTORY SHAPING AND EVALUATION

Trajectory optimization consists of determining a trajectory and control profile which, in some sense, is "best". The approach used in ENERGY to compare different trajectories is to assign a scalar cost to each trajectory. Typically, a general trajectory cost function has the form

$$J = \Phi(\underline{x}(R_f)) + \int_{R_0}^{R_f} L(\underline{x},\underline{u},R)\ dR \qquad \text{(A.2-1)}$$

where

J = scalar cost value

$\underline{x}(R_f)$ = final values of trajectory state variables (velocity, flight path angle, altitude, mass, and time)

$\underline{u}$ = control variables (pitch-angle, throttle, and roll)

R_0, R_f = initial and final values of independent variable (range)

L = scalar integrated cost function

Φ = scalar function of final state variables

The optimal or "best" trajectory is the one which provides the lowest cost value.

The inclusion of numerous penalty functions, terminal conditions, $\Phi(\underline{x},(R_f))$, and in-flight constraints, $L(\underline{x}, \underline{u}, R)$, in program ENERGY provides a wide degree of flexibility in shaping and evaluating trajectory and control profiles. A summary of the penalty functions which can be specified in ENERGY is presented in Table A-1.

A simple example demonstrates how these penalty functions can be used for trajectory optimization. If it is desired that a trajectory terminate at a particular altitude, H_D, and not exceed a maximum Mach number, $MACH_{MAX}$, while minimizing fuel use, Δm, the appropriate cost function to minimize would be given as

TABLE A-1

TRAJECTORY PENALTY FUNCTIONS

Terminal Constraints $\phi(\underline{x}(R_f))$	State Constraints $L(\underline{x},\underline{u},R)$	Control Constraints $L(\underline{x},\underline{u},R)$
Altitude	Maximum Altitude	Maximum Throttle
Flight Path Angle	Minimum Altitude	Minimum Throttle
Mass	Excluded Altitude Band	Maximum Pitch Angle
Velocity	Maximum Altitude Rate	Minimum Pitch Angle
Time	Maximum Mach Number	Maximum Angle-of-Attack
	Buffet Limits	Minimum Angle-of-Attack
	Maximum IAS	
	Minimum IAS	

$$J = C_1(H_D - H(R_f))^2 + C_2(\Delta m) + \int_{R_0}^{R_F} L(\text{MACH})\, dR \qquad \text{(A.2-2)}$$

where

$$L = \begin{cases} C_3\ (\text{MACH}_{MAX} - \text{MACH})^2, & \text{if MACH} > \text{MACH}_{MAX} \\ 0, & \text{if MACH} < \text{MACH}_{MAX} \end{cases} \qquad \text{(A.2-3)}$$

and C_1, C_2, C_3 are positive scalars.

Examination of the cost function of Eq. (A.2-2) shows an increase in cost for missing the desired terminal altitude, for using a large amount of fuel, Δm, or for exceeding the maximum Mach number along the trajectory.

The penalty functions listed in Table A-1 show that program ENERGY can describe the characteristics of a desired trajectory in some detail. In keeping with the flexible structure of the program, the list of penalty functions can be modified or expanded to take into account any other desirable trajectory characteristics.

A.3 PROGRAM APPLICATIONS

Sections A.1 and A.2 described the modular structure of program ENERGY and the methods of determining a cost for each trajectory, in order to compare different trajectory and control profiles. The present section briefly describes the major program modules and demonstrates how they can be executed in appropriate order to perform complex trajectory and guidance algorithm analysis.

A list of the major computational blocks and a description of their functions is given below:

- Trajectory Generation - Given an initial vehicle state (velocity, altitude, flight path angle, and mass) and control profile, the trajectory generation logic integrates forward from the initial conditions the complete trajectory profile. Either open-loop, ad hoc, or linear-optimal perturbation guidance algorithms can be employed.

- Cost Computation - For each complete trajectory, a scalar cost is computed as described in Section A.2.

- Partial Derivatives - The partial derivatives of the vehicle dynamics and the penalty functions with respect to the state and control variables are evaluated along the computed trajectory.

- Steepest-Descent Control Perturbation - Using the conditions and partial derivatives of the nominal trajectory, this program section integrates the costate variable equations backward from the terminal conditions and computes the control perturbation history to most effectively reduce trajectory costs.

- Linear-Optimal Gain Computation - Given a nominal trajectory to follow, this routine solves the optimal regulator control problem to determine linear perturbation guidance gains. The solution to the optimal regulator problem is achieved by computing the steady-state values of a matrix Riccati equation.

Flow diagrams depicting three of the major trajectory analysis techniques which can be exercised with ENERGY are presented in Fig. A-2. These diagrams demonstrate how the ordering of the program's computational blocks can be rearranged to perform significantly different forms of trajectory analysis.

Many of the computational blocks are used for more than one type of trajectory analysis. The trajectory generation block, for example, is used for steepest-descent optimization, for parametric optimization, and for optimal perturbation guidance computations. In each application, however, the guidance algorithm is chosen to fit the specific needs of the problem. For steepest-descent optimization, trajectories are generated using open-loop guidance commands which are computed to minimize total trajectory cost. Parametric optimization trajectories utilize closed-loop guidance commands to fly the profiles which are specified by the parameters to be optimized. Linear-optimal guidance gain analysis requires trajectory generation with either open-loop or closed-loop guidance algorithms to define the nominal path and its associated linear model. Performance of the linear-optima guidance law is evaluated using both linear and nonlinear mathematical models.

Program ENERGY's applications can be made more complex by chaining together the analysis tools depicted in Fig. A-2. Rather than initiating the guidance gain computations with an arbitrary trajectory, the trajectory defined as a result of

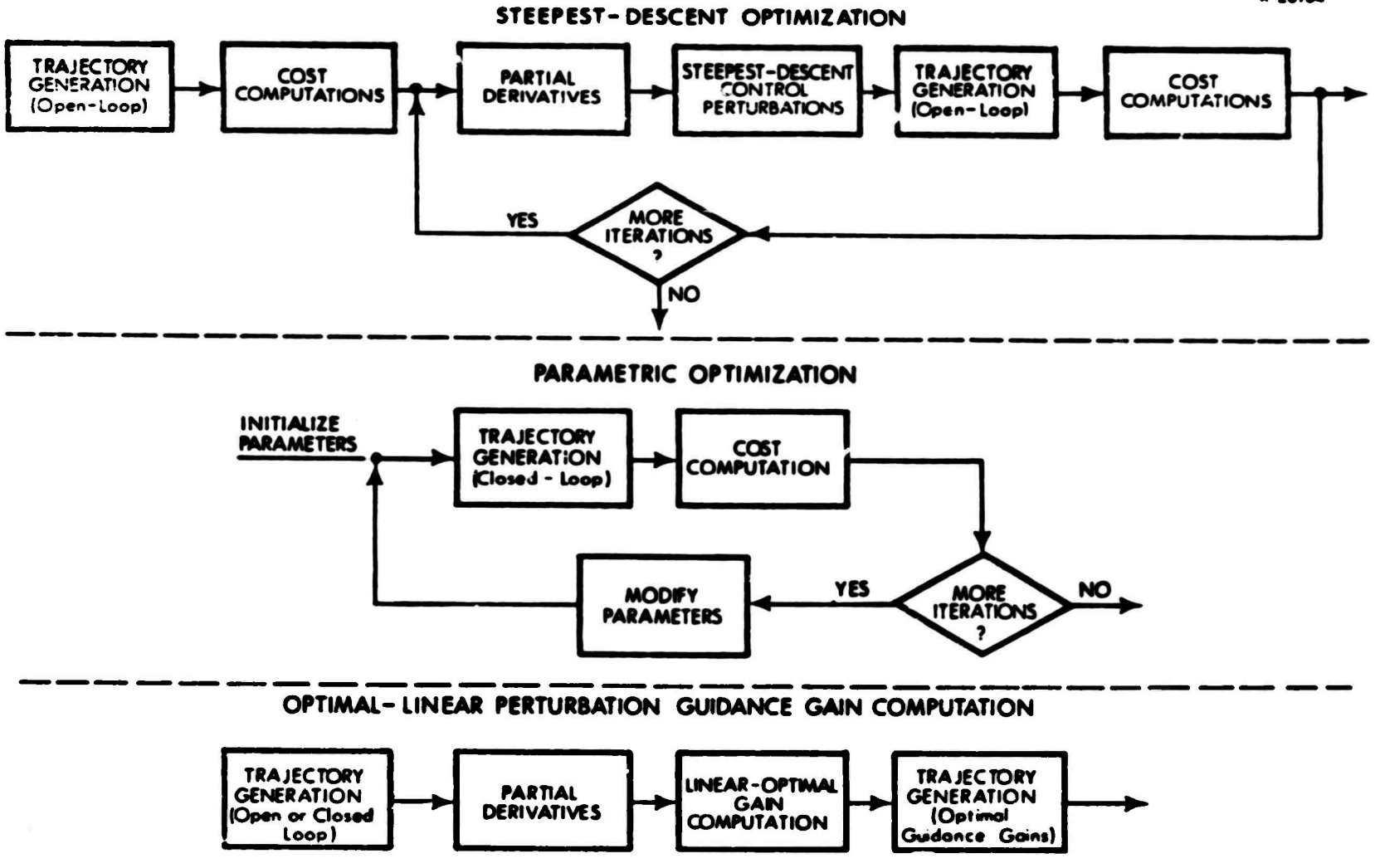

Figure A-2 Flow Diagrams of Trajectory Analysis Tools

steepest-descent or parametric optimization could be employed. The guidance gains then computed always would attempt to follow the optimal reference trajectory. Section A.4 shows that ENERGY's control logic facilitates this type of chaining operation.

A.4 PROGRAM CONTROL

The control logic of ENERGY provides for both sequential and iterative processing of the major trajectory analysis algorithms. Sequential processing enables chaining together specific program applications, such as trajectory optimization and optimal guidance gain computations. Iterative program operation is useful for examining the effects of vehicle or environmental variations on system performance (e.g., optimal trajectory shapes, nominal trajectory costs, on-board guidance algorithm operation, etc.).

The two modes of program operation -- sequential and iterative -- are controlled by the program's RUN-CASE-SWEEP control logic. This control logic is basically a set of nested repetitive loops as shown in Fig. A-3. The innermost loop is the SWEEP, the middle loop is the CASE, and the outer loop is the RUN type.

The RUN control point specifies the particular type of trajectory analysis to be performed, such as parametric trajectory optimization. A complete list of analysis options is given in Section A.1. The CASE control point specifies the desired terminal conditions and inflight constraints to be used in determining trajectory costs. The available penalty functions are presented in Section A.2. The SWEEP control point provides for modification of the

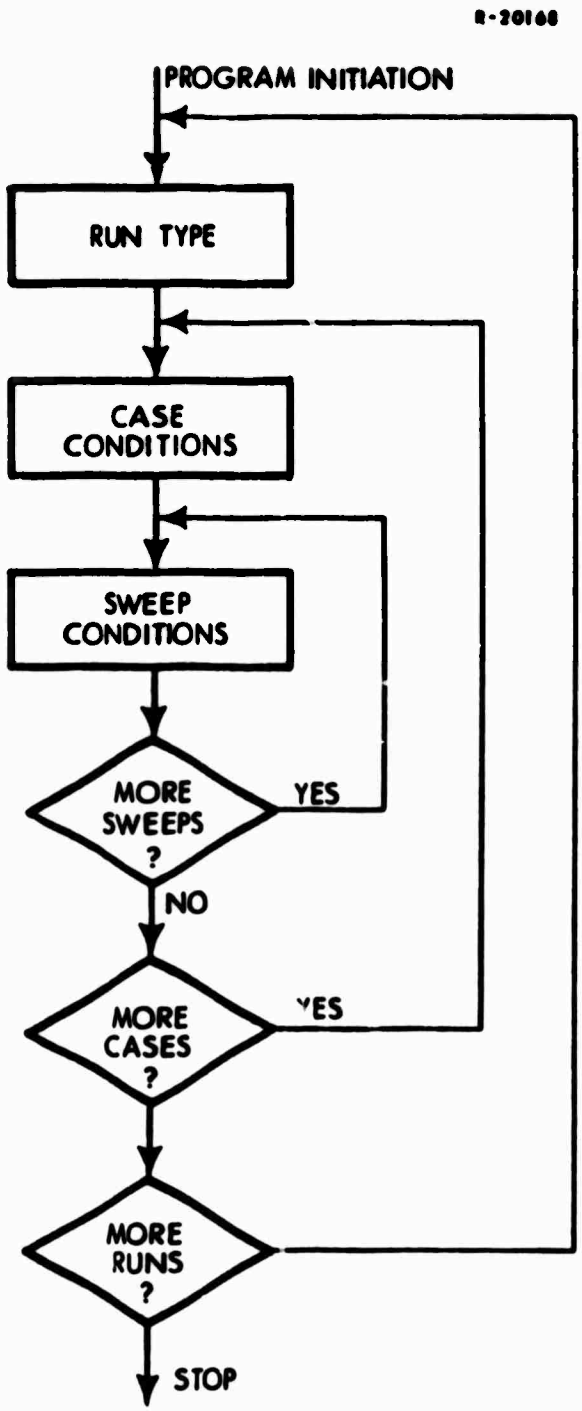

Figure A-3 RUN-CASE-SWEEP Control Logic

aircraft and environmental conditions. The conditions which can be modified at the sweep control point are:

- Initial vehicle state: Velocity, altitude, flight path angle, and mass.
- Aircraft modifications: Locations of vehicle c.g., number of engines operating.
- Environmental effects: Wind profile vs. position and altitude, atmospheric temperature variations.

The use of sequential analysis program operation is achieved by consecutively executing two RUN types. That is, if only one case and one sweep are specified for each RUN type, control looping occurs only at the RUN control point. By this means, an optimal guidance gain computation could be performed immediately following a trajectory optimization step. The optimized trajectory would, therefore, be available as the nominal profile to be used in the gain computation analysis.

Iterative program operation is achieved by specifying more than one CASE and/or SWEEP option for each RUN type. This iterative processing of multiple CASE or SWEEP options enables comparisons of trajectory costs as a function of changing vehicle and atmospheric conditions.

An example of program ENERGY output is illustrated in Fig. A-4, which is a partial listing of the 200-nm steepest-descent optimal trajectory. The columns of the flight path output are defined as follows:

ENERGY	Specific total energy times g, ft^2/sec^2
K.E.	Specific kinetic energy times g, ft^2/sec^2
HEIGHT	Altitude, ft

VELOCITY	True airspeed, fps
GAMMA	Flight path angle, deg
RANGE	Range to go, nm
XI	Heading Angle, deg
AGO	Azimuth Angle, deg
MACH	Mach number
ALPHA	Angle of attack, deg
PHI	Roll angle, deg
L/D	Lift-to-drag ratio
DYNP	Dynamic pressure, psf
GLOAD	Load factor, "g"'s
CL	Lift coefficient
CD	Drag coefficient
TIME	Elapsed time, sec
IJK	Step number
IHLF	Number of step-size halvings
PITCH	Pitch angle, deg
THROTL	Throttle setting, (0 to 1)
FLOW	Fuel flow rate, lb/hr
NRT	Normal-rated thrust, lb
WEIGHT	Vehicle weight, lb
FORCE	Thrust, lb
WT/DELTA	Weight divided by pressure ratio, lbs
DELTA	Atmospheric pressure ratio
HDOT	Climb rate, ft/min
SR	Specific range, nm/lb of fuel
IAS	Indicated airspeed, kt

The flight path listing is followed by particulars of the optimization, including terminal errors, penalty costs of the trajectory and dollar costs of the mission.

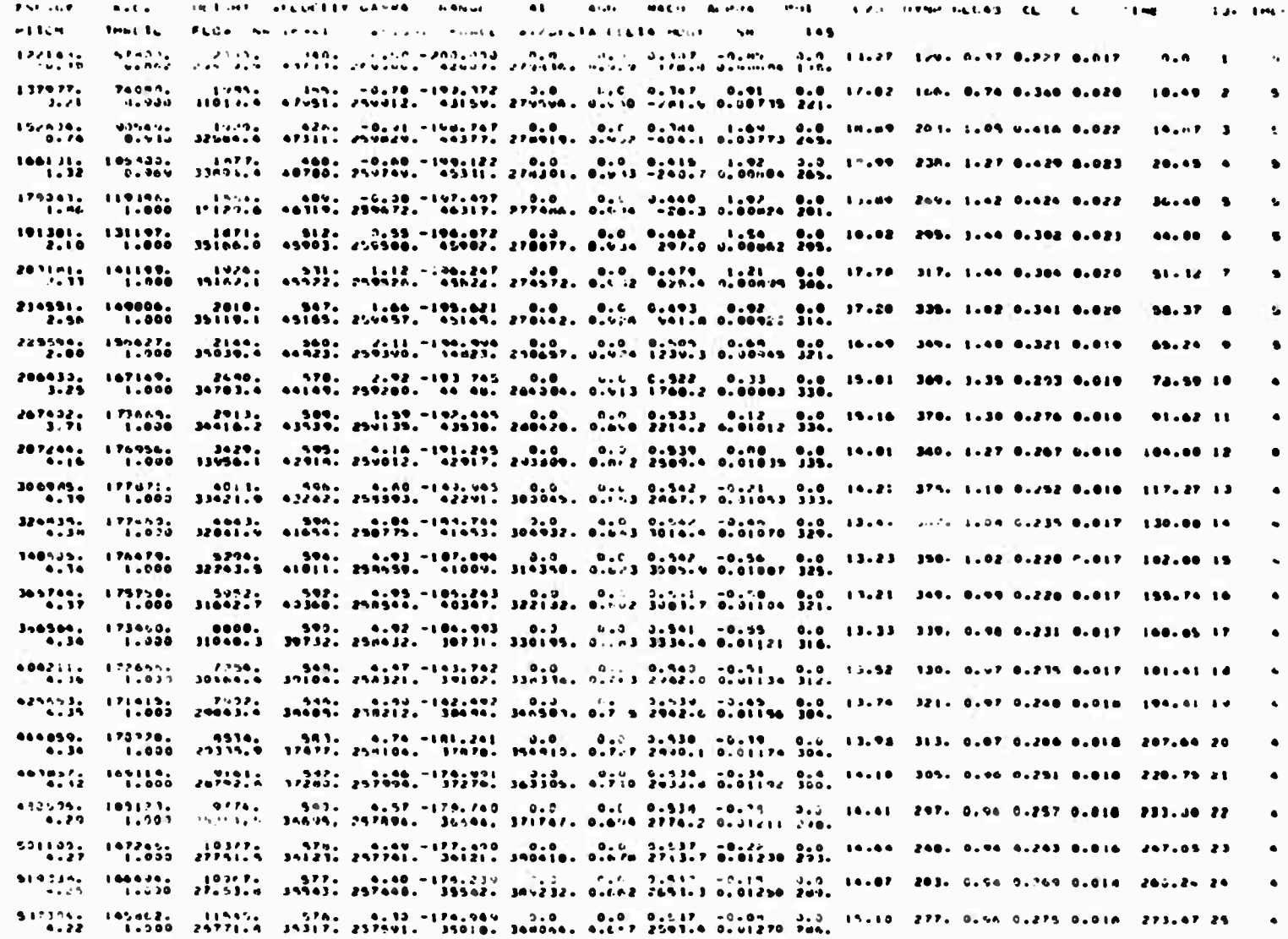

Figure A-4 Segments of 2,000-nm Steepest-Descent Trajectory Listing. (Throttle-Down Begins at 1098.44 Sec)

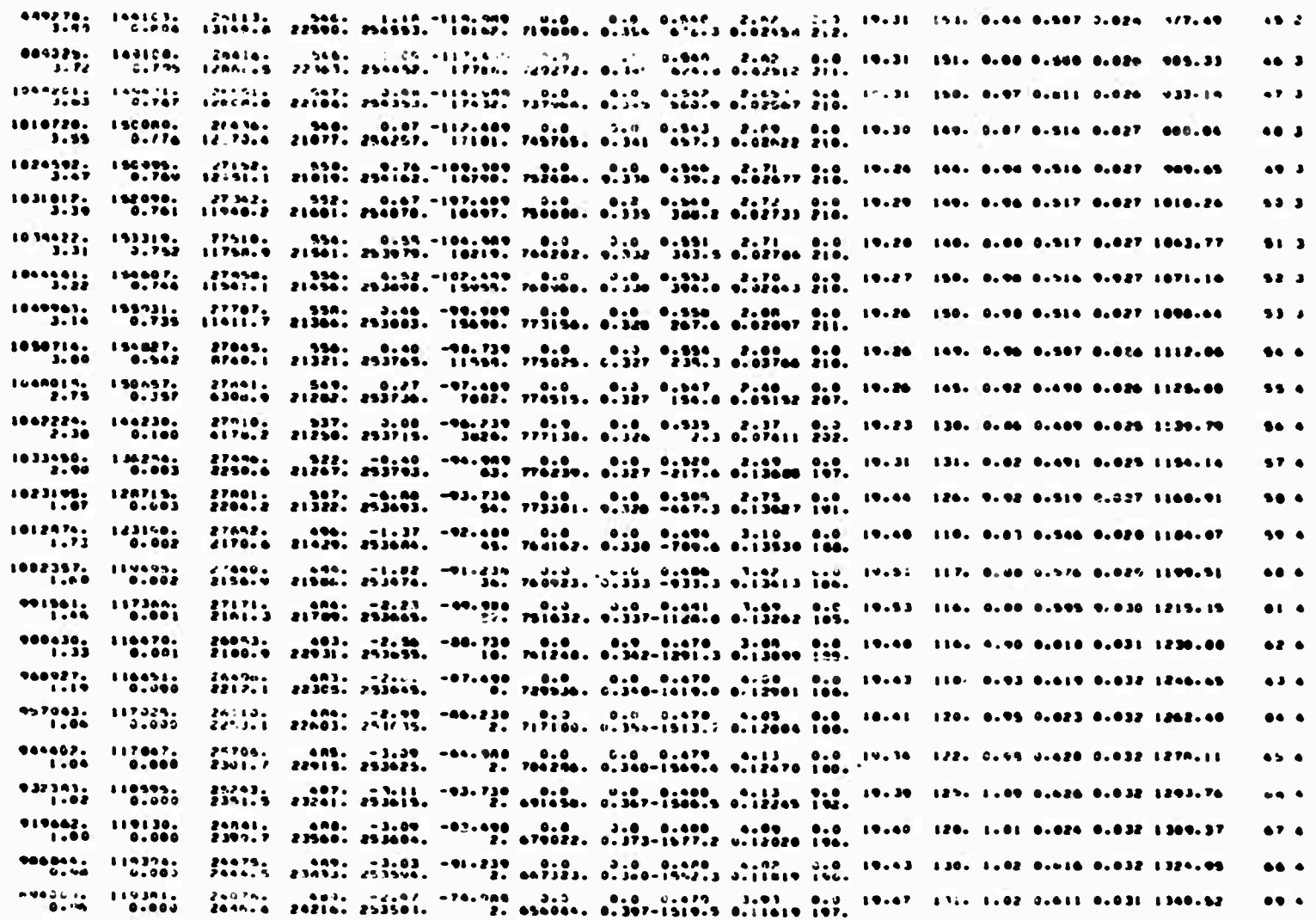

Figure A-4 Segments of 2,000-nm Steepest-Descent Trajectory Listing. (Throttle-Down Begins at 1098.44 Sec) (Continued).

```
220791.    59972.    5328.     365.  -2.50   -12.409    0.0     0.0   0.315    4.67    0.0   16.46   122.  1.00 0.040 0.033 2310.36    90 3
   1.88     0.333   2498.3   64431. 252738.         2. 363024.  0.032  -534.5 0.06433   193.

199628.    56626.    3323.     337.  -2.60    -9.980    0.0     0.0   0.306    4.70    0.0   19.35   110.  1.00 0.059 0.034 2341.30    97 3
   2.10     0.333   2472.2   65029. 252701.         3. 299198.  0.053  -910.0 0.06930   107.

182765.    54753.    3979.     331.  -2.52    -8.730    0.0     0.0   0.306    5.11    0.0   19.17   110.  1.02 0.072 0.030 2363.79    98 4
   2.56     0.033   2788.3   60351. 252603.         4. 292480.  0.104  -872.5 0.07625   105.

169659.    52051.    3656.     323.  -2.37    -7.400    0.0     0.0   0.293    5.45    0.0   18.99   111.  1.02 0.719 0.036 2607.08    96 4
   3.09     0.000   2642.1   66900. 252605.         0. 288996.  0.076  -799.6 0.07220   101.

156531.    48812.    3340.     312.  -2.28    -6.238    0.0     0.0   0.283    5.85    0.0   18.79   105.  1.01 0.781 0.080 2630.99   100 6
   3.56     0.030   2447.8   67668. 252440.         8. 285737.  0.004  -760.4 0.07552   176.

143444.    65365.    3046.     301.  -2.20    -4.980    0.0     0.0   0.273    6.33    0.0   18.57    90.  0.99 0.790 0.063 2485.79   101 4
   4.07     3.300   2227.0   68052. 252632.        12. 282595.  0.096  -712.2 0.08000   170.

136403.    61523.    2695.     298.  -2.24    -4.303    0.0     0.0   0.207    6.88    0.0   18.30    55.  1.01 0.033 0.045 2468.56   162 5
   4.03     0.000   2104.8   64395. 252626.        14. 281035.  0.099  -693.4 0.08293   167.

130030.    61400.    2752.     288.  -2.19    -3.730    0.0     0.0   0.280    7.37    0.0   18.18    91.  1.01 0.072 0.060 2481.58   103 5
   5.10     0.000   1962.0   66673. 252610.        16. 279509.  0.904  -660.0 0.45686   166.

123212.    39204.    2830.     280.  -2.16    -3.113    0.0     0.0   0.253    7.05    0.0   18.03    86.  1.01 0.911 0.051 2494.96   104 5
   5.71     3.000   1801.0   69002. 252529.        17. 270029.  0.909  -629.4 0.09210   100.

110358.    37041.    2.07.     272.  -2.16    -2.400    0.0     0.0   0.240   [illegible]    0.0   17.86    82.  1.00 0.952 0.053 2506.73   105 5
   6.23     0.130   1627.9   69340. 252002.        10. 276570.  0.013  -600.7 0.09092   155.

100855.    36623.    2326.     266.  -2.19    -1.808    0.0     0.0   0.238    8.66    0.0   17.75    77.  0.98 0.992 0.056 2522.04   .06 5
   6.67     0.060   1656.2   69679. 252596.        17. 275126.  0.019  -606.1 0.10746   151.

103351.    33100.    2174.     257.  -2.38    -1.244    0.0     0.0   0.232    9.50    0.0   17.73    74.  0.94 1.000 0.356 2537.37   107 5
   7.12     0.000   1304.0   50009. 252591.        13. 273007.  0.923  -641.1 0.11072   147.

 90072.    32157.    2005.     256.  -2.78    -0.622    0.0     0.0   0.227   10.37    0.0   17.73    72.  0.92 1.000 0.056 2552.21   100 5
   7.62     0.030   1221.0   53309. 252505.         0. 271807.  0.020  -731.3 0.12276   166.

 93340.    32166.    1909.     256.  -3.18     0.000    0.0     0.0   0.226   11.38    0.0   17.73    72.  0.93 1.000 0.056 2567.16   109 5
   6.20     0.030   1722.2   00590. 252500.         0. 269967.  0.930  -663.7 0.12264   166.

ENERGY    K.E.    HEIGHT  VELOCITY GAMMA   RANGE     XI     AGO    MACH   ALPHA    PHI    L/D  DYNP GLOAD  CL    CD    TIME      IJK IMLP
PITCH     THROTL  FLOW    NRT(FNM)        WEIGHT    FORCE  WT/DELTA DELTA HDOT    SR     IGS

ITERATION =   2     FUNCTION EVALUATION =    0

      GAIN ARRAY AM
0.33252E 01    0.46210E 00

      TERMINAL ERRORS
VELOCITY        FLIGHT PATH    ALTITUDE      MASS          TIME          MACHD         WOVOLO
-0.86450E 02  -0.31793E 01   -0.19132E 03   0.74200E 04   0.75672E 04   -0.49056E 00   -0.10701E 97

      TERMINAL COSTS
VELOCITY        FLIGHT PATH    ALTITUDE      MASS          TIME          CTMACH        CTMDEL        CTLIN
0.76734E 00   0.10100E 00   0.30009E 05   0.74200E 00   0.0           0.0           0.0           0.0

      INTEGRATED COSTS
        TRAJECTORY
   MMAX        HDOTMAX       MACHMAX       DYNPMAX       MMIN          MACLMN        MACLMX        IGOMN         IASMX
0.0          0.0           0.0           0.0           0.0           0.0           0.0           0.0           0.0
        CONTROL
   THROTLMN    THROTLMAX     PITCHMN       PITCHMAX      ALPHAMN       ALPHAMAX
0.0          0.0           0.0           0.0           0.0           0.0           0.0           0.0

TOTAL COST =    0.75085E 00

MISSION COSTS
       FUEL COST (AT 35 CENTS / GAL.) = $    396.49
TIME BASED COST (AT 400 DOLLARS / HRS.) = $    205.24
                           TOTAL COST = $    601.73
```

Figure A-4 Segments of 2,000-nm Steepest-Descent Trajectory Listing. (Throttle-Down Begins at 1098.44 Sec) (Continued).

APPENDIX B

MATHEMATICAL MODEL OF THE C-141A AIRCRAFT

The investigation of aircraft fuel minimization techniques has concentrated on the C-141A aircraft, and mathematical models of the C-141A have been included in the computer program ENERGY which performed all the trajectory analysis related to this task.

Five sources of vehicle data have been used for defining the vehicle model (Refs. 1, 2, 32, 47, and 48). These sources provide what is believed to be a vehicle model with a high degree of fidelity. The appropriate equations and the data which comprise the model are presented in the following sections of this appendix.

B.1 C-141A AERODYNAMIC MODEL

The aerodynamic data model for the C-141A aircraft has been obtained from Ref. 48. The model computes the aircraft's coefficients of lift and drag, C_L and C_D, as functions of angle of attack (α), Mach number (M), altitude (h), center of gravity (c.g.), total engine thrust (F), and dynamic pressure (q). Because this study employs only throttle setting and pitch angle as guidance commands, the vehicle's flap and spoiler settings are assumed to be zero. As only two-degree-of-freedom dynamics are used for optimization, the total pitching moment on the vehicle also is assumed to be zero, i.e., the vehicle is trimmed.

With the above assumptions, the computations needed to compute C_L and C_D are as follows. First, the basic lift coefficient is computed as

$$CLBAS = CLALP \cdot CRCLA \cdot (\alpha - CRALO \cdot \alpha_0) \qquad (B.1\text{-}1)$$

where

CLALP (M) = lift curve slope
CRCLA(M,h) = lift flexibility parameter
α_0(M) = zero-lift angle of attack
CRALO(M,h) = zero-lift flexibility parameter.

The total lift coefficient is then given by

$$C_L = CLBAS - 0.2979(CMIT \cdot STAB) \qquad (B.1\text{-}2)$$

where

CMIT = pitch moment coefficient due to stabilator deflection
STAB = Stabilator deflection angle

The coefficient 0.2979 is the ratio of the aircraft's reference chord to tail moment arm and reflects the fact that the tail provides lift as well as pitching moment.

The zero total pitching moment assumption allows the quantity CMIT · STAB to be expressed in terms of the other pitching moments acting on the vehicle. Making these substitutions results in

$$C_L = \frac{CLBAS(1+0.2979 \cdot CMCL \cdot CRCMC)+0.2979(CMO \cdot CRCMO+CMTH)}{[1-0.2979(CCG-0.241)]} \qquad (B.1\text{-}3)$$

where

CMCL(M) = pitching moment coefficient due to lift
CRCMC(M,h) = CMCL flexibility parameter
CMO(M) = pitching moment
CRCMO(M,H) = CMO flexbility parameter
CMTH = pitch moment due to thrust

The thrust-induced pitching moment, CMTH, which appears in Eq. (B.1-3) is computed from the engine thrust and dynamic pressure as

$$CMTH = F/(17960 \cdot q) \qquad (B.1\text{-}4)$$

Having computed the vehicle's lift coefficient, the drag coefficient is determined as a function of C_L and M, i.e.,

$$C_D = (CDCCL(M, C_L)) \qquad (B.1\text{-}5)$$

Either total lift coefficient (C_L) or wing lift coefficient (CLBAS) could be used to compute the drag coefficient (Eq. (B.1-5)). The first approach neglects trim drag, as the down load on the tail (required for static trim) is not considered explicitly. Since CLBAS is greater than C_L, trim drag is included in the second approach. C_D has been computed using C_L for optimal and conventional flight path computations and using CLBAS in the specific range analyses.

The computations of vehicle C_L and C_D described in Eqs. (B.1-1), (B.1-3) and (B.1-5) necessitate performing table lookups to obtain appropriate values of the tabulated data. The table lookups are performed using either linear or cubic polynominal interpolation. The linear lookup routines provide satisfactory results for all trajectory

simulations. The cubic interpolations are employed whenever partial derivatives of the data are required, as this information is available with the cubic interpolation routines.

The actual data values used in the computation of vehicle lift and drag are in the form of single- and two-dimensional data arrays. To complete the C-141A aerodynamic model specification, these data values are presented below.

The data tables are stored as functions of Mach number, altitude, and C_L. The arrays which define the values of the Mach number-only dependent variables are:

- Lift curve slope (CLALP(M))
- Zero lift angle-of-attack (α_0(M))
- Pitching moment coefficient due to lift (CMCL(M))
- Pitching moment (CMO(M))

The data points for these variables as a function of Mach number are shown in Table B-1.

TABLE B-1

MACH NUMBER-DEPENDENT AERODYNAMIC VARIABLES

Mach number	CLALB	α_0	CMCL	CMO
0.0	0.0835	-3.37	-0.246	0.085
0.1	0.0851	-3.39	-0.245	0.084
0.2	0.0867	-3.41	-0.244	0.083
0.3	0.0882	-3.43	-0.241	0.080
0.4	0.0900	-3.45	-0.242	0.080
0.5	0.0917	-3.46	-0.247	0.082
0.6	0.0937	-3.48	-0.254	0.085
0.65	0.0968	-3.42	-0.257	0.089
0.7	0.0998	-3.36	-0.260	0.092
0.75	0.1076	-3.27	-0.255	0.098
0.77	0.1100	-3.22	-0.263	0.096
0.8	0.1055	-3.25	-0.283	0.100
0.83	0.0870	-3.28	-0.311	0.080
0.86	0.0861	-2.56	-0.317	0.061
0.9	0.1030	-1.30	-0.293	0.115

The data points for those variables which are functions of two independent variables are the following:

- Lift flexibility parameter (CRCLA(M,h))

M \ h(ft)	0	20,000	40,000
0.0	1.00	1.00	1.00
0.1	1.00	1.00	1.00
0.2	.983	.992	.994
0.3	.949	.976	.987
0.4	.900	.952	.976
0.5	.854	.926	.966
0.6	.806	.995	.955
0.65	.775	.870	.944
0.70	.744	.845	.933
0.75	.712	.816	.912
0.77	.712	.804	.893
0.80	.712	.796	.883
0.83	.712	.810	.905
0.86	.712	.814	.994
0.90	.712	.749	.873

- Zero-lift angle-of-attack flexibility parameter (CRALO(M,h))

M \ h(ft)	0	20,000	40,000
0.0	1.00	1.00	1.00
0.1	1.00	1.00	1.00
0.2	1.00	1.00	1.00
0.3	1.00	1.00	1.00
0.4	1.00	1.00	1.00
0.5	.985	1.00	1.00
0.6	.955	.985	1.00
0.65	.947	.980	1.00
0.70	.938	.975	1.00
0.75	.926	.958	1.00
0.77	.926	.948	.994
0.80	.926	.926	.981
0.83	.926	.913	.971
0.86	.926	1.016	1.00
0.90	.926	1.547	1.00

- CMCL flexibility parameter (CRCMC(M,h))

M \ h(ft)	0	20,000	40,000
0.0	1.00	1.00	1.00
0.1	1.00	1.00	1.00
0.2	.960	.988	1.00
0.3	.904	.968	.988
0.4	.833	.939	.976
0.5	.755	.890	.951
0.6	.679	.846	.939
0.65	.624	.807	.920
0.70	.568	.768	.900
0.75	.421	.715	.908
0.77	.421	.681	.880
0.80	.421	.640	.877
0.83	.421	.663	.905
0.86	.421	.590	.739
0.90	.421	.585	.717

- CMO flexibility parameter (CRCMO(M,h))

M \ h(ft)	0	20,000	40,000
0.0	1.00	1.00	1.00
0.1	1.00	1.00	1.00
0.2	.938	.988	1.00
0.3	.807	.928	.964
0.4	.709	.860	.930
0.5	.567	.756	.889
0.6	.436	.670	.851
0.65	.383	.639	.833
0.70	.330	.608	.814
0.75	.260	.550	.780
0.77	.260	.520	.770
0.80	.260	.490	.765
0.83	.260	.440	.774
0.86	.260	.466	.740
0.90	.260	.496	.617

- Drag Coefficient (CDCCL(M,C_L))

M \ C_L	0.1	0.2	0.3	0.4	0.5	0.6	0.7	0.8
0.0	.0156	.0166	.0185	.0213	.0253	.0304	.0366	.0432
0.1	.0156	.0166	.0185	.0213	.0253	.0304	.0366	.0432
0.2	.0156	.0166	.0185	.0213	.0253	.0304	.0366	.0432
0.3	.0156	.0166	.0185	.0213	.0253	.0304	.0366	.0432
0.4	.0156	.0166	.0185	.0214	.0254	.0304	.0366	.0432
0.5	.0157	.0166	.0186	.0216	.0257	.0308	.0368	.0438
0.6	.0160	.0168	.0189	.0221	.0262	.0313	.0375	.0450
0.65	.0163	.0171	.0192	.0224	.0266	.0318	.0385	.0473
0.70	.0166	.0174	.0195	.0228	.0270	.0323	.0394	.0495
0.75	.0176	.0182	.0202	.0234	.0276	.0333	.0432	.0612
0.77	.0183	.0189	.0210	.0240	.0283	.0347	.0493	.0707
0.80	.0209	.0215	.0234	.0267	.0320	.0423	.0664	.0872
0.83	.0325	.0330	.0353	.0393	.0476	.0670	.0775	.0855
0.86	.0470	.0475	.0498	.0536	.0610	.0770	.0829	.0883
0.90	.0590	.0595	.0610	.0637	.0697	.0817	.0865	.0900

B.2 C-141A THRUST MODEL

The installed thrust model of the C-141A aircraft provides the normal rated thrust, NRT, of each of the aircraft's engines. The model included in program ENERGY was provided by the fuel management studies of Ref. 2.

Altitude, Mach number, and non-standard atmospheric temperature effects on NRT are accounted for in the current engine model. A thirteen-term polynomial, which is a function of these parameters, is evaluated to determine engine thrust. The NRT equation is given by

$$\begin{aligned} NRT = {} & 5763.499 - 498.8629 \cdot UN - 5590.819 \cdot HN \\ & - 123.8276 \cdot UN^2 - 136.1916 \cdot UN \cdot MN \\ & + 77.995 \cdot MN^2 + 1177.55 \cdot UN \cdot HN + 731.959 \cdot MN \cdot HN \\ & + 1609.4427 \cdot HN^2 + 108.217 \cdot UN \cdot MN \cdot HN \\ & - 875.1862 \cdot UN \cdot HN^2 - 805.6959 \cdot MN \cdot HN^2 \\ & + 385.875 \cdot HN^3 \end{aligned} \qquad \text{(B.2-1)}$$

where

NRT = normal-rated thrust (lb)
UN = normalized temperature deviation
HN = normalized altitude
MN = normalized Mach number

The normalized terms in Eq. (B.2-1) are computed as:

$$UN = \Delta TEMP/40. \qquad \text{(B.2-2)}$$

$$HN = (h-25500.)/29500. \qquad \text{(B.2-3)}$$

$$MN = (M-0.55)/0.25 \qquad (B.2\text{-}4)$$

where $\Delta TEMP$ is the temperature deviation (^{o}F) from the 1962 Standard Atmosphere, h is the aircraft altitude in feet, and M is the aircraft's Mach number.

The polynomial form of the NRT computation eliminates the need to execute numerous table interpolations. It also simplifies the evaluation of the partial derivatives of engine thrust with respect to the vehicle state, which is needed for trajectory and guidance gain optimization. The partial derivatives of NRT with respect to the vehicle state are computed in closed form by taking the appropriate partial derivatives of Eq. (B.2-1).

B.3 ENGINE FUEL FLOW MODEL

A general fuel flow model for the C-141A was obtained from Ref. 1. The data represents flow rates for a TF33 Pratt and Whitney engine installed on the C-141A aircraft.

Figure B-1 presents the fuel flow data in graphical form. In this figure, normalized flow rate is plotted as a function of normalized engine thrust for three Mach numbers. The atmospheric normalization factor, δ, is the ratio of atmospheric pressure at altitude, p_h, to pressure at sea-level, p_{SL}, i.e.,

$$\delta = p_h/p_{SL} \qquad (B.3\text{-}1)$$

The normalization factor, θ, is given by

$$\theta = TEMP_h/TEMP_{SL} \qquad (B.3\text{-}2)$$

where

$TEMP_h$ = temperature at altitude

$TEMP_{SL}$ = sea-level temperature

For the analysis of this study, engine thrust is computed simply as the product of throttle setting, T, and the engines' NRT,

$$F = T \cdot NRT \qquad \text{(B.3-3)}$$

where throttle setting ranges between 0 and 1.

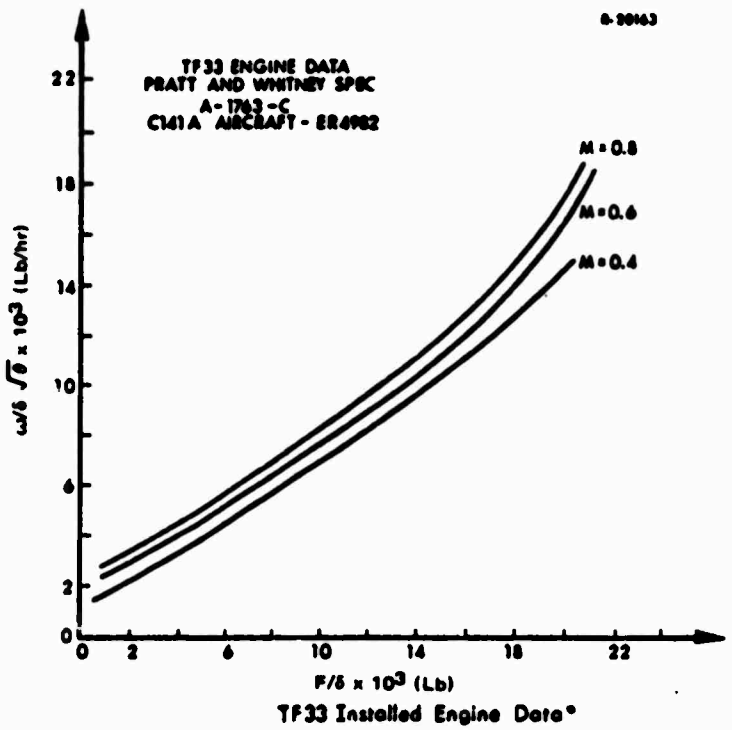

Figure B-1 TF33 Installed Engine Data*

*Fuel flow rates modeled in program ENERGY have been increased by 11 percent to match C-141A Category II Flight Performance Test results.

The data presented in Fig. B-1 is incorporated in program ENERGY as a two-dimensional table lookup. Fuel flow data is stored as a function of engine thrust and Mach number. As with the vehicle aerodynamic data, linear table interpolation is used for most trajectory analysis. For those functions which require partial derivatives of fuel flow rate with respect to the vehicle state, cubic interpolation routines are employed to accurately determine the required derivatives.

In order to validate the C-141A vehicle model of program ENERGY, the maximum range factor and best Mach number were computed for a wide range of aircraft altitudes and weights. The results of this study then were compared with the data available from the C-141A Category II Performance Tests (Ref. 47). It was found that the range factor performance of the simulated vehicle was approximately 11 percent too high. The fuel flow rates depicted in Fig. B-1 were increased by this percentage and the range factor comparisons repeated. The close agreement between the modeled results and those of the vehicle tests is shown in Fig. B-2. The trajectory analysis performed in the current study employed the fuel flow data adjusted by the 11 percent factor in order to represent an actual vehicle as accurately as possible.

B.4 VEHICLE LOADING CONDITIONS

Typical C-141A vehicle weights and fuel loadings are documented in Ref. 32. Those values which were useful for the current program development are listed here:

- Maximum ramp weight: 318,000 lb
- Maximum normal landing weight: 257,500 lb
- Maximum flight fuel load: 148,120 lb

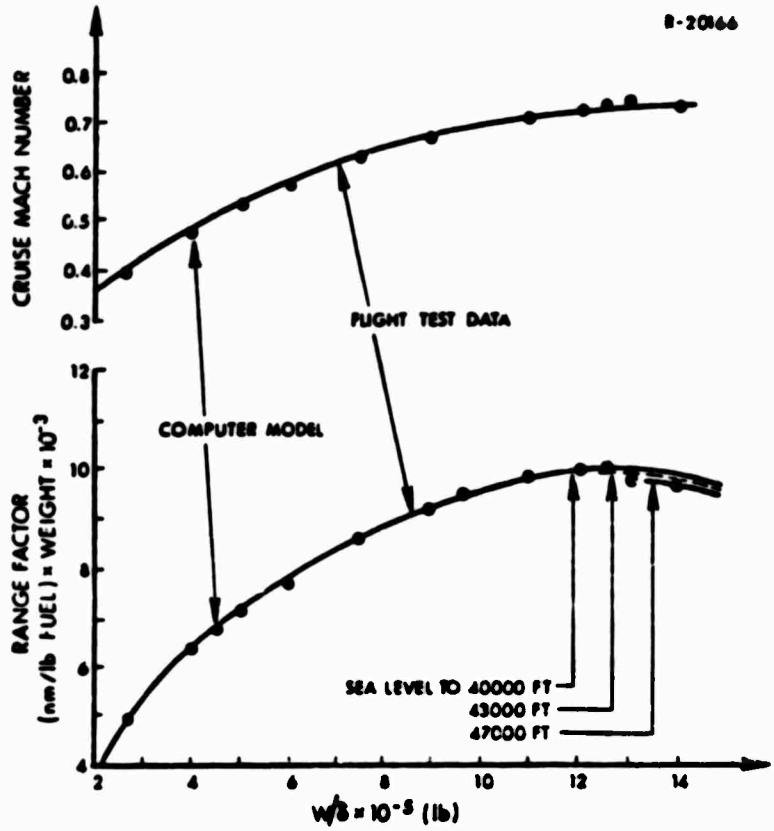

Figure B-2 Comparison of Vehicle Model and Actual Aircraft Performance

The vehicle reference area, needed for computations of specific force on the vehicle was obtained from Ref. 45 as 3,228 ft^2. At a maximum vehicle weight of 318,000 lb, level "1-g" flight would necessitate a wing loading on the order of 99 lb/ft^2.

REFERENCES

1. Seinfeld, R.D., Sobocinski, R.S. and Kommrusch, F.G., "Mission Control Fuel Management Techniques for Aircraft," AFFDL-TR-67-95, Aug. 1967.

2. Stephan, P.W. and Sworder, S.C., "Fuel Management Computer Investigation," AFFDL-TR-70-148, Dec. 1970.

3. Miele, A., Flight Mechanics, Addison-Wesley, Reading, 1962.

4. Perkins, C.D. and Hage, R.E., Airplane Performance Stability and Control, J. Wiley & Sons, New York, 1949.

5. Teren, F. and Daniele, C.J., "Optimal Cruise Trajectories for Supersonic Airplanes," NASA TN D-6707, Mar. 1972.

6. Speyer, J., "On the Fuel Optimality of Cruise," Journal of Aircraft, Vol. 10, No. 12, Dec. 1973, pp. 763-765.

7. Schultz, R.L., "Fuel Optimality of Cruise," Journal of Aircraft, Vol. 11, No. 9, Sept. 1974, pp. 586-587.

8. Bryson, A.E., Jr., Desai, M.N. and Hoffman, W.C., "Energy-State Approximation in Performance Optimization of Supersonic Aircraft," Journal of Aircraft, Vol. 6, Nov.-Dec. 1969, pp. 481-488.

9. Parsons, M.G., Bryson, A.E., Jr. and Hoffman, W.C., "Long-Range Energy-State Maneuvers for Minimum Time to Specified Terminal Conditions," AIAA Paper 73-229, New York, Jan. 1973

10. Zagalsky, N.R., Irons, R.P., Jr. and Schultz, R.L., "Energy State Approximation and Minimum-Fuel Fixed-Range Trajectories," Journal of Aircraft, Vol. 8, No. 6, June 1971, pp. 488-490.

11. Schultz, R.L. and Zagalsky, N.R., "Aircraft Performance Optimization," Journal of Aircraft, Vol. 9, No. 2, Feb. 1972, pp. 108-114.

12. Zagalsky, N.R., "Aircraft Energy Management," AIAA Paper 73-228, New York, Jan. 1973.

REFERENCES (Continued)

13. Nichols, M.A. and Hedrick, J.K., "The Sensitivity of Optimal Flight Paths to Variations in Aircraft and Atmospheric Parameters," Proceedings of the 1973 JACC, Columbus, June 1973.

14. Ardema, M.D., "Approximations in the Minimum Time-to-Climb Problem," NASA TMX-62,292, Aug. 1973.

15. Thomas, A.N., Porter, J.L., et al., "Results of an Investigation of Propulsion Management Systems for Advanced Military Aircraft," AFFDL-TR-71-136, Oct. 1971.

16. Schiro, J.A. and Shykula, T.J., "Flight Evaluation of Optimal Commands for F-106 Minimum Time Climb and Acceleration," AFFDL-TR-73-32, Mar. 1973.

17. Johnson, D.T., "Evaluation of Energy Maneuverability Procedures in Aircraft Flight Path Optimization and Performance Estimation," AFFDL-TR-71-58, Nov. 1972.

18. Kelley, H.J., "Aircraft Maneuver Optimization by Reduced-Order Approximation," in Control and Dynamic Systems, Vol. 10, Advances in Theory and Applications, Academic Press, New York, 1973.

19. Calise, A.J., "On the Use of Singular Perturbation Methods in the Solution of Variational Problems," Proceedings of the 1973 JACC, Columbus, June 1973.

20. Kelley, H.J. and Edelbaum, T.N., "Energy Climbs, Energy Turns, and Asymptotic Expansions," Journal of Aircraft, Vol. 7, No. 1, Jan.-Feb. 1970, pp. 93-95.

21. O'Connor, J.T., "Aircraft Range Optimization using Singular Perturbations," Ph.D. Thesis, M.I.T., June 1973.

22. Grose, G.G., Landy, R.J., Marsh, R.G., and Turner, R.D., "Analysis and Simulation of Variable Throttle/ Energy Management Concepts for Fighter Aircraft," AFFDL-TR-74-138, Nov. 1974.

23. Grose, G.G., Marsh, R.G., and Turner, R.D., "Interface of Fighter Throttle/Energy Management Functions with DAIS," AFFDL-TR-75-60, June 1975.

24. Coleman, H.J., "USAF Faces Major Boost in Fuel Cost, Aviation Week & Space Technology, Vol. 103, No. 9, Sept. 1, 1975, pp. 18-19.

REFERENCES (Continued)

25. Communications and Memoranda from the Air Force Flight Dynamics Laboratory, 1975.

26. Bryant, W.B., Hoffman, M.A., Navoy, A.J. and Pastan, H.L., Cruise Control Techniques for Turbojet Aircraft," WADC TR-55-246, July 1955.

27. Martin, R.W., "Centralized Flow Control," Journal of ATC, Sept. 1970, pp. 5-8.

28. Kulikowski, A.J., "En Route Speed Control Techniques," Journal of ATC, May 1971, pp. 5-8.

29. Kulikowski, A.J., "Airspeed and ATC," Journal of ATC, May-June 1973, pp. 5-7.

30. Anon., "Chapter 8-Flight Planning," The MAC Command Post Regulation, MAC Regulation 55-3, Vol. I, Scott Air Force Base, Oct. 17, 1973.

31. Anon., "Delta's Automated Flight Control Helps Reduce Exposure to CAT," Journal of ATC, July 1972, pp. 19-31.

32. Anon., "C-141A Flight Handbook," Technical Order T.O. 1C-141A-1-1, U.S. Government Printing Office, Washington, Feb. 1971.

33. Anon., "U.S. Standard Atmosphere, 1962," U.S. Government Printing Office, Washington, 1962.

34. Laughlin, T.F., Jr., "L-1011 Fuel Conservation Considerations," Lockheed (Informal) Memorandum, Dec. 1973.

35. Flight Technical Section, "Fuel Conservation," Boeing Airliner, Jan. 1974, pp. 3-12.

36. Grey, Jerry, ed., Aircraft Fuel Conservation: An AIAA View," New York, June 1974.

37. Gravelle, J.A., "Evaluation of an Airborne Thrust Computing System, Vol. I: System Performance Evaluation," ASD-TR-75-2, May 1975.

38. Athans, M. and Falb, P.L., Optimal Control, McGraw-Hill, New York, 1966.

39. Bryson, A.E., Jr. and Ho, Y.C., Applied Optimal Control, Ginn-Blaisdell, Waltham, 1969.

REFERENCES (Continued)

40. Jacob, H.G., "An Engineering Optimization Method with Application to STOL-Aircraft Approach and Landing Trajectories," NASA TN D-6978, Sept. 1972.

41. Deyst, J., Kriegsman, B., and Marcus, F.J., "Entry-Trajectory Design to Minimize Thermal-Protection-System Weight," MIT CSDL E-2614, Nov. 1971.

42. Stengel, R.F., "Optimal Transition from Entry to Cruising Flight," Journal of Spacecraft and Rockets, Vol. 8, No. 11, Nov. 1971, pp. 1126-1132.

43. Palsson, T., et al, "Optimal VTOL Flight Paths under Constraints," AIAA Paper 70-550, New York, May 1970.

44. Stengel, R.F., "Strategies for Control of the Space Shuttle Transition," Journal of Spacecraft and Rockets, Vol. 10, No. 1, Jan. 1973, pp. 77-84.

45. Stengel, R.F., "Optimal Guidance for the Space Shuttle Transition," Journal of Spacecraft and Rockets, Vol. 11, No. 3, Mar. 1974, pp. 173-179.

46. Zeldin, S. and Speyer, J.L., "Maximum Noise Abatement Trajectories," AIAA Paper 72-665, New York, June 1972.

47. Roe, C.W. and Cross, C.S., "C-141A Category II Performance Tests," USAF FTC-TR-66-9, Aug. 1966.

48. Larson, H.B., Zimmer, C.R., Roberts, L.D., Bunnel, J. and Lair, D., "Military Transport (C-141) Fly-by-Wire Programs," AFFDL-TR-74-52, Vol. I, April 1974.

49. Enright, W.H., Hull, T.E. and Lindberg, B., "Comparing Numerical Methods for Stiff Systems of ODEs," University of Toronto, Technical Report No. 69, Sept. 1974.

50. Lindberg, B., "Optimal Stepsize Sequences and Requirements for the Local Error for Methods for (Stiff) Differential Equations," University of Toronto, Technical Report No. 67, May 1974.

51. Balakrishnan, A.V., and Neustadt, L.W., ed., Computing Methods in Optimization Problems, Academic Press, New York, 1964.

REFERENCES (Continued)

52. Dommasch, D.O., Sherby, S.S. and Connolly, T.F., Airplane Aerodynamics, Pitman, New York, 1967.

53. Wetmore, W.C., "Stretch of C-141A Fleet Termed Possible by 1980," Aviation Week & Space Technology, Vol. 103, No. 10, Sept. 8, 1975, pp. 47-48.

54. Kwakernaak, H. and Sivan, R., Linear Optimal Control Systems, Wiley-Interscience, New York, 1972.

55. Price, C.F. and Koenigsberg, W.D., "Adaptive Control and Guidance for Tactical Missiles," Vols. I and II, TR-170-1, The Analytic Sciences Corp., June 1970.

56. Hall, B.A., and Trainor, W.V., et al, "Modular Digital Missile Guidance System Study," Raytheon Co. Mission Systems Division, Report No. BR-8073, June 1973.

57. Stengel, R.F., Broussard, J.R., and Berry, P.W., "The Design of Digital-Adaptive Controllers for VTOL Aircraft," Technical Report No. TR-640-1, (NASA CR-144912), The Analytic Sciences Corp., Oct. 1975.

58. Lee, T.H., Adams, G.E., and Gaines, W.M., Computer Process Control: Modeling and Optimization, John Wiley & Sons, New York, 1968

59. Pike, H.E., Jr., "Software Production for Minicomputers," IEEE Proceedings, Vol. 61, No. 11, Nov. 1973, pp. 1544-1556.

60. Anon., "Computer Monitoring Shaves Fuel Use," Aviation Week & Space Technology, Vol. 101, No. 23, Dec. 23, 1974, pp. 30-36.

☆ U. S. GOVERNMENT PRINTING OFFICE: 1976 — 657-640/573